The effect of the magnetic and optical field on hydrogen production via alkaline water electrolysis

Paranos, Matej

University of Zagreb
Faculty of Mechanical Engineering and Naval Architecture

Matej Paranos

THE EFFECT OF THE MAGNETIC AND OPTICAL FIELD ON HYDROGEN PRODUCTION VIA ALKALINE WATER ELECTROLYSIS

DOCTORAL DISSERTATION

Zagreb, 2024

University of Zagreb
Faculty of Mechanical Engineering and Naval Architecture

Matej Paranos

THE EFFECT OF THE MAGNETIC AND OPTICAL FIELD ON HYDROGEN PRODUCTION VIA ALKALINE WATER ELECTROLYSIS

DOCTORAL DISSERTATION

Supervisor:
Assoc. Prof. Ankica Kovač, Ph.D.

Zagreb, 2024

Sveučilište u Zagrebu
Fakultet strojarstva i brodogradnje

Matej Paranos

UTJECAJ MAGNETSKOGA I OPTIČKOGA POLJA NA UČINKOVITOST PROIZVODNJE VODIKA ALKALNOM ELEKTROLIZOM VODE

DOKTORSKI RAD

Mentor:
Izv. prof. dr. sc. Ankica Kovač

Zagreb, 2024.

ZAHVALA

Zahvaljujem Hrvatskoj zakladi za znanost na potpori kroz projekt DOK-2018-09-9405 u okviru kojega je izrađen ovaj doktorski rad.

Prije svega, zahvaljujem se svojoj mentorici Ankici Kovač na komentarima i svesrdnoj pomoći koju mi je pružala tijekom izrade ovog doktorskog rada. Hvala joj na prilici da svoje obrazovanje okrunim ovom doktorskom disertacijom te zakoračim u svijet znanosti te na svakoj pruženoj prilici da napredujem. Hvala joj na sreći i veselju koju smo iskusili u svim lijepim trenucima kao i na podršci i vodstvu u onim teškim. Hvala joj što je bila odlična šefica i što je sudjelovanje na projektu za mene bio gušt, a ne samo posao.

Hvala članovima Povjerenstva, prof. dr. sc. Vesni Alar, izv. prof. dr. sc. Goranu Krajačiću i prof. dr. sc. Sanji Martinez na velikoj podršci, te svim stručnim savjetima i komentarima koji su utkani u ovaj doktorski rad. Također zahvaljujem i prof. emer. dr. sc. Frani Barbiru i dr. sc. Đuri Drobcu na vremenu uloženom u čitanje i komentiranje radnih verzija doktorskoga rada koji su uvelike doprinijeli njegovoj kvaliteti. Zahvaljujem se i svojoj kolegici s kojom sam dijelio ured, Doriji Marciuš, za sve trenutke koje smo proveli zajedno u Laboratoriju, što smo bili jedan drugome podrška u bremenitim vremenima i zajedno slavili sve naše uspjehe. Jedno veliko hvala i laborantima Milanu Šulentiću i Krunoslavu Uroiću koji su bezrezervno i srdačno priskakali u pomoć kad god je trebalo, koji su svojim savjetima i mudrostima oplemenili moj rad i bez kojih rad u Laboratoriju ne bi bio isti.

Neizmjerno sam zahvalan svim svojim prijateljima, ljudima koji mi vraćaju osmijeh na lice i kada je najteže, rastjeruju čak i one najcrnje oblake, koji me motiviraju da dajem 120% od sebe i uvijek stremim najboljem. Hvala dragom Bogu na nebu i Dinamu na zemlji što postoje i što su uvijek tu.

Zahvaljujem se i svim profesorima na poslijediplomskom studiju, kao i kolegama, bivšima i sadašnjima, te djelatnicama Fakulteta strojarstva i brodogradnje, a posebno kolegama sa Zavoda za energetska postrojenja, energetiku i okoliš.

Za kraj, najveća hvala mojim roditeljima Mirjani i Tihomiru, bez čije ljubavi, žrtve i podrške ne bih nikada bio to što jesam. Hvala im za neiscrpnu podršku i strpljenje tijekom provedbe projekta i izrade doktorata. Hvala im što su me odgojili da budem čovjek. U ovaj rad utkan je i njihov trud. Hvala za sve.

U Ivanić Gradu dana 29.08.2023. godine,

Matej Paranos

Ovaj doktorski rad posvećujem svom pokojnom dedi Štefu, koji mi je još kao klincu objasnio kako funkcionira motor s unutarnjim izgaranjem i koji me je uvijek poticao na strojarsko razmišljanje. Znam da bi bio preponosan da je doživio dan kada sam upisao strojarski fakultet prije 12 godina i zato, ovaj rad je njemu u čast!

BIBLIOGRAPHY DATA

Keywords:	Hydrogen technologies; Alkaline electrolyzer; Magnetic field; Optical field; Ni foam electrodes
Scientific area:	Technical Sciences
Scientific field:	Mechanical Engineering
Institution:	University of Zagreb Faculty of Mechanical Engineering and Naval Architecture
Thesis supervisor:	Assoc. Prof. Ankica Kovač, PhD
Number of pages:	114
Number of figures:	49
Number of tables:	10
Number of references:	90
Date of examination:	*July 15th, 2024*
Thesis defence Committee:	Assoc. Prof. Goran Krajačić, PhD University of Zagreb Faculty of Mechanical Engineering and Naval Architecture, Zagreb, Croatia Prof. Vesna Alar, PhD University of Zagreb Faculty of Mechanical Engineering and Naval Architecture, Zagreb, Croatia Prof. Sanja Martinez, PhD University of Zagreb Faculty of Chemical Engineering and Technology, Zagreb, Croatia
Archive:	University of Zagreb Faculty of Mechanical Engineering and Naval Architecture

TABLE OF CONTENTS

LIST OF FIGURES

LIST OF TABLES

NOMENCLATURE

Symbol	Unit	Description
A_E	mm^2	Area of the cut section of the upper tank
a	$-$	Difference between the threshold values for measurement uncertainty
a_h	mm	Difference between the threshold values for the level of the electrolyte measurement
a_I	A	Difference between the threshold values for electrical current measurement
a_p	Pa	Difference between the threshold values for barometric pressure measurement
a_T	K	Difference between the threshold values for temperature measure
a_U	V	Difference between the threshold values for voltage measurement
B	T	Magnetic flux density
B_{HS}	mT	Magnetic flux density on the Hall sensor
E_I	J	Energy input
E_O	J	Energy output
g	ms^{-2}	Gravitational acceleration
h_{ae}	mm	Distance between the bottom of the volume in the lower tank and the top of the volume in the upper tank
h_e	mm	Distance between levels of the electrolyte in the upper tank and lower tank
h_{lt}	mm	Distance between the level of the electrolyte in the lower tank and the bottom of the volume of the lower tank (Level of the electrolyte in the lower tank)
h_{l1}	mm	Level of the electrolyte in the lower tank before the start of the experiment
h_{l2}	mm	Level of the electrolyte in the lower tank after the end of the experiment
h_{ut}	mm	Distance between the level of the electrolyte in the upper tank and the top of the volume of the upper tank (Level of the electrolyte in upper tank)
h_{u1}	mm	Level of the electrolyte in the upper tank before the start of the experiment
h_{u2}	mm	Level of the electrolyte in the upper tank after the end of the experiment

Symbol	Unit	Description
HHV_{H_2}	$MJkmol^{-1}$	Higher heating value of hydrogen
I	A	Electrical current
I_E	A	Electrical current in the process of water electrolysis
LHV_{H_2}	$MJkmol^{-1}$	Lower heating value of hydrogen
M_e	$kgmol^{-1}$	Molar mass of the electrolytic gas
M_{H_2}	$kgmol^{-1}$	Molar mass of the hydrogen
M_{H_2O}	$kgmol^{-1}$	Molar mass of the water
M_{O_2}	$kgmol^{-1}$	Molar mass of the oxygen
m	kg	Mass
m_e	kg	Mass of the produced electrolytic gas
$m_{e'}$	kg	Mass of the produced gas in electrolyzer
m_w	kg	Mass of used water
m_{H_2}	kg	Mass of produced hydrogen
m_{H_2O}	kg	Mass of vapor in produced gas in electrolyzer
P_I	Ws	Power output
p	Pa	Pressure
p_a	hPa	Measured barometric pressure
p_{a_1}	hPa	Measured barometric pressure before the start of the experiment
p_{a_2}	hPa	Measured barometric pressure after the end of the experiment
p_e	Pa	Pressure of the electrolytic gas
p_s	Pa	Saturation pressure of water
R_e	$Jkg^{-1}K^{-1}$	Individual gas constant for the electrolytic gas
R_{un}	$Jmol^{-1}K^{-1}$	Universal gas constant
t	s	Duration of the experiment
T	K	Temperature
T_e	$°C$	Temperature of the produced electrolytic gas
T_{e_1}	$°C$	Temperature of the produced electrolytic gas before the start of the experiment
T_{e_2}	K	Temperature of the produced electrolytic gas after the end of the experiment
U	V	Voltage
U_E	V	Voltage in the process of the water electrolysis
U_L	V	Voltage applied on the LED
U_{HS}	mV	Output voltage on the Hall sensor

Symbol	Unit	Description
u	$-$	Measurement uncertainty
u_h	mm	Measurement uncertainty for the level of the electrolyte measurement
u_I	A	Measurement uncertainty for the electrical current measurement
u_p	Pa	Measurement uncertainty for the barometric pressure measurement
u_T	K	Measurement uncertainty for the temperature measurement
u_U	V	Measurement uncertainty for the voltage measurement
V	m^3	Volume
V_e	mm^3	Volume of the produced electrolyte gas
V_{av}	mm^3	Extra volume in the volume of the threaded plug
y_{H_2}	$-$	Molar share of hydrogen in the electrolytic gas
η	%	Energy efficiency
η_e	%	Energy efficiency of the process of water electrolysis
η_{Lf}	%	Energy efficiency given by mathematical model with LED on foam electrodes
η_{Ls}	%	Energy efficiency given by mathematical model with LED on smooth electrodes
η_{mf}	%	Energy efficiency given by mathematical model with magnetic field on foam electrodes
η_{ms}	%	Energy efficiency given by mathematical model with magnetic field on smooth electrodes
η_0	%	Efficiency of the electrolyzer without application of the external field
ρ_e	kgm^{-3}	Density of the electrolyte

LIST OF ABBREVIATIONS

Abbreviation	Full meaning
3D	Three-dimensional
CO_2	Carbon dioxide
DAQ	Data acquisition system
DC	Direct current
GHG	Greenhouse gas emission
H_2O	Water
HRS	Hydrogen refuelling station
KOH	Potassium hydroxide
LED	Light emitting diode
Ni	Nickle
PEL	Power Engineering Laboratory
PEM	Proton exchange membrane
RES	Renewable energy sources
U-I	Electrical current-voltage
UNIZAG FSB	University of Zagreb, Faculty of Mechanical Engineering and Naval Architecture

ABSTRACT

In this doctoral dissertation, the influence of the magnetic and optical fields on the process of alkaline water electrolysis has been analysed. For that purpose, an experimental setup was designed and an electrolyzer was constructed. In the scope of the research implementation of the nickel (Ni) foam electrodes instead of smooth surface Ni electrodes was analysed. Based on the experimental results an adjustment of the mathematical model for the calculation of energy efficiency was proposed. The results of the research have been presented in detail, and conclusions were drawn out. Positive effects of the influence of the magnetic and optical fields, as well as the application of foam electrodes are observed, which means that the original hypothesis of the research was confirmed.

Keywords: Hydrogen technologies, Alkaline electrolyzer, Magnetic field, Optical field, Ni foam electrodes

EXTENDED ABSTRACT

A development of hydrogen technologies is rapidly increasing worldwide, among which is hydrogen production in alkaline electrolyzers. The main topic of this doctoral thesis is the research of the influencing factors on the energy efficiency of the alkaline electrolyzer. The analysed influencing factors include the application of the magnetic and optical field, and an implementation of the Ni foam electrodes, respectively.

The first chapter of the doctoral dissertation is INTRODUCTION. In this chapter it was given a view on the energy transition from a fossil fuel-based economy to the hydrogen-based economy, towards a carbon-neutral society. Then follows detailed analysis of the state of the art of hydrogen technologies, with a focus on the hydrogen production via alkaline water electrolysis. At the end there were given thesis objectives, hypothesis, methods, and plan of research.

Following an introduction, the chapter 2. EXPERIMENTAL RESEARCH details a description of the experimental setup. First, the application of the magnetic and optical fields is analysed. The development and design adaptation of the electrolyzer and electrodes were presented in detail. The process of measurement and data processing is elaborated, including the calculation of energy efficiency.

The next chapter is ADAPTATION OF EXPERIMENTAL RESULTS IN a MODEL where the adjusted version of the mathematical model for calculation of energy efficiency was presented. Based on the results of the experimental measurements, a model has been adjusted by using MATLAB/Simulink software.

The chapter RESULTS includes the results of the experimental research and comparison with adjusted mathematical model. The results have been analysed in detail, and conclusions were drawn out.

The final chapter is CONCLUSION in which the summary of the research was given, with elaborated results. Analysis of the confirmation of hypothesis was given and scientific contributions were listed. At the end, it was presented planned future research.

PROŠIRENI SAŽETAK

Razvoj vodikovih tehnologija u velikom je porastu diljem svijeta, među kojima je i proizvodnja vodika u alkalnim elektrolizatorima. Glavna tema ovoga doktorskoga rada je istraživanje utjecajnih čimbenika na energetsku učinkovitost alkalnoga elektrolizera. Analizirani utjecajni čimbenici uključuju primjenu magnetskoga i optičkoga polja, te primjenu elektroda od Ni pjene.

Prvo poglavlje doktorske disertacije je UVOD. U ovom poglavlju prikazan je pogled na energetsku tranziciju s gospodarstva temeljenoga na fosilnim gorivima na gospodarstvo temeljeno na vodiku, prema ugljično neutralnom društvu. Zatim slijedi detaljna analiza trenutnog stanja vodikovih tehnologija, s fokusom na proizvodnju vodika alkalnom elektrolizom vode. Na kraju su opisani ciljevi rada, hipoteza, metode, te plan istraživanja.

Nakon uvoda, u poglavlju EKSPERIMENTALNA ISTRAŽIVANJA detaljno je opisana eksperimentalna staza. Najprije je analizira primjena magnetskoga i optičkoga polja, a potom je detaljno prikazan razvoj i prilagodba dizajna elektrolizatora i elektroda. Razrađen je postupak mjerenja i obrade podataka, uključujući i proračun energetske učinkovitosti.

Sljedeće poglavlje je MATEMATIČKI MODEL gdje je prikazana prilagođena verzija matematičkoga modela za proračun energetske učinkovitosti. Na temelju rezultata eksperimentalnih mjerenja model je prilagođen korištenjem softvera MATLAB/Simulink te je prikazana uspješnost prilagodbe.

U poglavlju REZULTATI prikazani su rezultati eksperimentalnoga istraživanja koji su detaljno analizirani te su doneseni zaključci.

Završno poglavlje je ZAKLJUČAK u kojemu je dan sažetak istraživanja s razrađenim rezultatima. Opisana je analiza potvrde hipoteze s navedenim znanstvenim doprinosima istraživanja. Na samom kraju predstavljena su planirana buduća istraživanja.

1. INTRODUCTION

In a world that is steaming towards a carbon-neutral society, hydrogen technologies are recognized as an indispensable part of the global energy transition. Hydrogen can be even considered as an essential part since the ultimate goal of zero carbon dioxide (CO_2) and greenhouse gasses (GHG) emissions. In synergy with renewable energy sources (RES), hydrogen can serve as a long-term energy storage solution, enabling a great balance of the electro-energy grid [1]. Hydrogen produced by using RES is generally known as renewable/clean/green hydrogen, while hydrogen produced from fossil fuels, is know as gray or blue hydrogen. In term of green energy transition, gray and blue hydrogen are unacceptable because of enormous CO_2 emission [2]. Considering how renewable hydrogen is an excellent link to the RES, with skyrocketing investment in RES in the last twenty years, more and more investments have been made in the research and development of hydrogen technologies. The main reason for this is the maturing of awareness of the consequences of human action on the atmosphere and the environment [3]. Due to the growing problems with climate change, the need for carbon-neutral energy systems has been recognized becoming clear that clean energy has no alternative [4].

The basic principle of the utilisation of hydrogen technologies is understanding that hydrogen is not an energy source, but an energy carrier [5]. The electricity produced by RES, if cannot be utilised in the given moment, can be stored in the form of chemical energy in hydrogen by powering the process of water electrolysis, where water is split into oxygen and hydrogen [6]. The hydrogen then can be stored as a gas in high-pressure tanks, liquified in cryogenic tanks or in metal hydride storage units [7]. Then, when need for the electricity arise, hydrogen can be used in the fuel cells. In fuel cells, the chemical energy stored in hydrogen is converted back into electrical energy [8]. In the process of utilisation of hydrogen, for the storage of electrical energy, conversion from one form of energy into another (electrical energy to chemical energy), and then back from the second form to the first one (chemical energy to electrical energy), causes the losses in the process. The problem of efficiency of those two energy conversions is one of the reasons why hydrogen technologies were long time neglected. Thus, efficiency of the first energy conversion, and the ways how to increase that efficiency, is the main topic of the research of this work.

Research carried out in the scope of this doctoral dissertation was conducted in the Power Engineering Laboratory (PEL), at the University of Zagreb, Faculty of Mechanical Engineering and Naval Architecture (UNIZAG FSB). The main feature of the PEL is its extensive history of experimental research in areas of clean energy technologies [9], climate changes, materials like nickel, Ni [10], RES [11] and storage with a special focus on hydrogen technologies [12]. An autonomous hydrogen production system was developed [13], which resulted in the development of the First Croatian hydrogen-powered bicycle and First Croatian Hydrogen Refuelling Station (HRS) [14]. That HRS was installed in front of the PEL [15] and it represents one of the first pieces of hydrogen infrastructure in Croatia. The goal in the coming decades is to develop hydrogen infrastructure in Croatia [16], with PEL as the one of the few key places for generating scientific development. By adoption of the Croatian Hydrogen Strategy by 2050 (*Cro: Hrvatska strategija za vodik do 2050. godine*) by the Croatian Parliament [17], hydrogen is set to have an inclusive role in almost all energy sectors [18] and the research development will only increase [19]. By expanding knowledge of hydrogen technologies, PEL aims to stay at the forefront of Croatian hydrogen knowledge generation by researching and implementing novel technologies, such as electrochemical hydrogen compression [20].

1.1 Research overview

With the rise of global awareness of the climate change, the harmful effects of CO_2, and GHG emissions, the research in the RES and hydrogen has significantly increased all over the globe [21]. With the energy transition in full swing [22], developments in hydrogen infrastructure [23], transportation and storage [24], utilisation of RES [25], and hydrogen production [26] are bringing results as the application of hydrogen technologies is growing [27]. An interesting field of research proved to be production of the renewable hydrogen, with the main goal to increase the efficiency of the process [28] and reduce the cost of producing the hydrogen [29]. Two main types of electrolyzers, are Proton Exchange Membrane (PEM) electrolyzers [30] and Alkaline electrolyzers [31]. These technologies are more mature in comparison to other types of electrolyzers, like Solid Oxide electrolyzers, which are still mostly in the early research phase [32], [33], [34]. The research on the efficiency [35] of the alkaline water electrolysis [36], and implementation of beneficial applications [37], is ongoing and it is a main research area of this work as well.

Research of alkaline water electrolysis is primarily focused on the increase of the efficiency of the process [38] and lowering cost of the maintenance by researching the materials of the electrodes [39]. To increase energy efficiency, many influencing factors were researched [40]. These factors are temperature [41], the gap between electrodes [42], the application of different materials [43], impact of the application of ultrasound [44], fluctuating voltage [45], electrical current [46] and power supply [47], and pulsating potential [48]. The usage of three-dimensional (3D) electrodes [49] advances the research in the usage of foam electrodes [50], where the influence of pore size [51] and oxygen evolution was conducted [52]. An example of the application of the influencing factor is sunlight [53], especially if used in combination with foam electrodes [54]. For analysis of alkaline water electrolysis [56], model processes [57] and compare results with the experimental research [58], a mathematical models were adjusted [55].

Finally, amongst various innovative research, quite promising appeared to be the application of the magnetic field in alkaline water electrolysis [59]. The application of a magnetic field indicated an increase in current density [60]. Therefore, other research has been conducted to determine the level of efficiency gains in basic systems [61]. Promising initial results increased the number of studies using magnetic fields, including examining the influence of Lorentz force on multi-electrode electrolyzer systems [62] and consequently, hydrogen production [63]. This provides positive results of the usage of the magnetic field [64], by using experimental approach [65] and model adjustment [66] as the research methods [67]. Analysis of oxygen [68] and hydrogen [69] bubble evolutions further improved the knowledge about gas generation on the electrodes [70]. The main impact the magnetic field has on the alkaline water electrolyzer is the creation of Lorentz force [71]. It enhances the removal of newly generated bubbles from the surface of the electrodes [72]. Other research is focused on the strengthening of the magnetic field [73], and the application of non-uniform magnetic fields [74], with the same goal of analysing the impact on the efficiency [75]. Investigation of different cost-effective electrodes under a magnetic field [76] opens the way for combining multiple applications on the same research. Analysis of the implementation of the foam electrodes under the application of the magnetic field [77] confirmed the improvement of energy efficiency [78]. The different combinations of the two fields can be in analysis of the combining effects of the implementation of the magnetic and optical fields [79]. The last three papers served as main motivation for this research. The goal of this research is to go a step further and analyse the effects of three different applications: magnetic field, optical field, and foam electrodes.

1.2 Research objectives

Research objectives are:

1. To experimentally prove the influence of magnetic and optical fields on increasing the efficiency of the alkaline water electrolysis.

2. To adjust a mathematical model of water electrolysis, which will be used for the calculation and development of future alkaline electrolyzers.

1.3 Hypothesis

Hypothesis of the scientific research is:

"The application of an external magnetic and optical field to the process of alkaline water electrolysis increases the efficiency of the alkaline electrolyzer with Ni foam electrodes."

This hypothesis was tested by conducting experimental research on laboratory-made alkaline electrolyzer.

1.4 Research methods

Two main research methods used in this scientific research were experimental research and mathematical modelling. The focus is placed on experimental research, with the design of the alkaline electrolyzer. The secondary research method is the adjustment of existing mathematical modelling for the alkaline electrolyzer with the implementation of the effects of the magnetic and optical field on the process.

1.4.1 Experimental research

The most accurate way to prove or disprove the defined hypothesis is to test it on the electrolyzer. Therefore, the experimental research was chosen to be the main method of research. All experimental work was conducted in the PEL of the UNZAG FSB. An essential part of the experiment was the development of the alkaline electrolyzer. The final design of the electrolyzer was created after initial research with less complex equipment. Alongside the development of the electrolyzer, the whole experimental setup was developed, including power

equipment, connection equipment, measurement equipment, recording and analysing equipment to protection equipment.

1.4.2 Mathematical modelling

Since experimental research cannot provide results for more than a few chosen points under specific parameters, a mathematical model was adjusted to analyse any point of interest between those tested in the experiment. It represents a secondary research method in the overall scope of this thesis. The model presents an adjustment of the existing mathematical model that describes the calculation of the efficiency of the alkaline water electrolysis process. Its main purpose is to simplify and intensify the development of future alkaline electrolyzers with the application of magnetic and optical fields.

1.5 Research plan

The research plan was developed under the mentorship of Assoc. Prof. Ankica Kovač. The plan was designed to optimise the complex design of the experimental setup in each time period. It is divided according to the following basic points:

1. Introduction to the physical basis of the field of research of water electrolysis and alkaline electrolyzer through experimental work and theoretical research. Since this work is based on experimental research, for the preparation of the doctoral thesis it was necessary to get acquainted with the work in the laboratory, the basics of experimental setup, and the development of experimental work.

2. Development of an alkaline electrolyzer with smooth surface Ni electrodes, complete experimental setup with the appropriate measuring devices, and conduction of the first experimental research. Processing and analysing measurement data and results on the basic concept is a major step in developing the main experimental setup.

3. Introduction of an external source of magnetic field using permanent neodymium magnets or electromagnets, that create an intense magnetic field in the interelectrode space of the electrolyzer. The basic premise of the success of the implementation of the experimental work is to enable the overlap of the magnetic field and the interelectrode space between the two electrodes, which will enable the creation of the Lorentz force.

4. Application of external green light to the process of water electrolysis: It is necessary to provide such a design that will allow the action of spectral radiation on the interelectrode space where bubbles of hydrogen and oxygen gases are formed.

5. Application of Ni foam electrodes instead of smooth surface Ni electrodes with which initial experiments were to be performed. That will ensure a change in the geometric structure of the electrodes by providing a larger contact surface between the electrolyte and the electrode surface.

6. Development of the adequate design of electrolyzer, design of the experimental setup, and conduction of experiments, including data collection and processing, and the subsequent analysis of the impact of its combined effect on the process.

7. Adjustment of a mathematical model to perform separate analyses to be compared with the results of the experiment.

8. Writing a doctoral dissertation with detailed description of the experiment and installation of the experimental setup ensuring the reproducibility of the experiments. It also includes presentation and analysis of experimental results and their comparison with the results of the adjusted mathematical model, together with analysis of confirmation/refutation of the hypothesis with the analysis of the achieved objectives.

2. EXPERIMENTAL RESEARCH

Experimental research is the main method of research of this doctoral thesis. Therefore, great care is placed on the design of the experimental setup and conduction of the experiments. An essential part of the experimental setup is an alkaline electrolyzer. As stated in the hypothesis, the influence of magnetic and optical fields on the process of water electrolysis was analysed. While the application of the optical field is relatively easy to implement in the design of the electrolyzer, the implementation of the directed magnetic field is quite problematic from the construction side. A request of having magnetic field withing the electrolyzer has great impact on the shape and overall geometry of the electrolyzer. For that reason, external fields applied in experiments with accompanying equipment are described in detail.

Additional equipment consists of power and connection elements and measurement equipment. Since scientific research is a *live* process, the experimental setup was changing and growing during the research, becoming ever bigger and more complex. In the last part of this chapter, the experiment was explained in detail.

2.1 Magnetic field

Application of the magnetic field in the electrolyzer proved to be a challenging task. First, the application of the magnetic field created engineering problems since the usage of ferromagnetic materials is limited if not completely avoided in the vicinity of the magnetic field. That effectively eliminated option of using commercially available alkaline electrolyzers in the research and the focus shifted towards laboratory-made electrolyzer. The second problem was sheer inexperience in dealing with magnets and magnetic fields. This meant slowly introduction of magnets and the application of neodymium permanent magnets in the first phase of the research. Based on initial experiments, it was concluded that permanent magnets cannot create sufficient magnetic fields, and only the implementation of electromagnets will enable creation of the magnetic fields with better properties, which proved correct.

Over the course of the research, conflicting aims in the design clashes:

- the goal to increase the strength of the magnetic field imply a reduction of the space between the north and south pole of magnets, while on the other hand

- construction of the electrolyzer demand as much space as it can get for better properties of the construction.

Maintaining the constant directed magnetic field also proved to be no easy task, as magnets facing opposite poles have the intention to connect, creating strong forces between them. To prevent connection, the geometry of the apparatus that is used should enable movement for easier operation and handling, and at the same time security for the operator and equipment.

2.1.1 Permanent magnets

The first conclusive research was conducted with permanent magnets in the shape of cubes of 25x25x25 mm. Since experiments demand the ability to apply and remove magnetic fields, the magnet's application must be portable and easily accessible. In that purpose magnet's adjustable holding device was made. It was made of wood, aluminium, and copper, with iron plates, intended for keeping magnets separated one from another. The magnets were set into positions with opposite poles facing each other. Since the force that is keeping magnets connected to the iron plates is stronger than those of their mutual attraction, a stable inhomogeneous magnetic field was created between them. Distance between magnets can be manually adjusted. With the reduction of the distance between magnets two observations emerged: First, the magnetic flux density of the field increased, and second, the field became more homogeneous. Measurements of the magnetic field were conducted with laboratory-made Hall sensor and were described in the later subchapters. The other way to increase the magnetic flux density of the magnetic field by permanent magnets was the addition of a second pair of magnets. However, that proved to be insufficient as the increase was limited and the addition of the third pair would yield even smaller benefits in terms of the magnetic flux density increase.

Distance between magnets in the experiment was determined by the thickness of the upper tank of the Electrolyzer 3, used in initial experiments. Therefore, magnets were separated at 25 mm. The inhomogeneous magnetic field was measured in 3D with the Hall sensor and mapped in detail. The magnetic flux density at the surface of the magnets was approximately 630 mT, at the centre of the plate where the magnetic flux density is highest. From the centre towards the edges of the surface, magnetic flux density slightly dropped, and then plummeted near the edge of the magnet's cube. As the Hall sensor is moved away from the surface, towards the middle between two magnets, the magnetic flux density value drops. In the middle of the field, 12.5 mm forms both edges of the magnets, it reaches the minimum, with approximately 380 mT at the centre, projected to the surface of the magnets. As sensor move from the centre of the

projected plane of the magnet's surface to the projected edge of the magnet's cube, the magnetic flux density value slightly drops towards the edges and beyond, but there is no sudden drop in values like that one measured near the surface.

The created magnetic field was directed from the north face of one magnet toward the south face of the second magnet with the electrolyzer in between. More precisely, the electrodes of the electrolyzer in Electrolyzer 3 were 25 mm high and were placed so the top of the electrodes was in the same plane as the top surface of the magnets facing each other. Electrodes were also separated 25 mm one from another, therefore, creating the interelectrode space that was overlapping with the magnetic field. The combination of the magnetic and electric forces creates the Lorentz force, which is perpendicular to both (Figure 1).

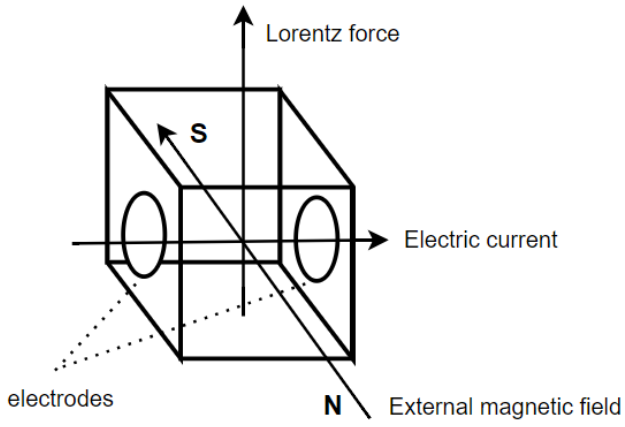

Figure 1. Visual presentation of the Lorentz force

2.1.2 Electromagnets

After analysis of the results of initial experiments with permanent magnets and Electrolyzer 3, it was confirmed that the application of magnets had a visual and a positive impact on efficiency. The results also suggested that with the increase of the magnetic flux density of the field, the increase in the efficiency of the water electrolysis is higher as well. In other words, the stronger the magnetic field the higher the efficiency increase. The main problem with permanent magnets is the lack of flexibility in the creation of magnetic fields of different strengths and shapes. To increase or decrease the strength of the field, additional pairs of magnets would be needed to add or remove. The secondary problem was the fact that the magnetic field was inhomogeneous. It *de facto* meant that with the change in the distance between magnets, the shape of the field would change, and the fields would not be compatible for comparison. Therefore, the reduction or increase of the distance between magnets was not

optional. The problem could be eliminated by the implementation of electromagnets, where the magnetic flux density of the created magnetic field could be regulated by the electrical current in the coils.

For the research the electromagnet AGEM 5520 of Schwarzbeck Mess-Elektronik was acquired. Electromagnets can generate strong magnetic fields above 2 T. It was designed for experimental applications. Depending on the required magnetic flux density, the air gap between poles can be adjusted continuously. The magnet poles come with a partial conical shape that is close to the test volume. This is to improve accessibility and to better optimize the achievable magnetic flux density. From the safety aspect, the locking of the coils is achieved by the usage of hand levers for each coil [80]. It was purchased with a complementary power supply that was described separately later in the chapter. Its two main regulations systems were adjustable airgap between magnets and change of electrical current. Basically, by reducing the distance between magnets and increasing the electrical current on the power supply, the magnetic flux density was increasing in the test volume (Figure 2).

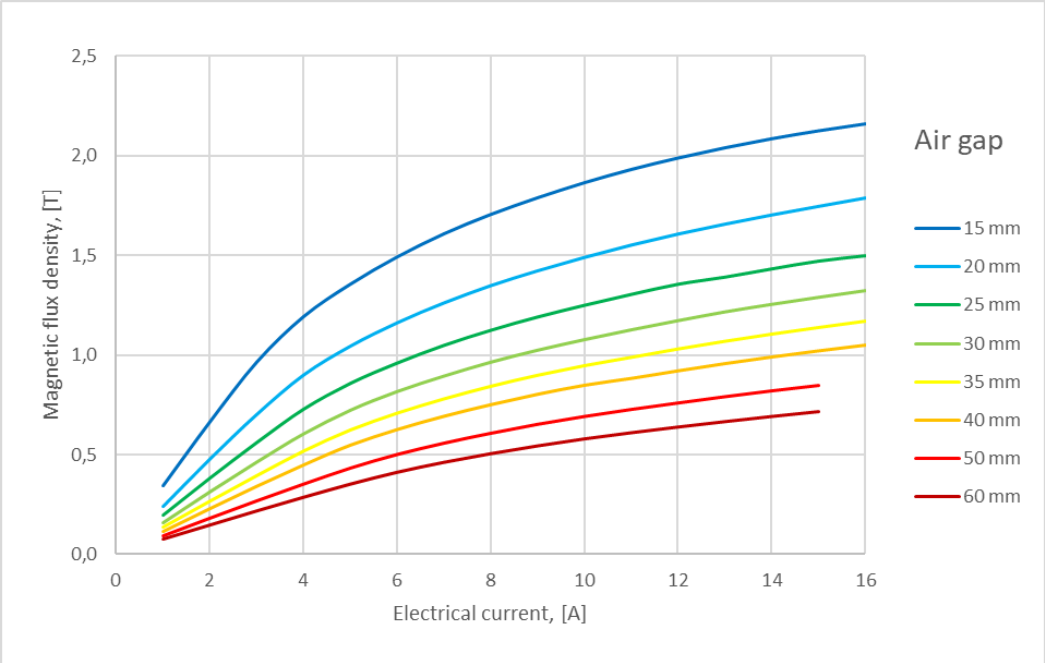

Figure 2. The magnetic flux density of the created magnetic field in the dependence of air gap between magnets and electrical current [80]

2.2 Light

The application of the optical field was introduced in the final phase of experimental research with Electrolyzer 4. Since the creation of the magnetic field was a more complex problem, the design of the electrolyzer was subordinated to it. The optical field was introduced into the electrolyzer through the integration of light-emitting diodes (LEDs). The LED light serves as an additional energy source that can positively impact the electrolysis process. When LED light is employed in the electrolysis process, it serves as more than just an additional energy source. It has several beneficial effects that optimize various aspects of the electrochemical reactions. While LEDs may not have the same energy levels as some other light sources, they still can provide influence.

One key aspect of the LED's contribution is delivery of photons with specific energy levels. As these photons are absorbed by the electrode materials, they induce a photoexcitation process, elevating electrons to higher energy states. This heightened electron activity enhances the electrochemical reactions involved in water splitting. The interaction between the LED light and the electrode materials acts as a catalyst, expediting the conversion of water into hydrogen and oxygen. Moreover, LED light tackles overpotential challenges in electrolysis. Overpotential is the extra voltage needed to start a specific electrochemical reaction. Introducing LED light uses photon energy to decrease this overpotential, making the process more energy efficient. This lowers overall energy consumption and boosts hydrogen gas production efficiency. The effects of LED light on alkaline water electrolysis extend beyond the direct contributions to energy levels. Photons, interacting with electrode materials, induce subtle yet impactful changes in surface properties. These alterations enhance the catalytic activity of the electrodes, with different light wavelengths selectively influencing these modifications. This improves the catalytic efficiency of the electrodes, optimizing reaction kinetics and further enhancing overall electrolysis efficiency. It's crucial to note that while the potential benefits of LED light are evident, optimal conditions for leveraging these effects are still under ongoing research. Factors influencing outcomes include light intensity, wavelength, and electrode material choice. Researchers are actively exploring and refining these parameters for optimal results [81].

In the scope of this research, the energy consumption of the LED was not calculated into the overall energy efficiency calculation for several reasons. First, this research is based on the research of the energy efficiency of the effects applied on the process, not overall all energy

efficiency of the electrolyzers. For example, if the study showed potential, the energy of the Sun with the application of wavelengths filters can be applied, excluding any energy consumption in the overall energy efficiency calculation. Second, neither the energy for the electromagnet is calculated for the overall energy efficiency calculation and the energy consumption of the electromagnet is by several powers larger than those of the LED. Finally, the energy consumption of the LED in the experiment is not significant for the calculation of the energy efficiency since the power consumption of the LED is by several powers lower than those of the electrolyzer. For example, the error operator is making while reading the scale of the level of the electrolyte in the upper tank, even when that reading is as precise as it can be, is by several powers more impactful on the energy efficiency calculation than exclusion of the energy consumption of the LED of the calculations. The LED was incorporated in the design of the threaded plug on the top of the upper tank in the electrolyzer (Figure 3).

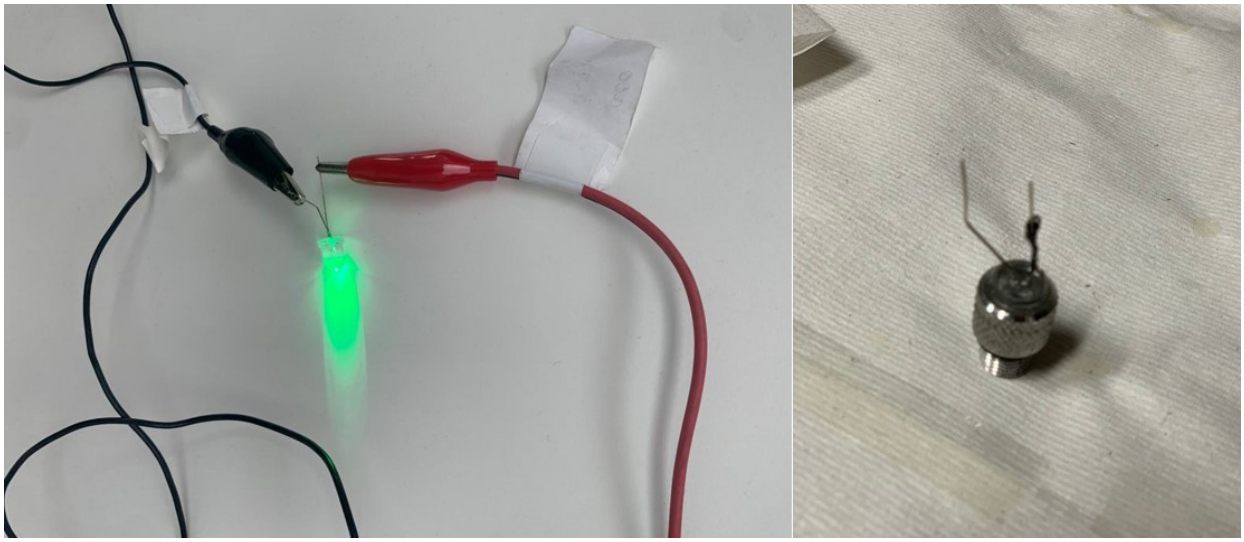

Figure 3. Testing of the LED (left) and the LED incorporated in the threaded plug (right)

The LED related to a separate power supply that was described later in the chapter.

2.3 Electrolyzer

Electrolyzer is an essential part of the experimental setup, and it is basically the centrepiece of the whole scientific research. Type of the electrolyzer is an alkaline electrolyzer with one pair of electrodes. The main demand for the design of the electrolyzer was to enable the application of the external magnetic and optic field. More precisely, the external magnetic field had to overlap with the interelectrode space, while the light created by the LED had to illuminate the

same space. The application of the latter was not as problematic as the application of the external magnetic field. Therefore, the development of the design of the electrolyzer was mainly focused on the application for the permanent neodymium magnets in the beginning, and later, electromagnets.

2.3.1 Electrodes

Electrodes used were laboratory-made, for the specific design of the used electrolyzer. There were two main types of electrodes, smooth surface Ni electrodes and Ni foam electrodes. In the scope of the research, their comparison was analysed.

2.3.1.1 Smooth Ni electrodes

In initial experiments with the Electrolyzer 3 only smooth Ni electrodes were used. Therefore, there were two types of design, depending on where were placed in the electrolyzer.

2.3.1.1.1 Smooth Ni electrodes for Electrolyzer 3

Electrodes used in the Electrolyzer 3 were connected to the electrolyzer upper tank on the bottom of the upper tank, and they were positioned vertically. The Ni plate (20x25 mm, thickness of 1 mm) was welded on the copper rod (ϕ4 mm). The *face* of the electrode was directed to the face of the opposite electrode with the intention of hydrogen and oxygen bubble generation limited only to the *face* of the electrode. For that purpose, the rest of the *body* of the electrode, including the copper rod, and the *back* and the *sides* of the Ni plate, were coated and isolated with the base-solution-resistant glue. The main feature is that the level of the interelectrode space can be adjusted in height.

2.3.1.1.2 Smooth Ni electrodes for Electrolyzer 4

Smooth Ni electrodes for Electrolyzer 4 were made of the same materials. However, there were two main differences. First, the Ni plates were smaller than in the previous version (10x20 mm, thickness of 1 mm), since the device was thinner in the upper tank (Figure 4). Second, the plate was not welded alongside the rod, but the rod was welded perpendicular to the *back* side of the plate, since in Electrolyzer 4 electrodes were in a horizontal position. Its main feature is that distance between electrodes can be adjusted. Electrodes were also coated and isolated with the base-solution-resistant glue with the exception to the *face*.

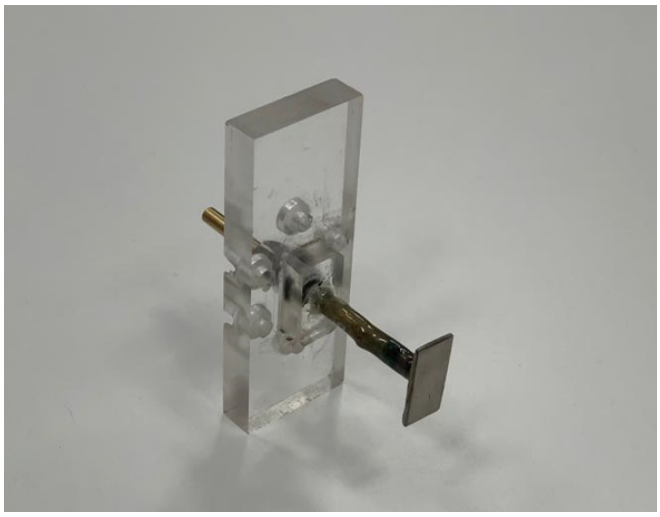

Figure 4. Smooth Ni electrode for Electrolyzer 4 on the electrode holder part

2.3.1.2 Ni foam electrodes

The Ni foam electrodes were regular smooth surface Ni electrodes with additional Ni foam elements (Figure 5). Metal foams in general, are material structures with high porosity where water solutions can reach, effectively increasing the contact surface between electrodes and electrolyte [82]. In this case, on the *face* of the smooth electrode is glued a 2 mm thick plate of Ni foam (10x20 mm, thickness of the foam 2 mm). For that purpose, the two-component epoxy glue was used, and its *sides* were coated and isolated with the base-solution-resistant glue. The duration of connection was tested in strong base solutions. Since the design of the electrodes and electrolyzers enables adjustment in the axial direction, the distance between the two electrodes can be regulated. Therefore, it was possible to adjust the volume of interelectrode space to be identical to the smooth electrodes, enabling research that would compare the efficiency of the electrolyzer depending only on the type of electrode used.

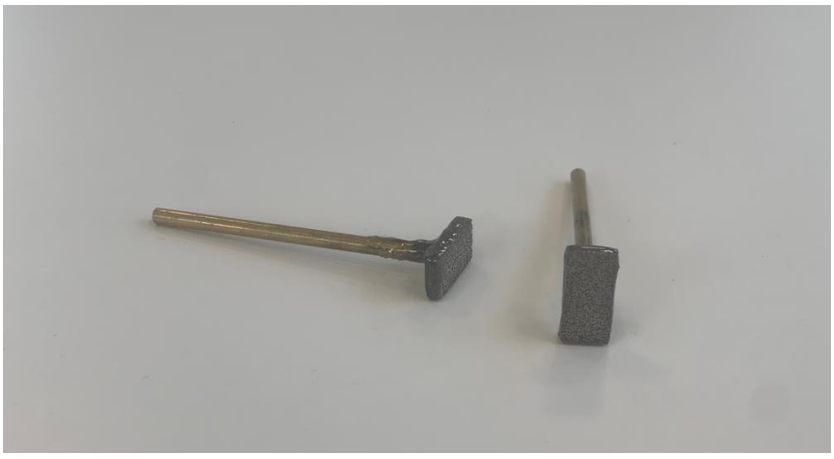

Figure 5. Ni foam electrodes

2.3.2 Electrolyte

The function of the electrolyte is the generation of an adequate environment for the transport of electrons via ions. In this research, a 25% water solution of potassium hydroxide (KOH) was used as the electrolyte. The main reason for the usage of 25% KOH water solution is the fact that in the PEL of UNIZAG FSB, 25% KOH water solution is used regularly for all experiments in alkaline water electrolysis. A new batch of electrolytes was prepared for every new set of experiments, and it was not reused in later experiments. It was always prepared on the same weighing scale, with 50 g of electrolyte and 150 g of de-ionised water, strictly following establish internal PEL's procedure. The KOH used in this research was commercially obtained and water was prepared at the Water, Fuel and Lubricant Laboratory of the UNIZAG FSB.

2.3.3 Design of the electrolyzer

As the introduction to the research, two smaller electrolyzers were designed. In the internal classification of PEL, those electrolyzers were listed as Electrolyzer 1 and Electrolyzer 2. After preliminary research, it was concluded that a bigger electrolyzer is needed for proper experiments considering the measurement of the magnetic field efficiency on the process. The third electrolyzer, Electrolyzer 3, was designed and built with the idea that an external magnetic field created by permanent magnets can be applied. Scientific research, whose results were presented at the conference, was conducted, and the idea of the application of stronger magnetic fields arose. For that purpose, the electromagnet that enabled stronger magnetic fields up to 2 T was included. In order to accommodate the usage of electromagnet the last design was built as an Electrolyzer 4.

2.3.3.1 Design of the early experimental versions of the electrolyzer

The development of the design of the early experimental versions of the electrolyzer can be easily divided into two parts. The first two versions were small-scale, easy-to-build prototypes meant to be used few times only, primarily intended for the acquisition of certain knowledge. The third version of the electrolyzer, however, was a much more complex device capable of repeated experiments on which comprehensive research can be conducted. Therefore, they are divided into pre-research and research designs.

2.3.3.1.1 Pre-research designs

To visualise the process of water electrolysis, and more importantly, the effect the application of the magnetic field has on it, the basic device was designed. The idea was to quickly design a device that will be able to visually show any differences between two processes, with and without magnets. For that purpose, Electrolyzer 1 was built. It consisted of a simple plexiglass tube with two thin electrodes connected to an electrical circuit. The wooden frame was supportive construction that was supposed to hold small magnet plates of neodymium magnets that were easy to handle. The used magnets were very small and weak, that were easy to handle and operate, but the connection force created between them at a small distance make them nearly impossible to place in the same spot. Therefore, the second design was built. Electrolyzer 2 had flat sides that were optimal for the application of the magnetic plates. It also had edges so that magnetic plates were confined in the walls, therefore reducing the chance of slipping and unsupervised connection that could result in damage and injury.

The second design proved to be adequate for the purpose it should serve. The early experiments conducted on the Electrolyzer 2 showed that there is a visible difference in the process when magnets were applied and when they were not applied. Moreover, the experimental results showed that an open design with the opening above the device will not be adequate. With higher voltage values the reaction of hydrogen and oxygen production was too intense and the drops of electrolyte were slipping out of the device.

2.3.3.1.2 Research design

With knowledge accumulated in the early experiments, the design for Electrolyzer 3 (Figure 6) was approved and the device was built. Considering only size, Electrolyzer 3 was a bigger device. Its construction consisted of two parts, the upper and the lower tank, where the upper tank was closed toward the upper surface and the lower was open to the atmosphere. They were interconnected with the small tube, ensuring that electrolytes can move from one tank to another. The upper tank was closed due to the reason that electrolyte in the upper tank does not have contact with the open atmosphere. Earlier experiments showed that bubbles of hydrogen and oxygen upon reaching the surface of the electrolyte pull micro-drops of the electrolyte into the atmosphere, therefore preventing the accurate measurement of the produced hydrogen.

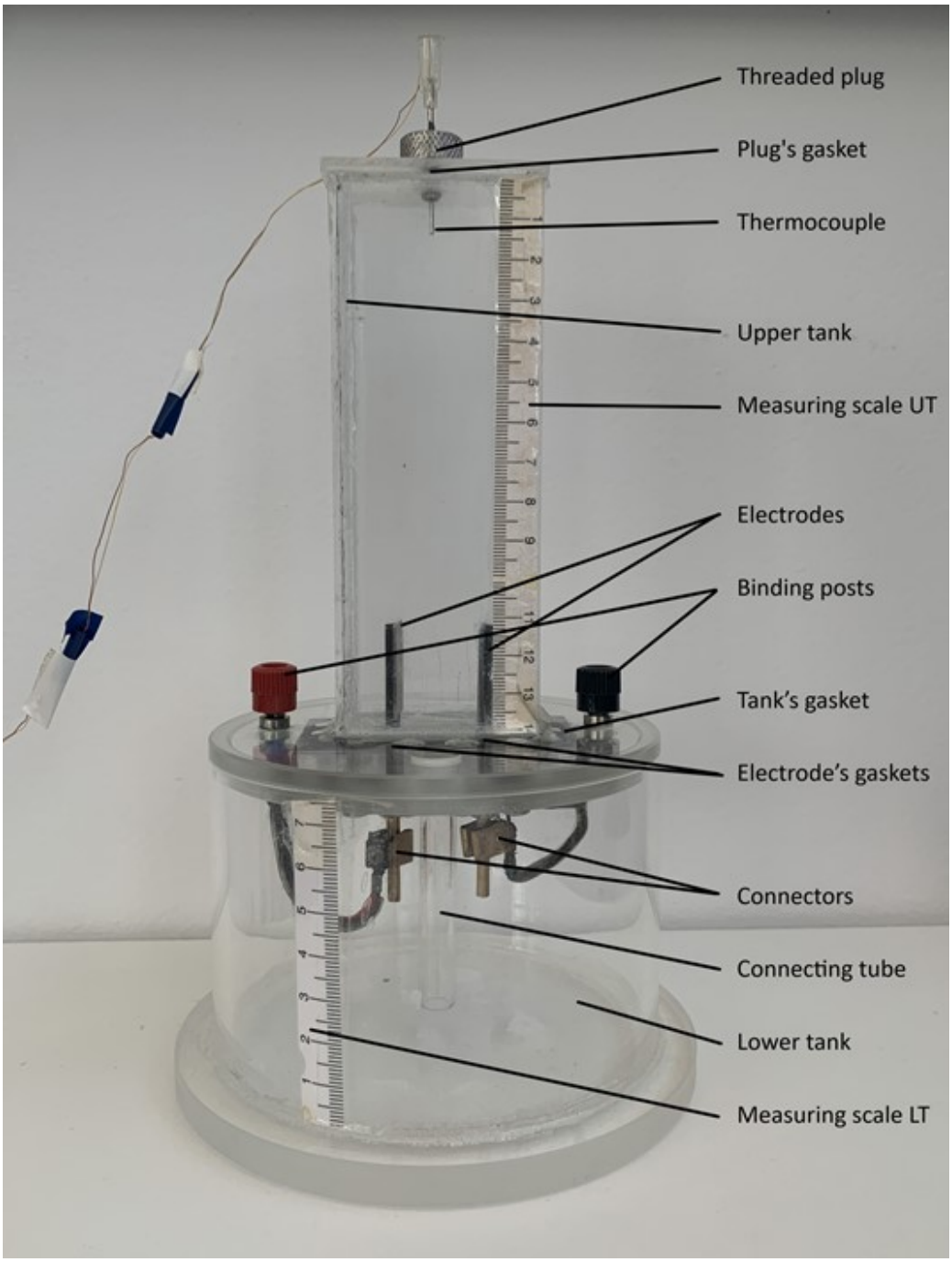

Figure 6. Electrolyzer 3

Electrolyzer housing was made of polymethyl methacrylate, commonly known as plexiglass. Sides were connected by epoxy adhesive resistant to alkaline solutions since the electrolyte used in the experiments was 25% KOH solution. On the top of the upper tank, a threaded plug with the incorporated thermocouple was inserted. The plug seat was sealed with a gasket and the thermocouple was connected to the data acquisition system (DAQ). Electrodes were inserted into the upper tank through the bottom side of the tank that also holds the tube. The bottom side was attached to the upper part of the construction with 14 stainless steel

nonmagnetic screws. All slits were sealed with gaskets, preventing the possible leaking of the electrolyte through construction connections. The lower part of the electrodes, therefore, entered the area of the lower tank via electrical connectors linked with binding posts. Binding posts were installed to enable easier connections of the electrolyzer to the electrical circuit.

2.3.3.2 Design of the final version of the electrolyzer

Experience in the work with alkaline electrolyzers and magnets the was gained, and the need for a new design of electrolyzer arose. Also, some disadvantages in the operation of the Electrolyzer 3 were noticed and set to be eliminated or reduced. Therefore, due to geometric restrictions with the implementation of new equipment, flawed design in previous versions, and new knowledge and experience gained, the final version of the electrolyzer was created. As explained before, in the Laboratory's intern classification it was listed as Electrolyzer 4 (Figure 7).

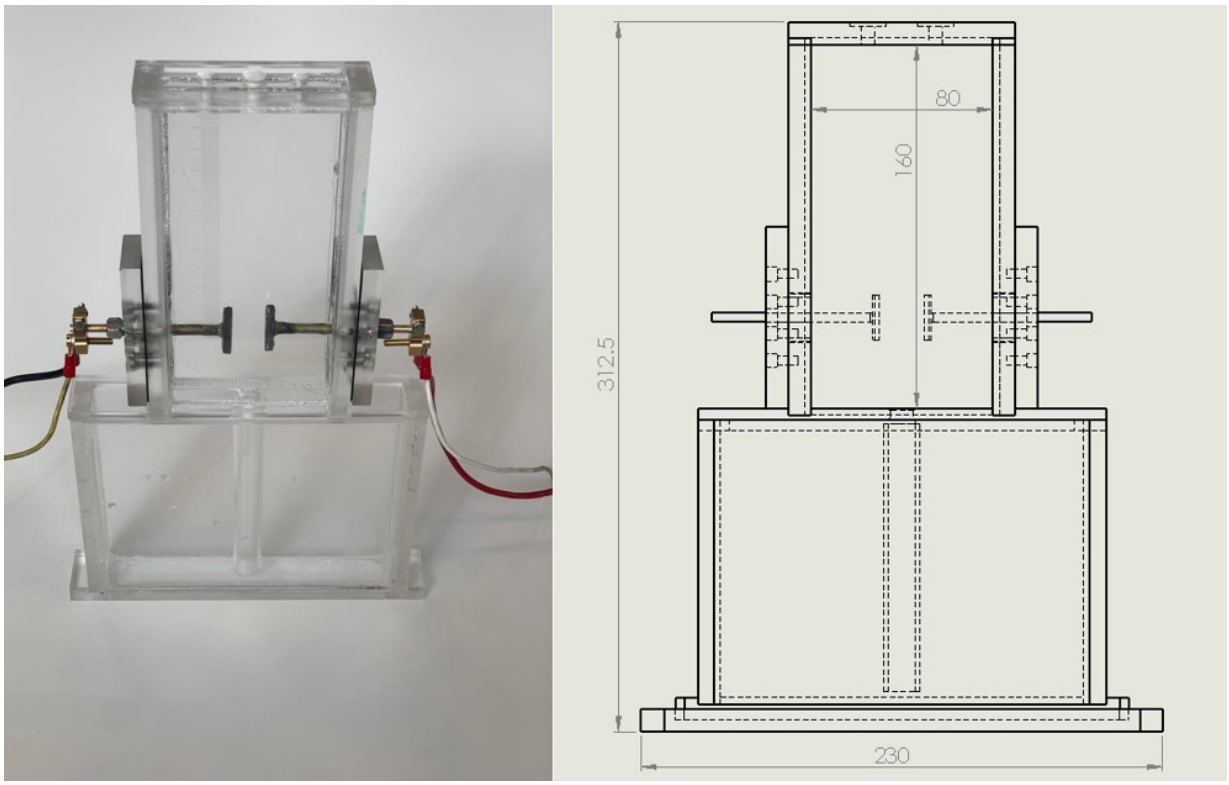

Figure 7. Electrolyzer 4

2.3.3.2.1 Geometric restrictions

For the creation of a stronger magnetic field, an electromagnet had to be used. The strength of the magnetic field depends on mainly two parameters: the electric current and the distance between two poles of electromagnets. To maximise the strength of the magnetic field that can

be created, the distance between poles was minimised, up to the safety limit of 15 mm. The limit was also conditioned by the size of the materials used for the construction of the electrolyzer. Since the electromagnet has a bulge in the shape of a partial cone (Figure 8) with a height of 7.5 mm on each coil, the available space for overall thickness was 30 mm for the rest of the construction.

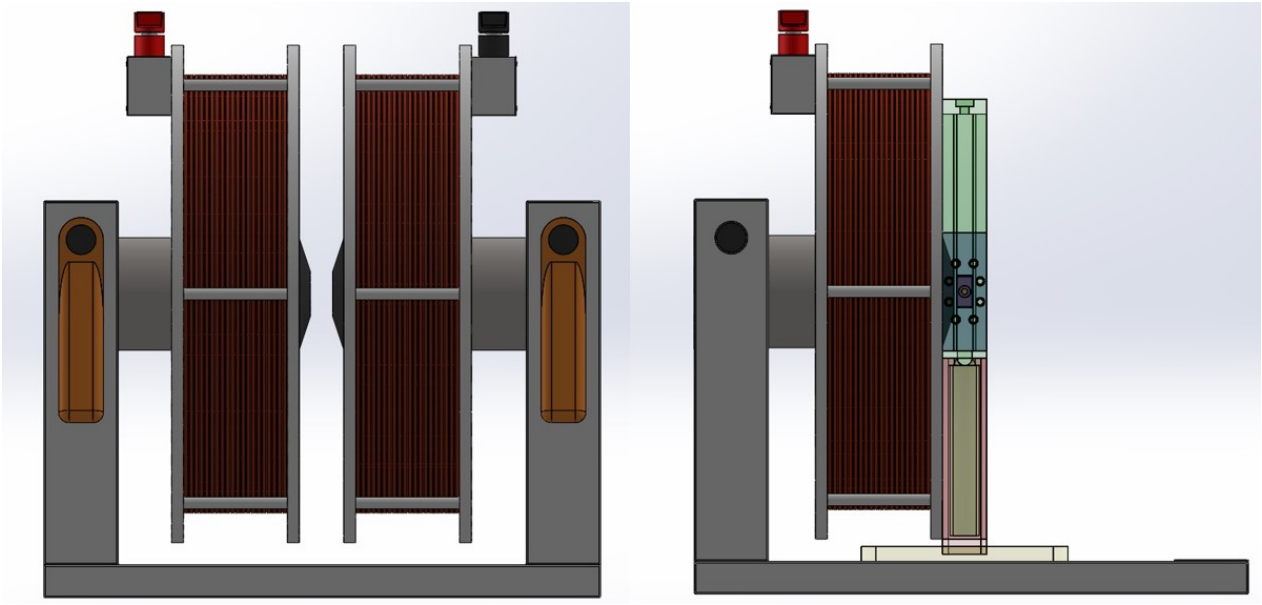

Figure 8. Model of electromagnet and placement of the electrolyzer inside of electromagnet

2.3.3.2.2 Challenges with Electrolyzer 3

There were several challenges with the design of the Electrolyzer 3 that needed to be fixed, most notably the challenge of electrodes. Electrodes in Electrolyzer 3 were positioned in the bottom of the upper tank, and they were adjustable in height. Since part of the research was a comparison of the efficiency between smooth and foam electrodes, the thickness of the foam connected to the nickel plate presented a challenge because it reduced the distance between two electrodes. In that case, the space between two foam electrodes would always yield higher efficiency due to space difference and not the other factors.

The second challenge was with the corrosion of the copper-made electrodes in the space under the upper tank. This was caused because some amount of the electrolyte was needed in the lower tank, and the lower part of electrodes were in the volume of the lower tank. Therefore, the copper rod of electrodes was exposed to the mildly corrosive atmosphere. It presented challenge since the connection with the rest of the electric circuit was realised in that space. Such design demanded a high maintenance factor and preparation for the experiment.

Therefore, the positioning of the electrodes in Electrolyzer 4 was from the sides of the upper tank, and not the bottom as in Electrolyzer 3. That enabled the movement in the axial direction and regulation of space between electrodes. It also presented easier maintenance and connection of the device with the rest of the electrical circuit.

2.3.3.2.3 Upper tank

An upper tank of the Electrolyzer 4 was the main part of the whole device. It houses electrodes and the production of hydrogen was generated there. Most of the measurements were focused on the upper tank and it was the most delicate to operate. Dimensions of the block-shaped volume inside were 180x80x11 mm, except for the small pockets of volume on the top and the bottom. Since the latter was not significant for measurements, the focus was on two pockets of volume on the top of the tank. They were created by threaded plugs for measurement purposes. First was created by the thermocouple for temperature measurement. The second pocket was an extra pocket created by the gap in the plug that enables the green light from the LED incorporated in the plug to reach the electrolyte.

The sides that lean onto electromagnets were made of 2 mm plexiglass and were retracted in the frame of the upper tank. In that way, an electrolyzer could be fitted in the electromagnet when the distance between two poles was 15 mm and between two coils 30 mm. The space between the two sides was 11 mm, and that determined the width of the electrodes. Electrodes used in the Electrolyzer 3 were 20 mm wide since the space between the two magnets was restricted to 25 mm.

2.3.3.2.4 Lower tank

The lower tank is part of the electrolyzer that holds the upper part, enabling the connection of the fluid with the atmosphere for pressure measurement. It also functions construction holder that makes it harder for the device to fall over during operation, therefore reducing the chance of damage.

2.3.3.2.5 Electrode holders

Two electrode holders are separate pieces of the Upper tank (Figure 9). Their function was to adjust electrodes in the desired position. They were intended as removable parts for easier maintenance and management of electrodes. They were connected with 6 non-magnetic stainless-steel screws with rubber gaskets to prevent leakage.

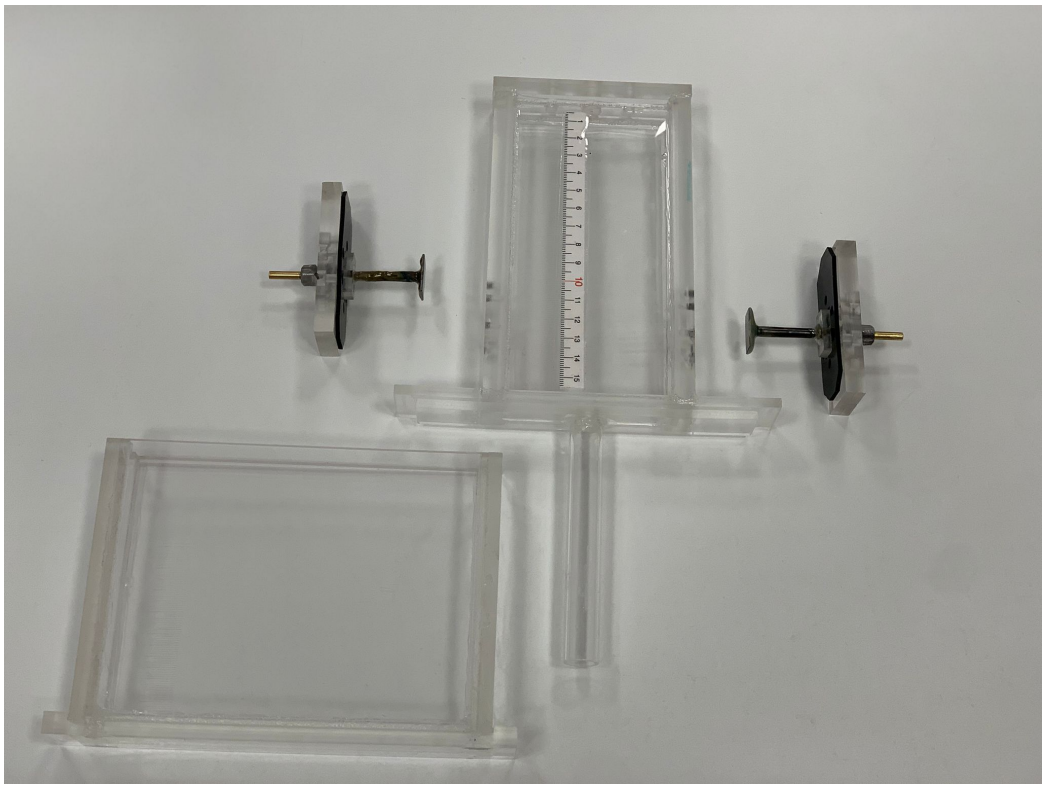

Figure 9. Main parts of Electrolyzer 4

2.3.4 Principle of operation of the alkaline electrolyzer

Considering the mode of operation, Electrolyzer 3 and Electrolyzer 4 operated on similar principles. Before the activation of the system, the upper tank was filled with the electrolyte and the lower tank was filled to the level above the end of the tube connecting both tanks. The upper tank was filled in a way that it was turned upside down and placed on a specially made holder. Then the electrolyte was poured into the upper tank up until the end of the tube. Some amount of electrolyte was poured into the lower tank, and then, by manoeuvring the upper tank in regular position, and holding the exit of the tube covered so no electrolyte spills out the electrolyzer, was completed and set in working position. When the electrolyzer was filled with electrolyte the device was set in the prepared spot. For example, if working with the electromagnet, then the electrolyzer was placed between the north and south pole of the electromagnet with interelectrode space overlapping with the directed magnetic field. When the device was positioned, electrodes were connected in the electrical circuit, according to the experimental scheme for a specific experiment.

Other supporting equipment and measurement equipment were turned and a final check before start was conducted. If analysing the electrical current-voltage (U-I) characteristic of the

electrolyzer, the measurement of the produced hydrogen was not a priority, and measurement equipment was recording needed data. For the experiment considering the efficiency of the water electrolysis process, hydrogen production measurement was critical. Therefore, the amount of hydrogen was measured by reading of the level of the electrolyte in the upper tank. Detailed calculation of energy efficiency in a single experiment was detailly described in later chapters. When the process of water electrolysis started, the production of oxygen and hydrogen was accrued on the electrodes in the upper tank. The bubbles evolved on the electrodes and when they reached the proper size they detached into electrolyte and moved towards the upper part of the upper tank. There the hydrogen and oxygen were collected and formed a block-shaped volume that was pushing the electrolyte down. A smaller volume of the electrolyte in the upper tank was used for the generation of hydrogen and oxygen, and a bigger amount was pushed into the lower tank via a tube. When was time to stop the hydrogen production, the experiment was stopped and the level of the electrolyte in the upper tank was measured.

2.4 Power and connection equipment

There were two main power sources used. For the electromagnet, a direct current (DC) power supply of 5 kW and for water electrolysis and LED multichannel laboratory power supply of smaller power.

2.4.1 Electromagnet DC power supply

For the electromagnet, Heinzinger PTN 250-20, a 5 kW DC power supply was acquired. The maximum values it can reach are 250 V and 20 A. It uses three-phase current and such electrical wiring needed to be secured. Since the whole experimental set up was located around the hand-made table, the power source had to be delivered near it. For that purpose, a laboratory power box with a three-phase current jack was constructed enabling power sources for both three-phase and one-phase equipment.

2.4.2 Three-channel DC power supply

Although it is possible to use separate power supplies for every individual purpose, during the experiment it was quite easier and more suited to have all regulatory equipment in the same place. Not only it was easier to operate the experiment and manage the changes, but it also required less space. Therefore, multichannel laboratory DC power supply Owon ODP3033 with

two channels of 30 V and 3 A and one channel for 6 V and 3 A was selected for the experiment. On one channel the power for the LED was secured via cables and connected with the crocodile connectors to the wires of the LED. The voltage was checked via voltmeter and was not recorded by DAQ. The second channel was used for the water electrolysis. It was connected to the power box, and from it connected to the electrolyzer. There was one laboratory ammeter checking the electrical current and two voltmeters checking the voltage on the electrolyzer and on the power supply. The DAQ recorded the voltage on the electrolyzer and on the power supply as well as on the resistance shunt, for electrical current measurement, which was also checked by an additional voltmeter.

2.5 Measurement equipment

Measurement is an essential part of any experimental research and without proper equipment for collecting and recording data, experimental research could not be described for scientific purposes. The data analysed in this research can be divided into two groups, depending on whether it was collected by DAQ or not. Most of the data collected by DAQ was better suited for the calculation of efficiency, while data collected by other means have another purpose.

2.5.1 Data acquisition system (DAQ)

The data acquisition system of National instruments was used for collecting and recording a large amount of data. It allows easier and continuous management of the experiment as there is no need to separately measure data. In the scope of this research, DAQ was used for collecting data about operating voltage, operating electrical current, and temperature with time recording, enabling to compare separate data as they happened in the same time. All the data was collected by registering voltage output and for values of temperatures and electrical current transformed in corresponding units.

2.5.1.1 Voltage

Measurement of the operating voltage was used in two places in the experimental setup. The main measurement of voltage was directly on the electrodes. The second connector was collecting voltage data on the power supply output. The difference between the measured units represents the electrical losses in the circuit that are not related to the electrolyzers, but other connections.

2.5.1.2 Electrical current

In the experimental setup, the third voltage measurement unit was connected to the resistance shunt of known resistance. The shunt was incorporated in the multipurpose electrical box for visual management of the processes during the experiment. Its purpose was to record values of electrical current.

2.5.1.3 Temperature

A temperature was measured in three positions. For that purpose, K-type thermocouples were used since this type is exclusively used in Laboratory. The most important measurement of the temperature was of produced electrolytic gas in the electrolyzer. That thermocouple was designed as a part of the threaded plug (Figure 10). The second thermocouple was measuring the temperature of the air inside the volume of the lower tank, above the free surface of the electrolyte while the third thermocouple was measuring the ambient temperature outside the electrolyzer.

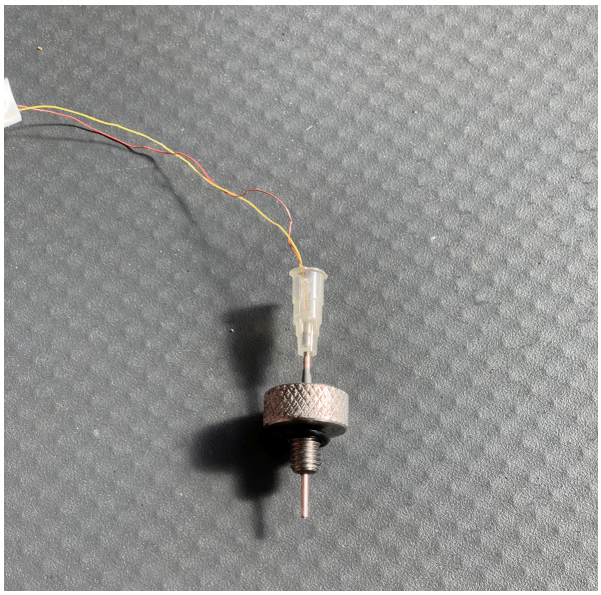

Figure 10. The K-type thermocouple incorporated in the threaded plug

2.5.2 Measurement without DAQ

Although most data used in calculations of the efficiency of the water electrolysis was collected by DAQ, for some measurements standard measurement equipment, procedures and devices were used. Reasons for the application of such devices vary. Some measurements, like visual scale reading, do not have realistic alternatives while others are easier to carry out without the usage of DAQ, like mapping of the magnetic field. However, most of the measurement

equipment during experiments was used since it was easier for the operator to rely on the data from such equipment, like handy multimeters, and act accordingly if needed.

2.5.2.1 Digital multimeters

Some multimeters were fixed parts of the experimental setups, such as the Hewlett-Packard 3478A multimeter. It was used as an ammeter for the visual control of electrical current during the experiment conduction.

Other, smaller units, like handy multimeters were used for different purposes since they were easier to change from one place in the experimental setup to the other. There were also a lot of situations where measurements were needed during testing. A wide variety of handy multimeters was used. All of them were calibrated and constantly checked during research.

2.5.2.2 Magnetic flux density measurement

For the measurement of the magnetic flux density, a laboratory-made Hall sensor was built. It was consisting of a sensor on the tip of brass made stick that has a socket for the power connection, an aluminum made box with a battery and regulation electronic, connecting cables. It was used in combination with a multimeter, which is a voltmeter (Figure 11) [83].

The low voltage output of the Hall sensor was depending on the magnetic flux density registered on the sensor. It follows the linear function (1):

$$B_{HS}\,[mT] = 5.14368\,U_{HS}\,[mV] - 51.0997 \tag{1}$$

where, the measured magnetic flux density with the Hall sensor $\boldsymbol{B_{HS}}$ is given in mT, and the output voltage of the Hall sensor $\boldsymbol{U_{HS}}$ is in mV.

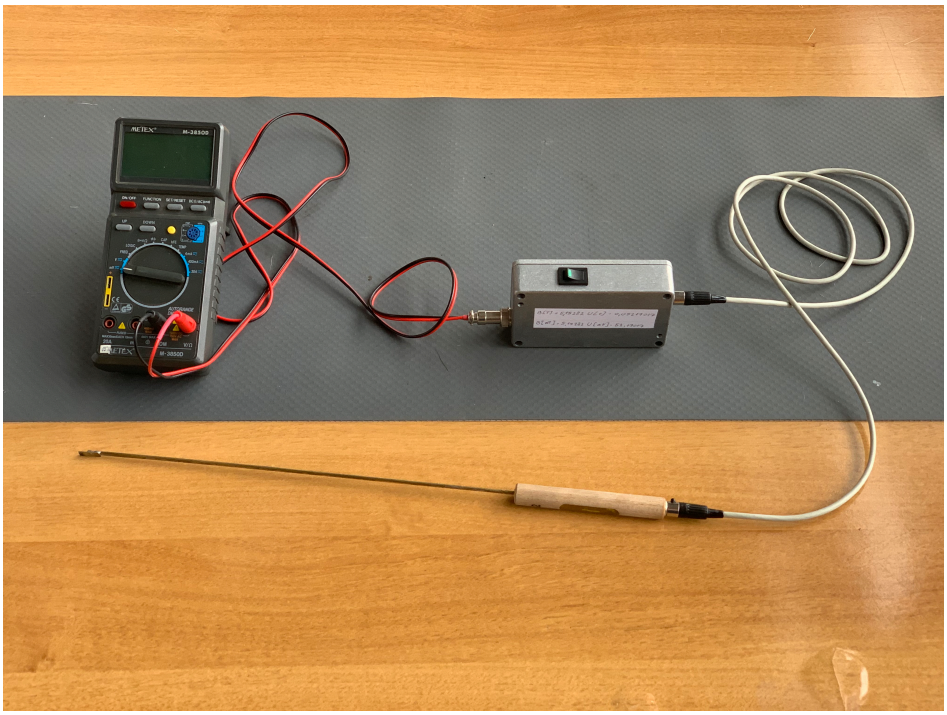

Figure 11. Setup for measurement of the magnetic flux density of the magnetic field

The sensor was not only capable of measuring the magnetic flux density, but it also measured the direction of the magnetic field. If the sensor was rotated at one point the voltage output would change depending on the side, it came across the field lines of the magnetic field. When the sensor was facing the north side of the magnetic field, and it was perpendicular to the field lines the voltage output would be maximum. When the sensor was rotated in the same spot, the voltage output would start to drop since the angle between field lines and the normal vector on the face of the sensor increased. As the sensor was rotated for 180° the output value would be minimal as the sensor was facing the south pole of the magnetic field. The referent voltage output, which indicated that there was no magnetic field in the area, was 10 mV. Therefore, if measured values were above that value, the sensor was facing the north side or any angle between the normal vector of the sensor and the fields lines that were in between 0° and 90°, while if the measured values are under 10 mV sensor is facing south side or angle between 90° and 180°. For that reason, when mapping a magnetic field, it was important to prevent the sensor from rotating and secure it so that it was always facing the north side of the field. To ensure that condition, the 3D linear translator was built (Figure 12).

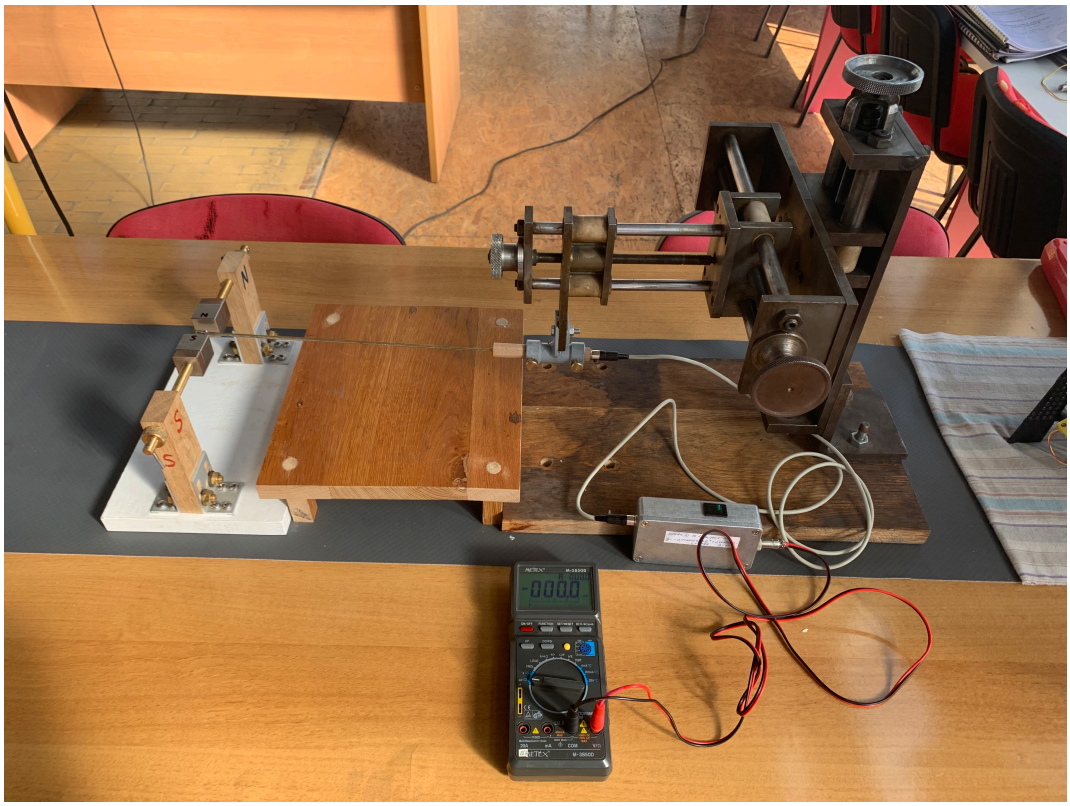

Figure 12. 3D mapping of the magnetic field with the 3D linear translator

2.5.2.3 Measurement of the barometric pressure

The barometric pressure in the experimental research was measured by hand testo 511 barometer. The measuring range of the instrument was between 300 hPa and 1200 hPa.

2.5.2.4 Hydrogen production measurement

Measurement of the produced hydrogen was done by measurement of the level of the electrolyte in the upper tank. There were two major assumptions that calculation of the hydrogen production was based on:

1. The produced electrolytic gas was the combination of hydrogen and oxygen in the mole ratio of 2:1 for the hydrogen with the additional share of water vapour in the produced gas in the electrolyzer
2. The produced electrolytic gas was on pressure and temperature near ambient conditions, and therefore the ideal gas law can be applied for calculation.

Since the geometry of the electrolyzer was known, by visual scale reading of the level of the electrolyte, the volume of the produced electrolyte gas, $\boldsymbol{V_e}$, was calculated (2):

$$V_e\ [mm^3] = A_E\ [mm^2] \cdot h_{ut}\ [mm] + V_{av}\ [mm^3]$$

(2)

where $\boldsymbol{A_E}$ is the area of the cut section of the upper tank, $\boldsymbol{h_{ut}}$ the distance between the level of the electrolyte in the upper tank and the top of the volume of the upper tank, and $\boldsymbol{V_{av}}$ the extra volume in the volume of the threaded plug for the delivery of optical field in the electrolyzer subtracted by the volume of the thermocouple incorporated in the second threaded plug.

The amount of the extra volume was $\boldsymbol{V_{av}} = 1321\ mm^3$.

The temperature of the produced electrolytic gas $\boldsymbol{T_e}$ was measured by a thermocouple in the threaded plug, and the pressure of the electrolytic gas $\boldsymbol{p_e}$ was measured by measurement of the barometric pressure in the surface of the and subtraction of the millimetre of the electrolyte (3):

$$p_e\ [Pa] = p_a\ [Pa] - \rho_e\ [kgm^{-3}] \cdot g\ [ms^{-2}] \cdot h_e\ [m]$$

(3)

where $\boldsymbol{p_a}$ is measured barometric pressure, $\boldsymbol{\rho_e}$ the density of the electrolyte used, $\boldsymbol{g}$ gravitational acceleration, and $\boldsymbol{h_e}$ the distance between the level of the electrolyte in the upper tank and the level of the electrolyte in the lower tank.

Density of the electrolyte was used for the 25% KOH water solution at the temperature of 20 °C and its amounted to $\boldsymbol{\rho_e} = 1240\ kgm^{-3}$ [84], Gravitational acceleration for the Zagreb area is $\boldsymbol{g} = 9.80665\ ms^{-2}$. Distance between levels of the electrolyte in the upper tank and lower tank $\boldsymbol{h_e}$ (Figure 13) was calculated by visual scale reading of levels by the operator and calculated (4):

$$h_e\ [mm] = h_{ae}\ [mm] - (h_{lt}\ [mm] + h_{ut}\ [mm])$$

(4)

where $\boldsymbol{h_{ae}}$ is the distance between the bottom end of the volume in the lower tank and the top of the volume in the upper tank, $\boldsymbol{h_{lt}}$ distance between the level of the electrolyte in the lower tank and the bottom of the volume of lower tank, and $\boldsymbol{h_{ut}}$ the distance between the level of the electrolyte in the upper tank and the top of the volume of the upper tank.

The value of the distance between the bottom end of the volume in the lower tank and the top of the volume in the upper tank was constant and amounted to $\boldsymbol{h_{ae}} = 287.7\ mm$.

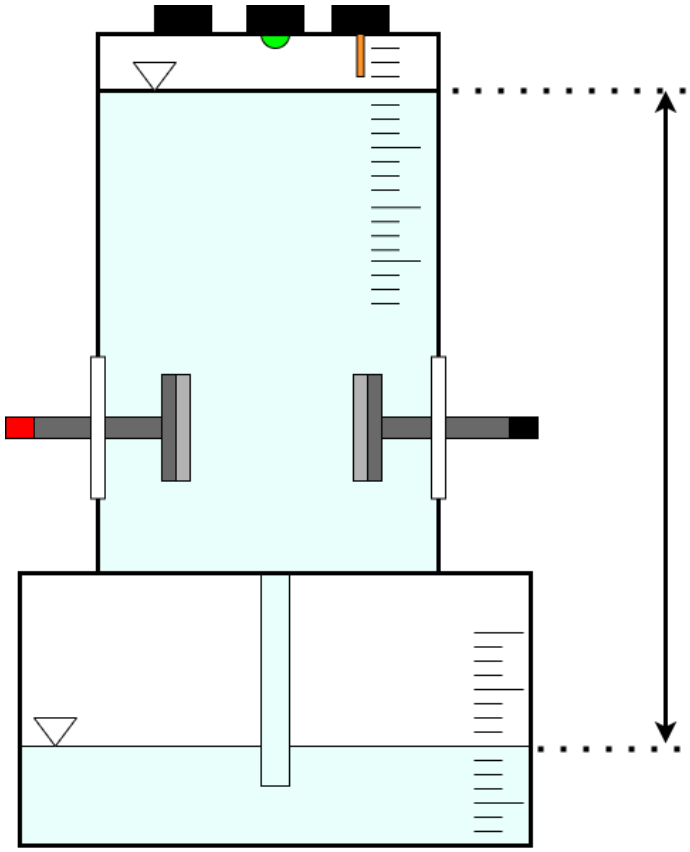

Figure 13. Schematic display of Electrolyzer 4

Since the calculation was based on the first assumption, the individual gas constant for the electrolytic gas $\boldsymbol{R_e}$ was calculated (5):

$$R_e\ [Jkg^{-1}K^{-1}] = R_{un}\ [Jmol^{-1}K^{-1}] \cdot M_e\ [kgmol^{-1}] \tag{5}$$

where $\boldsymbol{R_{un}}$ is universal gas constant and $\boldsymbol{M_e}$ the molar mass of the electrolytic gas.

Universal gas constant amounts to $\boldsymbol{R_{un}} = 8.314\ Jmol^{-1}K^{-1}$ [85]. The molar mass of the electrolytic gas $\boldsymbol{M_e}$ is also constant since the ratio of molecules of hydrogen and oxygen in the mixtures is constant 2:1, therefore it can be calculated (6):

$$M_e\ [kgmol^{-1}] = y_{H_2}\left(M_{H_2}\ [kgmol^{-1}] - M_{O_2}\ [kgmol^{-1}]\right) + M_{O_2}\ [kgmol^{-1}] \tag{6}$$

where $\boldsymbol{y_{H_2}}$ is molar share of hydrogen in the electrolytic gas, $\boldsymbol{M_{H_2}}$ molar mass of the hydrogen, and $\boldsymbol{M_{O_2}}$ molar mass of the oxygen. All values are constant. Molar share of hydrogen in electrolytic gas is consequence of 2:1 hydrogen and oxygen ratio and amounts to $\boldsymbol{y_{H_2}} = 2/3$,

the molar mass of hydrogen amounts to $\boldsymbol{M_{H_2}} = 2.0156\ gmol^{-1}$ and the molar mass of oxygen amount to $\boldsymbol{M_{O_2}} = 32.00\ gmol^{-1}$ [86].

With the data for temperature, pressure, volume, and properties of produced gas in the electrolyzer, the mass of the produced gas in the electrolyzer $\boldsymbol{m_{e'}}$ can be calculated by using the ideal gas law (7):

$$m_{e'}\,[kg] = \frac{(p_e\,[Pa] \cdot V_e\,[m^3])}{(T_e\,[K] \cdot R_e\,[Jkg^{-1}K^{-1}])} \tag{7}$$

where $\boldsymbol{p_e}$ is the pressure of the produced electrolytic gas, $\boldsymbol{V_e}$ volume of the produced electrolytic gas, $\boldsymbol{T_e}$ temperature of the produced electrolytic gas, and $\boldsymbol{R_e}$ individual gas constant of the produced electrolytic gas.

However, the produced gas in the electrolyzer is not exclusively electrolytic gas since the first major assumption indicates the existence of the water vapour in the gas. To calculate the amount of produced hydrogen, first is needed to eliminate the amount of vapour form the calculated gas. For that purpose, the mass of the vapourised water in the electrolytic gas $\boldsymbol{m_v}$ was calculated (9):

$$m_v\,[kg] = m_{e'}\,[kg]\left(\frac{M_{H_2O}\,[kgmol^{-1}]}{M_e\,[kgmol^{-1}]}\right)\left(\frac{p_s\,[Pa]}{p_e\,[Pa] - p_s\,[Pa]}\right) \tag{8}$$

where $\boldsymbol{m_{e'}}$ is the mass of the produced gas in the electrolyzer, $\boldsymbol{M_{H_2O}}$ molar mass of the vaporized water, $\boldsymbol{M_e}$ the molar mass of the electrolytic gas, $\boldsymbol{p_s}$ the saturation pressure of water, and $\boldsymbol{p_e}$ pressure of the electrolytic gas.

The saturation pressure of water $\boldsymbol{p_s}$ is not constant value and it depends on the temperature of the electrolytic gas $\boldsymbol{T_e}$. In the calculation, the saturation pressure was calculated for every measurement of temperature for specific calculation. Therefore, the values of the pressure saturation varied between 1950 kPa and 3150 kPa between individual measurements, depending on the measured temperature for those specific measurements. Consequently, the share of the mass of vapour $\boldsymbol{m_v}$ in the overall mass of the produced gas in the electrolyzer $\boldsymbol{m_{e'}}$ varied between 3% and 5%. For lower temperatures, the share was closer to 3%, and for higher it was closer to 5% [87].

After elimination of the vapour from the produced gas of the electrolyzer, the mass of the electrolytic gas $\boldsymbol{m_e}$ can be calculated (9)**:**

$$m_e\ [kg] = m_{e'}\ [kg] - m_v\ [kg] \tag{9}$$

where $\boldsymbol{m_{e'}}$ is the mass of the produced gas in the electrolyzer and $\boldsymbol{m_v}$ mass of the vapourised water in the electrolytic gas.

Since the production of hydrogen and oxygen was used in the form of water in the electrolyte, the law of the conversation of mass between water and produced electrolytic gas must be fulfilled, therefore the following applies (10):

$$m_e\ [kg] = m_w\ [kg] \tag{10}$$

where $\boldsymbol{m_e}$ is the mass of the produced electrolyte and $\boldsymbol{m_w}$ mass of used water. To calculate how much hydrogen was produced the following relation for the calculation of the mass of the produced hydrogen $\boldsymbol{m_{H_2}}$ applies (11):

$$m_{H_2}\ [kg] = m_w\ [kg] \frac{M_{H_2}\ [kgmol^{-1}]}{M_{H_2O}\ [kgmol^{-1}]} \tag{11}$$

where $\boldsymbol{m_w}$ is mass of used water which is the same amount as the mass of the produced electrolytic gas, $\boldsymbol{M_{H_2}}$ molar mass of the hydrogen, and $\boldsymbol{M_{H_2O}}$ molar mass of the water.

Molar masses are constant values. The molar mass of the hydrogen amount to $\boldsymbol{M_{H_2}} = 2.0156\ gmol^{-1}$ and molar mass of water amount to $\boldsymbol{M_{H_2O}} = 18.0153\ gmol^{-1}$ [86].

The measurement of the produced hydrogen was the most problematic in the whole experimental research since it completely relies on the skill of the operator that manages the process. The scale was engraved in the plexiglass on both tanks. It had lines for 1 mm and the objective resolution was 0.5 mm. Therefore, even the most skilled and experienced operator can make errors up to 0.25 mm in the reading. Measurement of the electrolyte levels created the biggest uncertainty in all measurements in the experiments which were analysed and described in a later subchapter in detail.

2.5.3 Measurement uncertainty

The source of measurement uncertainty can vary from the instruments used, object of measurement, conditions of measurement, method of measurement, the skill of the operator, and others. Since in the experimental research, there are numerous measurement positions, every measurement unit set for calculation was measured once. Type B of measurement uncertainty with squared distribution was used for the calculation of the measurement uncertainty (12):

$$u^2 = \frac{1}{3}\, a^2 \tag{12}$$

where $\boldsymbol{u}$ is measurement uncertainty and $\boldsymbol{a}$ the difference between the threshold values determined by specific factors for every type of measurement.

2.5.3.1 Measurement uncertainty of the voltage measurement

Before the measurement of the voltage via DAQ, the test was conducted in the Laboratory with the measurement of the same voltage via three additional voltmeters. The values of the measurement showed that all instruments were measuring the same value, only different resolutions of the instruments. Therefore, it was concluded that measurement via DAQ is reliable enough for the conduction of the experiments. For the calculation of measurement uncertainty for the voltage measurement $\boldsymbol{u_U}$, the value of the difference between the threshold values $\boldsymbol{a_U}$ was determent to be the 0.01 V, since it was the value of the resolution of the instrument with the lowest resolution done in testing. Therefore, the measurement uncertainty for the voltage measurement $\boldsymbol{u_U}$ was calculated (13):

$$u_U^2 = \frac{1}{3}\, a_U^2 \tag{13}$$

where $\boldsymbol{u_U}$ is the measurement uncertainty of the voltage measurement and $\boldsymbol{a_U}$ the difference between the threshold values for voltage measurement.

Since $\boldsymbol{a_U}$ was determent to amount to 0.01 V, the measurement uncertainty of the voltage measurement $\boldsymbol{u_U}$ was calculated to 0.0057735 V.

2.5.3.2 Measurement uncertainty of the electrical current measurement

Before the measurement of the electrical current via DAQ, the test was conducted in the Laboratory with the measurement of the same electrical current via two additional ammeters. The values of the measurement showed that all instruments were measuring the same value, only different resolutions of the instruments. Therefore, it was concluded that measurement via DAQ is reliable enough for the conduction of the experiments. For the calculation of measurement uncertainty for the electrical current measurement $\boldsymbol{u_I}$, the value of the difference between the threshold values $\boldsymbol{a_I}$ was determent to be the 0.001 A, since it was the value of the resolution of the instrument with the lowest resolution done in testing. Therefore, the measurement uncertainty for the electrical current measurement $\boldsymbol{u_I}$ was calculated (14):

$$u_I^2 = \frac{1}{3}\, a_I^2 \tag{14}$$

where $\boldsymbol{u_I}$ is measurement uncertainty of the electrical current measurement and $\boldsymbol{a_I}$ the difference between the threshold values for electrical current measurement.

Since $\boldsymbol{a_I}$ was determent to amount to 0.001 A, the measurement uncertainty of the electrical current measurement $\boldsymbol{u_I}$ was calculated to be 0.0005774 A.

2.5.3.3 Measurement uncertainty of the temperature measurement

Before the measurement of the temperature via DAQ, it was conducted calibration in the Process Measurement Laboratory of UNIZAG FSB. The maximum correction of the referent value was 0.07 °C. Therefore, it was concluded that measurement via DAQ is reliable enough for the conduction of the experimental research. For the calculation of measurement uncertainty for the temperature measurement $\boldsymbol{u_T}$, the value of the difference between the threshold values $\boldsymbol{a_T}$ was determent to be the 0.07 °C. Therefore, the measurement uncertainty for the temperature measurement $\boldsymbol{u_T}$ was calculated (15):

$$u_T^2 = \frac{1}{3}\, a_T^2 \tag{15}$$

where $\boldsymbol{u_T}$ is measurement uncertainty of the temperature measurement and $\boldsymbol{a_T}$ the difference between the threshold values for temperature measurement.

Since $\boldsymbol{a_T}$ was determent to amount to 0.07 °C, the measurement uncertainty of the temperature measurement $\boldsymbol{u_T}$ was calculated to be 0.0404 °C.

2.5.3.4 Measurement uncertainty of the barometric pressure measurement

The manufacturer of the barometric pressure measurement instrument used in the experimental research stated that the permissible tolerance of the instrument is 300 Pa. However, in the process of the calibration with the mercury barometer, the results were not crossing the 60 Pa difference, with the resolution of the device being 100 Pa. For the calculation of measurement uncertainty for the barometric pressure measurement $\boldsymbol{u_p}$, the value of the difference between the threshold values $\boldsymbol{a_p}$ was determent to be 100 Pa. Therefore, the measurement uncertainty for the barometric pressure measurement $\boldsymbol{u_p}$ was calculated (16):

$$u_p^2 = \frac{1}{3}\, a_p^2 \tag{16}$$

where $\boldsymbol{u_p}$ is measurement uncertainty of the barometric pressure measurement and $\boldsymbol{a_p}$ the difference between the threshold values for barometric pressure measurement.

Since $\boldsymbol{a_p}$ was determent to amount to 100 Pa, the measurement uncertainty of the electrical current measurement $\boldsymbol{u_p}$ was calculated to be 57.7 Pa.

2.5.3.5 Measurement uncertainty of the level of the electrolyte measurement

The scale used for the measurement of the level of the electrolyte in both tanks had a resolution of 1 mm. However, it was possible to read the values in the resolution of 0.5 mm. Therefore, the maximum error that can be taken in the reading of the value was 0.25 mm. For the calculation of measurement uncertainty for the level of the electrolyte measurement $\boldsymbol{u_h}$, the value of the difference between the threshold values $\boldsymbol{a_h}$ was determent to be the 0.25 mm. Therefore, the measurement uncertainty for the level of the electrolyte measurement $\boldsymbol{u_h}$ was calculated (17):

$$u_h^2 = \frac{1}{3}\, a_h^2 \tag{17}$$

where $\boldsymbol{u_h}$ is measurement uncertainty of the level of the electrolyte measurement and $\boldsymbol{a_h}$ the difference between the threshold values for the level of the electrolyte measurement.

Since $\boldsymbol{a_h}$ was determent to amount to 0.25 mm, the measurement uncertainty of the level of the electrolyte measurement $\boldsymbol{u_h}$ was calculated to be 0.144 mm.

2.5.3.6 Influence of the measurement uncertainty on the error of the calculated energy efficiency

To determine how significant an error in the calculation of energy efficiency is, the implementation of the maximum uncertainty was analysed on the example for the one individual experiment. For example, the experiment on smooth electrodes without the application of the magnetic or optical field was analysed. For the analysis, the *worst-case scenario* was applied with the goal to increase efficiency. The measured data of the experiment is given in **Table 1**, alongside information about the amount of measurement uncertainty and corresponding values when applied.

Table 1. Data of the individual experiment and measurement uncertainty with goal to increase the energy efficiency

	Property	**Values**	**Measurement uncertainty**	**Values after applying uncertainty**
	Electrodes	Smooth	-	
	Magnetic field	not applied	-	
	LED	not applied	-	
Values measured before the experiment	Level of electrolyte in upper tank	59.00 mm	±0.144 mm	58.856 mm
	Level of electrolyte in lower tank	43.50 mm	±0.144 mm	43.356 mm
	Temperature	22.42 °C	±0.0404 °C	22.4604 °C
	Barometric pressure	994.4 hPa	±0.577 hPa	993.823 hPa
Values measured after the experiment	Level of electrolyte in upper tank	70.50 mm	±0.144 mm	70.644 mm
	Level of electrolyte in lower tank	47.00 mm	±0.144 mm	47.144 mm
	Temperature	23.81 °C	±0.0404 °C	23.7696 °C
	Barometric pressure	993.60 hPa	±0.577 hPa	994.177 hPa
	Average voltage	2.4769 V	±0.0057735 V	2.471127 V
	Average electrical current	0.2128 A	±0.0005774 A	0.212223 A
	Energy efficiency	47.73%	-	-

The results of the analysis are presented in **Table 2**. From the analysed data it can be concluded that by far the biggest impact on the calculation of the energy efficiency has the error in the reading of the level of the electrolyte in the upper tank. In the specific experiment used for the analysis, the impact on the overall calculation can be more than 1.2%. The values can be lower or higher depending on which individual experiment is analysed, depending on the overall value of the level of the electrolyte in the upper tank. If the tank is almost full of electrolyte, the impact would be higher since the measurement uncertainty is affecting a higher part of the overall measurement, and when the tank is full of electrolytic gas, the impact is lower.

Table 2. Results of the values of energy efficiency changed after analysing the effect of the measurement efficiency with the goal to increase the efficiency

Application of measurement uncertainty	Value of energy efficiency	Difference
Original energy efficiency	**47.73%**	**0**
Level of electrolyte in upper tank	48.97%	+1.23%
Level of electrolyte in lower tank	47.73%	0.00%
Temperature	47.81%	+0.07%
Barometric pressure	48.05%	+0.31%
Voltage	47.85%	+0.11%
Electric current	47.86%	+0.13%
All uncertainties combined	**49.37%**	**+1.64%**

Of other measurements, measurement uncertainty of the barometric pressure measurement could have a significant impact as well, while other measurement uncertainties have a lower impact, with the reading of the level of the electrolyte in the lower tank basically having no impact at all. However, the measurement of barometric pressure, although having the potential to have a significant impact on calculation, in practice does not fulfil that potential. The reason for that is, that in general, most of the experiments have minimal changes in the barometric pressure before the process of the water electrolysis and after the process since the whole process is lasting 5 minutes. Therefore, if the error is in maximum values of measurement uncertainty, it would rarely be in the way the worst-case scenario is analysed.

Analog to the analysis of the *worst-case scenario* with the goal to increase efficiency, the opposite analysis was made with the goal to decrease efficiency. The measured data of the experiment is given in **Table 3**, alongside information about the amount of measurement uncertainty and corresponding values when applied.

Table 3. Data of the individual experiment and measurement uncertainty with goal to decrease the energy efficiency

	Property	Values	Measurement uncertainty	Values after applying uncertainty
	Electrodes	Smooth	-	
	Magnetic field	not applied	-	
	LED	not applied	-	
Values measured before the experiment	Level of electrolyte in upper tank	59.00 mm	±0.144 mm	59.144 mm
	Level of electrolyte in lower tank	43.50 mm	±0.144 mm	43.744 mm
	Temperature	22.42 °C	±0.0404 °C	22.3796 °C
	Barometric pressure	994.4 hPa	±0.577 hPa	994.977 hPa
Values measured after the experiment	Level of electrolyte in upper tank	70.50 mm	±0.144 mm	70.356 mm
	Level of electrolyte in lower tank	47.00 mm	±0.144 mm	46.856 mm
	Temperature	23.81 °C	±0.0404 °C	23.8504 °C
	Barometric pressure	993.60 hPa	±0.577 hPa	993.023 hPa
	Average voltage	2.4769 V	±0.0057735 V	2.482676 V
	Average electrical current	0.2128 A	±0.0005774 A	0.213377 A
	Energy efficiency	47.73%	-	-

The results of the analysis are presented in **Table 4**. From the analysed data it can be concluded that similar effects were caused by the same measurements. The measurement uncertainty of the measurement of the level of electrolyte in an upper tank had the biggest potential impact for the error in the calculation of energy efficiency. Therefore, after the analysis, the main conclusion was that the measurement of the level of the electrolyte in the upper tank is recognised as a critical measurement and specific instructions were followed by operator, with notice to give extra caution while reading the measurements of the level of the electrolyte in the upper tank. The same analogy of reading the measurement was implemented in every

measurement and more than one independent measurement was taken for every reading to minimise the potential for the error of the operator.

Table 4. Results of the energy efficiency's values changed after analysing the effect of the measurement efficiency with the goal to increase the efficiency

Application of measurement uncertainty	**Value of energy efficiency**	**Difference**
Original energy efficiency	**47.73%**	**0**
Level of electrolyte in upper tank	46.50%	-1.23%
Level of electrolyte in lower tank	47.73%	0.00%
Temperature	47.66%	-0.07%
Barometric pressure	48.05%	-0.31%
Voltage	47.62%	-0.11%
Electric current	47.42%	-0.31%
All uncertainties combined	**45.88%**	**-1.85%**

2.6 Experimental setup

For the successful realization of the experimental research, the experimental setup was designed (Figure 14). It is a simple electrical circuit with a DC power supply as an electrical source of energy and an electrolyzer as an electrical load. For better operating and monitoring conditions, a voltmeter and ammeter were installed. Its role is to help the operator keep a check on the current situation while conducting the experiment and ensure the reliability of the measured data since experiments are recorded. The DAQ simultaneously collects and records electrical current, voltage, and temperature data. The voltage of the process was measured at the binding posts of the electrolyzer, while an electrical current was measured by the measurement shunt that was implemented in the electrical circuit. Most elements of the experimental setup were positioned on or under the specially handmade heavy wooden table for the research with the electromagnet (Figure 15).

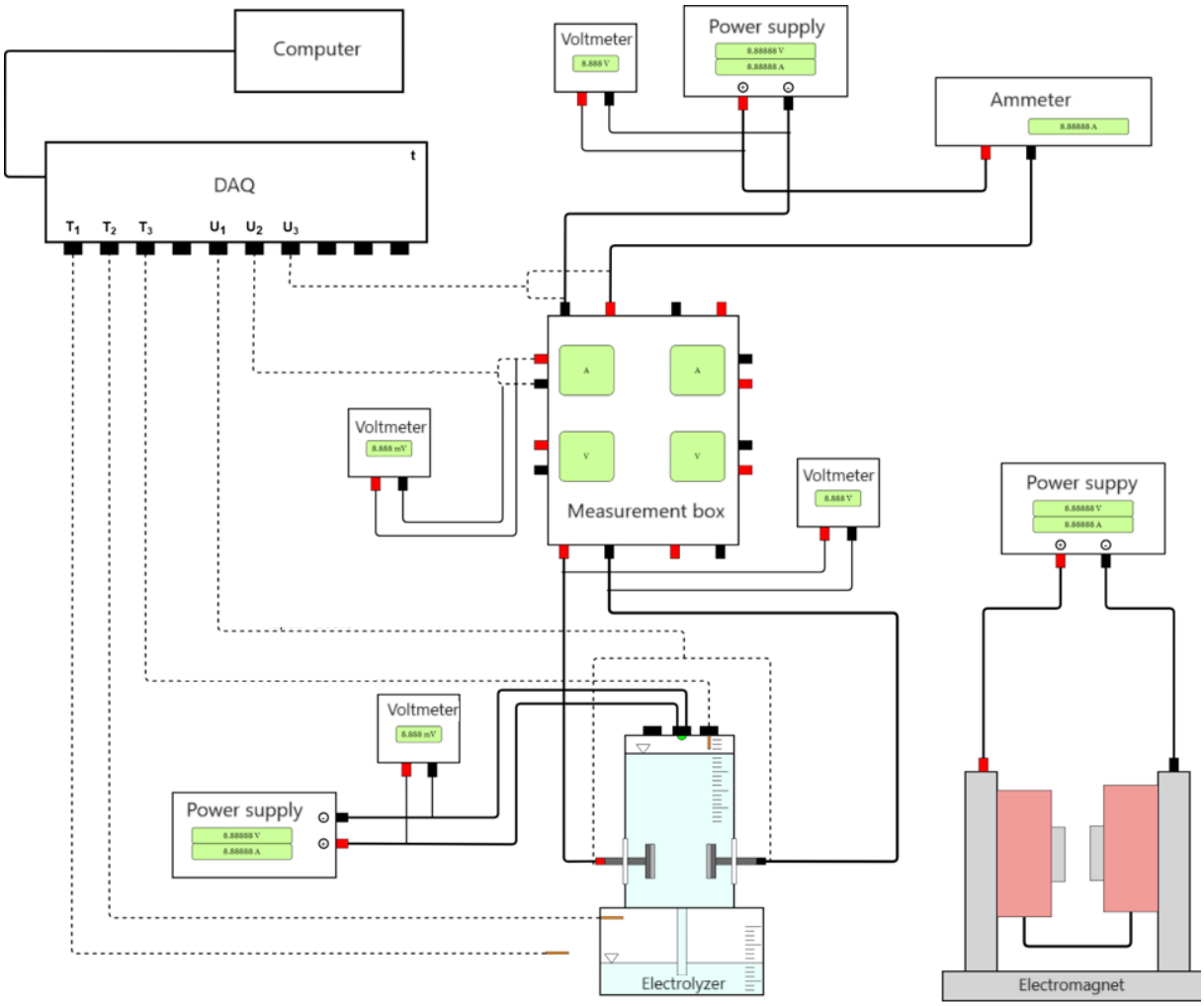

Figure 14. Schematic display of an experimental setup

The DAQ also registered temperature data, by measurement of voltage on a K-type thermocouple. There were three thermocouples installed, first measuring ambient temperature in the lower tank, second measuring temperature of produced gas in the upper tank via threaded plug thermocouple, and third recording ambient temperature around the device. The later thermocouple was incorporated into the threaded plug of the electrolyzer. The temperature of the gas was essential thermodynamic property needed for the calculation of the quantity of produced hydrogen.

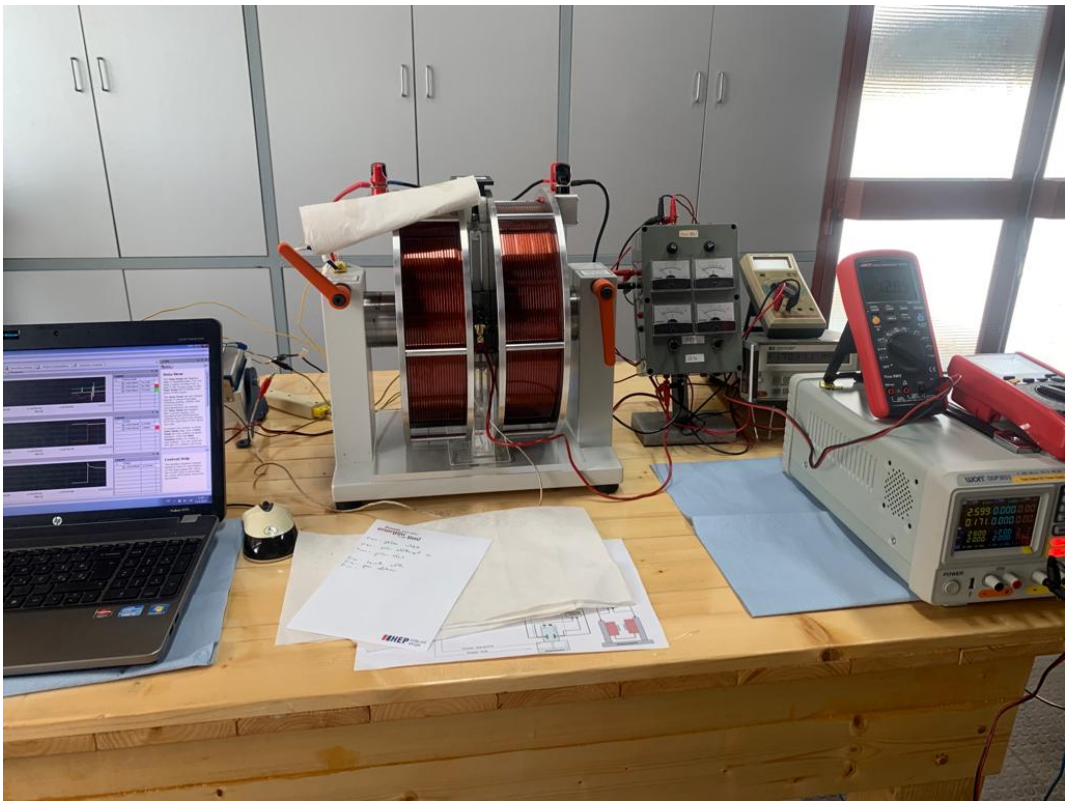

Figure 15. Experimental setup during the experimental research

Other measured thermodynamic properties used for calculation were not recorded by DAQ. The volume of the produced gas was observed from the scale. Since the cross-section of the upper tank was of known dimensions, by reading the level of the electrolyte in the upper tank, the volume was calculated. The same information was needed for the calculation of the pressure of the produced gas. In the experimental setup, there was no pressure gauge for direct measurement of the gas pressure. However, since produced gas was in direct contact with the electrolyte fluid, and electrolyte fluid was by the construction of the electrolyzer opened towards the atmosphere in the lower tank, by knowing the atmospheric pressure, the pressure of the produced gas was calculated. Therefore, the barometer was used for air pressure measurement. The main assumption in the experiment was that produced gas was the ideal mixture of hydrogen and oxygen in the 2:1 mole ratio. With the known chemical composition of the gas, the ideal gas law was implemented for the calculation of the mass of the produced gas, and later, the mass of hydrogen.

2.7 Experiment management

The main goal of the experimental research was to compare the efficiencies of the water electrolysis process depending on the influential factors. The effects of the influential factors observed in this research were:

- Implementation of Ni foam electrodes instead of smooth Ni electrodes.
- Application of the magnetic field in the interelectrode area.
- Application of the optical field in the interelectrode area.

Therefore, there were eight basic modes for electrolyzers. Other conditions should be aspired to be the same during the whole research, so their influence did not affect the results. The eight modes of the electrolyzer were:

- Smooth electrodes.
- Smooth electrodes with the magnetic field.
- Smooth electrodes with optical filed.
- Smooth electrodes with both magnetic field and optical field.
- Ni foam electrodes.
- Ni foam electrodes with the magnetic field.
- Ni foam electrodes with optical filed
- Ni foam electrodes with both magnetic field and optical field

The results of the experiments were primarily compared among each influential factor separately, but a combined analysis was also given. When considering electrodes, there were only two options to choose from, smooth Ni electrodes and Ni foam electrodes. When applying an optical field, and especially a magnetic field, there was a continuous range to set for the experiments. For example, in a separate analysis, under the same conditions experiments with different magnetic flux of the magnetic fields were conducted and analysed. But since that would create a big pool of separate conditions, in the primary analysis with eight basic modes only one magnetic field was used. The same analogy was applied to LED.

2.7.1 Aspired conditions for the conduction of the experiments

Since many known and unknown factors can affect the process of the water electrolyser, especially in experimental research on laboratory-made alkaline electrolyzers, a problem arose on how to prevent other external factors from interrupting research on energy efficiency. External factors like ambient temperature, ambient pressure, state of the electrodes, operating voltage, operating electrical current, and others have been researched to affect the energy efficiency. To prevent unwanted factors from interrupting the data, i.e., enabling only observed influential factors to impact the process, a series of preventive practices were implemented.

- To reduce the possibility of some imperfections in the electrolyzers and external conditions influencing the results, a bigger number of separate experiments were conducted. Therefore, if in one individual experiment, some unwanted factor affected the overall result, its impact was reduced or eliminated.
- To reduce the influence of environmental parameters, like the barometric pressure or ambient temperature, experiments were done in sets in a single day. Experiments included at least one individual experiment of each type so their comparison among them can be relevant. That way, the difference in external conditions was minimized, and results could be compared. Although the difference between conditions could exist among experiments of a different set, those were reduced to the minimum.
- The highest possibility of an error comes from the reading of electrolyte level due to the capillary effect of the wall of tank. Therefore, to reduce the impact of the error on the results among different experiments, all reading was done under the same principle. Therefore, if a mistake was made on one sample, it was an analogue to every other mistake in the research, therefore reducing the effect on the overall comparison.

2.7.2 Description of the individual experiment for calculation of energy efficiency

Preparations for each experiment were made the same way. Electrolyzer was cleaned and new electrodes were connected. Electrolyzer was filled up with a fresh batch of electrolytes and connected to the electrical circuit. The main switch was open, i.e., the electrical circuit was broken at that place. If used, electromagnets were turned on the pre-set value, as well as LED. Voltage for the LED was 3.4 V and it was constant for the duration of the experiment, and the voltage for the water electrolysis was adjusted to 2.5 V on the power source. Since the resistance

in the electrolyzer was variable over the duration of the experiment, the voltage slightly variated as well. The level of the electrolyte in the lower and upper tanks was measured. When everything was set, the check was conducted, DAQ turn on and settings adjusted, and the switch was lowered, and the electrical circuit connected. At that moment process of the water electrolysis started, and the generation of the bubbles of hydrogen and oxygen accordingly. The electrolyte in the upper tank soon stopped being transparent as it was filled with the small gas bubbles circulating in it before reaching the area of gas in the upper part of the upper tank. Every experiment was timed for a specific amount of time and when the time run off the switch was lifted, and the electrical circuit was broken. Electromagnet was turned off so electrolyzer could be approached. After all bubbles in the electrolyte reached the gas area at the top, the level of electrolyte in the lower and upper tanks was measured.

2.7.3 Calculation of an alkaline electrolyzer energy efficiency

In the scope of this research, a comparison of the efficiencies of the same electrolyzer was used when different conditions were applied. There were eight basic modes which can be compared, considering the usage of smooth or foam electrodes and application of magnetic and optical field, both, and none. Also, efficiencies can be compared based on the regulation of just one parameter. Since the efficiency of the regular electrolyzers solely depends on the voltage that is used for the experiment, all experiments were conducted under the same constant voltage or at least aspired to be. Therefore, the only possible option for the comparative analysis was a comparison of the energy efficiency.

2.7.3.1 Calculation of the input energy

In the calculation of energy efficiency, energy input represents electrical energy used to produce hydrogen. It was calculated by voltage and electrical current data collected via DAQ. The product of the voltage and energy current is power, but since data is collected in the time frame of every 1 second, it can be set to calculate the energy output for every second. The model was made to calculate average voltage values and average electrical current values between two recorded adjacent samples. Since the time frame was one second, the calculated power was power in the time frame of one second, i.e., energy. When all those samples were added up, the sum of small energy in every second represented the overall energy, used for hydrogen production, energy input, $\boldsymbol{E_I}$, was calculated. The procedure was basically the integration of the power input (18):

$$E_I\,[J] = \sum P_I\;[W \cdot s] = \int U_E I_E dt\;[V \cdot A \cdot s] \tag{18}$$

where $\boldsymbol{P_I}$ is power output, $\boldsymbol{U_E}$ operating voltage, and $\boldsymbol{I_E}$ operating electrical current.

2.7.3.2 Calculation of the output energy

In the calculation of the energy efficiency, energy output, $\boldsymbol{E_O}$, represents chemical energy stored in the hydrogen. It was calculated using higher heating value of hydrogen (19):

$$E_O\,[J] = m_{H_2}\,[mg]\frac{HHV_{H_2}[MJ \cdot kmol^{-1}]}{M_{H_2}[kg \cdot kmol^{-1}]} \tag{19}$$

where $\boldsymbol{m_{H_2}}$ is mass of produced hydrogen, $\boldsymbol{M_{H_2}}$ molar mass of hydrogen and $\boldsymbol{HHV_{H_2}}$ higher heating value of hydrogen [88]. For the calculation of the energy efficiency lower heating value of hydrogen $\boldsymbol{LHV_{H_2}}$ can be used as well. The efficiency of the process would be lower by ratio between $\boldsymbol{HHV_{H_2}}$ and $\boldsymbol{LHV_{H_2}}$. But, since the point of the research was a comparison of the energy efficiency between cases when were used magnetic field, optical field, Ni foam electrodes, or a combination of those parameters, it does not matter which heating value was used, since the difference will be the same. For the hydrogen higher heating values amounts to $\boldsymbol{HHV_{H_2}} = 286.18\,MJkmol^{-1}$, while lower heating value amounts to $\boldsymbol{LHV_{H_2}} = 241.1\,MJkmol^{-1}$ [86].

2.7.3.3 Calculation of the energy efficiency

After calculation of how much electrical energy was used in the process for hydrogen production and calculating how much hydrogen was produced, i.e., how much energy was stored in it, the energy efficiency $\boldsymbol{\eta_e}$ can be calculated (20):

$$\eta_e\,[\%] = 100\frac{E_O\,[J]}{E_I[J]} \tag{20}$$

where $\boldsymbol{E_O}$ is energy output, representing potential chemical energy of hydrogen and $\boldsymbol{E_I}$ energy input, representing electrical energy used for the hydrogen production.

3. ADAPTATION OF EXPERIMENTAL RESULTS IN A MODEL

In the scope of the research, a mathematical model was built using MATLAB/Simulink software [89]. The model represents the adjustment of the existing mathematical model that describes the process of alkaline water electrolysis whose purpose is to simplify and intensify the development of future alkaline electrolyzers with application of the magnetic and optical field. It was based on the calculation of energy efficiency described by equations (2)-(11) and (18)-(20). That set of equations represents the base for the model, upon which the part with the influence of external magnetic and optical fields was upgraded. Basically, the model is based on the fitting of the experimental data with second order polynomial. Considering that implementation of smooth or foam electrodes affects the results, those two cases have been considered. Moreover, the case for the implementation of the magnetic field was modelled separately from the case of the implementation of the LED. In that way, for Electrolyzer 4, four separate models were designed. The case of the electrolyzer model with smooth Ni electrodes and the application of the magnetic field was analysed in detail, while the other three cases follow the same analogy.

3.1 MATLAB/Simulink model for calculation of the effect of the magnetic and optical field on the energy efficiency of the Electrolyzer 4

A mathematical modelling was based on the calculation of energy efficiency described by equations (2)-(9) and (16)-(18). The main part of the model was developed around the calculation of energy efficiency $\boldsymbol{\eta}$ (*in Simulink:* eta) while the adjustment part, which calculate the effects of the magnetic and optical fields on the energy efficiency, was described by the function (Figure 16). The function was unique for each of the four cases and represents the variable part of the model. It is the second-degree polynomial function since it best describes the results of the experiment, calculated for the range of the magnetic flux density between 0 T and 2 T. For the model of the application of the LED, the range for it was between 2.8 V and 3.4 V.

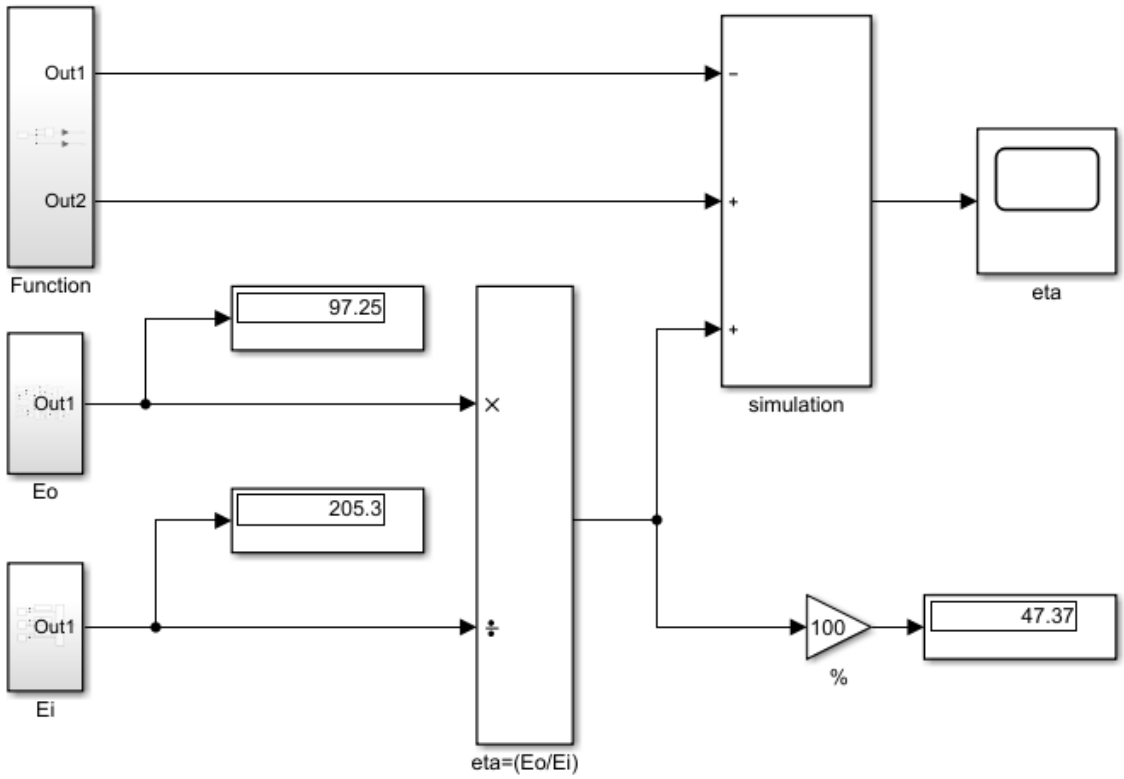

Figure 16. Mathematical model in MATLAB/Simulink for the Electrolyzer 4

3.1.1 Base of the model

In the base of the model, for calculation of the energy efficiency without application of any external field, the main division was in the subsystems for the calculation of the input energy, $\boldsymbol{E_I}$, and output energy, $\boldsymbol{E_O}$. In subsystem for energy input (Figure 17), the main equation is (18). The main difference in the model is a simplification of the way voltage and electrical current were obtained. In calculation, the power output was integrated for every second, while in the model, the average values of the voltage and the electrical current were used. The model can be expanded and additionally more developed in the future, for it, if necessary. Besides the input of voltage and electrical current in this subsystem, the third input was the duration of the experiment, more precisely, the duration of the process of the alkaline water electrolysis.

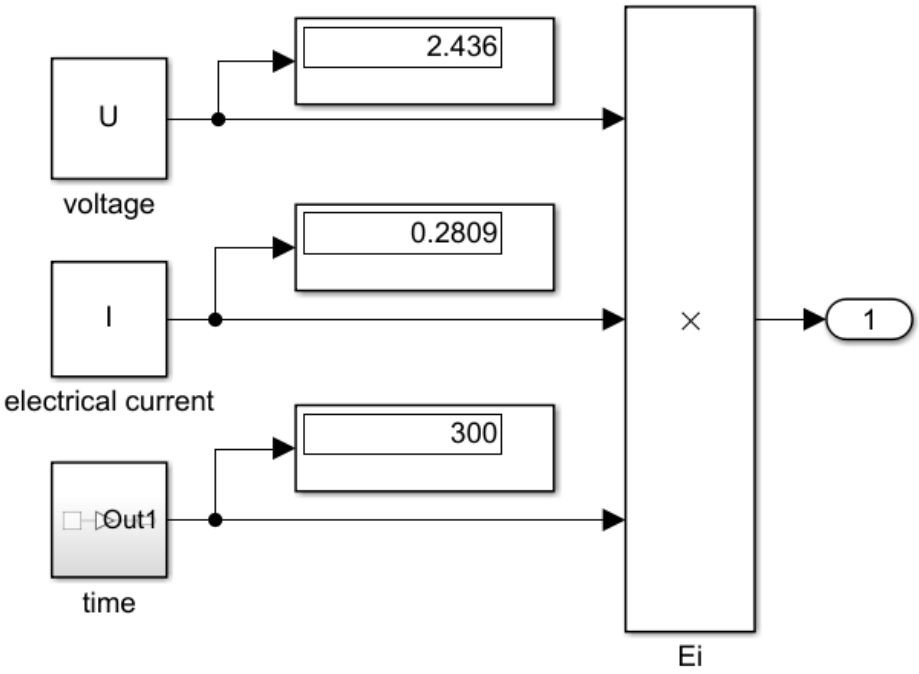

Figure 17. Subsystem of Simulink model for energy input

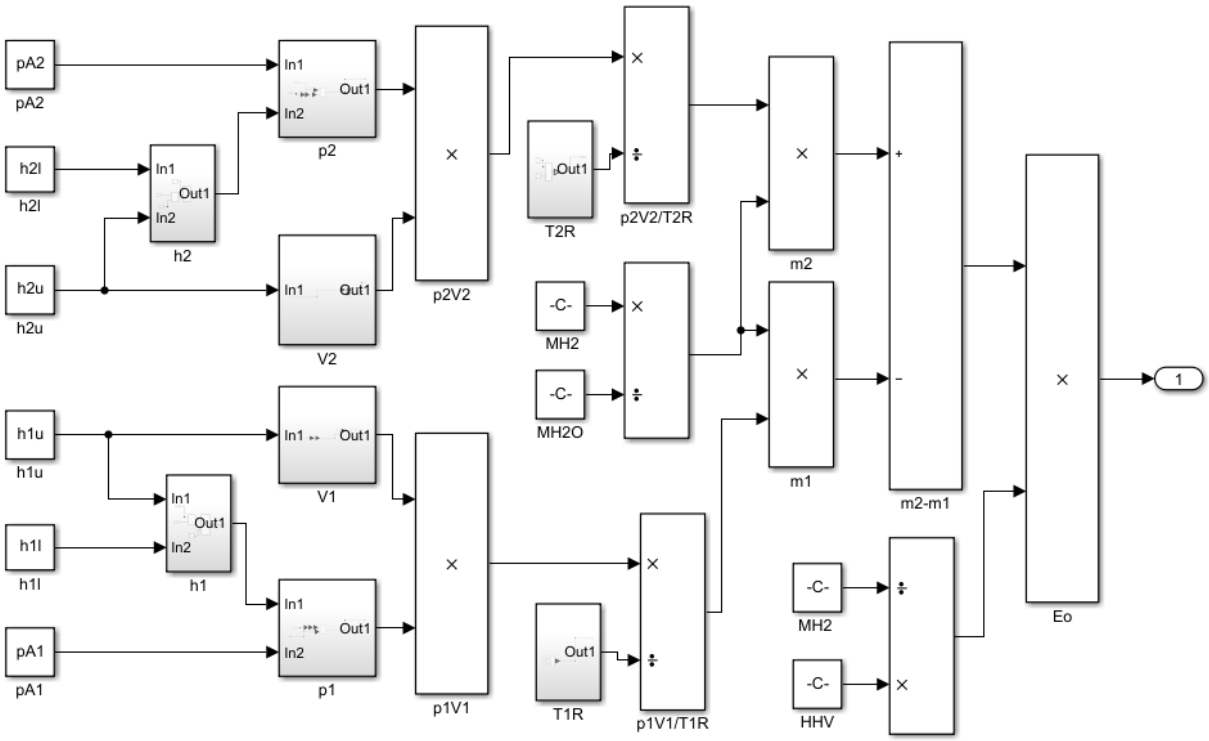

Figure 18. Subsystem of Simulink model for energy output

In subsystem of energy output (Figure 18) the main equation is (19). The system is the same as it was in the calculation. It has eight inputs: barometric pressure (in Simulink: pA), temperature (in Simulink: T) and levels of electrolyte in the upper tank (in Simulink: hu) and lower tank (in Simulink: hl). The values that were measured before have index 1, and values 2. The model can be expanded additionally if measurements of the levels of the electrolyte were to be collected during the duration of the process.

3.1.2 Variable part of the model

The variable part of the model is crucial causes it directly influences the energy efficiency of the electrolyzer. Upon a few measured points from the experimental measurements, a mathematical function was determined that best approximates results (Figure 19). It is a second-degree polynomial function. The input in the model was the whole range of the analysed value. For the magnetic field analysis, it was the magnetic flux density and for the LED it was a voltage. The range of the magnetic flux density was from 0 T to 2 T. For the LED, a voltage range was between 2.8 V and 3.4 V. In the case that voltage was decreased lower than 2.8 V the light would be very weak, barely visible, and soon non existing, while under the higher values of 3.4 V, the LED was not tested due to danger of damage on the LED. Considering the complication that the change of the LED on the equipment and the delays it would cause, potentially even completely shutting down the research, the values were limited at 3.4 V.

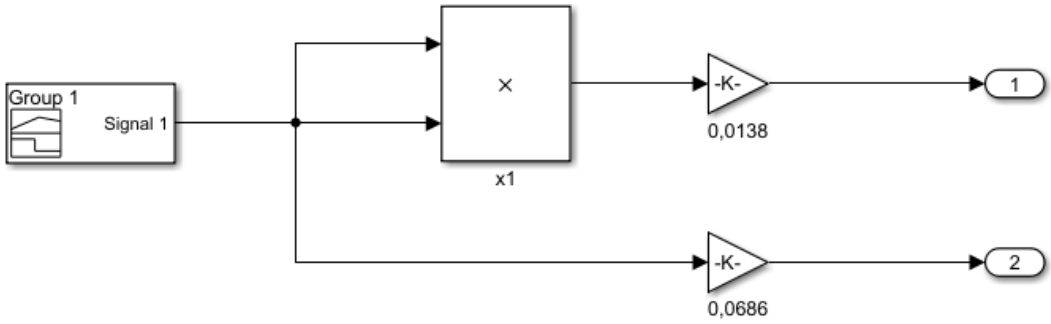

Figure 19. Variable subsystem of Simulink model with magnetic field application and smooth electrodes

3.2 Variations of the mathematical model

Since the usage of the smooth or the foam electrodes are treated as two different electrolyzers and since each applied external field is analysed separately, four different cases for the variable part of the mathematical model were made.

3.2.1 Mathematical model for case of the application of the magnetic field with smooth electrodes

For the model of the magnetic field with foam electrodes, the function in the variable subsystem of the model is (21):

$$\boldsymbol{\eta_{ms} = -0,0138\, B^2[T] + 0,0686\, B[T] + \eta_0} \tag{21}$$

where the $\boldsymbol{\eta_{ms}}$ is the resulting energy efficiency, $\boldsymbol{B}$ the magnetic field density and $\boldsymbol{\eta_0}$ the efficiency of the electrolyzer without application of the external field, calculated by the non-variable part of the model.

With the data from the experiment registered in the model, the final part was creating the linear regression signal of the magnetic flux density as an input. For the research of the application of the magnetic field, the range between 0 and 2 T was analysed. Therefore, the signal was a linear line from 0 to 2. Comparative analysis with the experimental results was discussed in the later chapter.

3.2.2 Mathematical model for other cases

All other cases were modelled analogically to the first case from the previous subchapter.

3.2.2.1 Mathematical model for case of the application of the magnetic field with foam electrodes

For the model of the magnetic field with the foam electrodes, the function in the variable subsystem of the model is (22):

$$\boldsymbol{\eta_{mf} = -0.0803\, B^2[T] + 0.1931\, B[T] + \eta_0} \tag{22}$$

where the $\boldsymbol{\eta_{mf}}$ is resulting energy efficiency, $\boldsymbol{B}$ the magnetic field density and $\boldsymbol{\eta_0}$ the efficiency of the electrolyzer without application of the external field, calculated by the non-variable part of the model.

3.2.2.2 Mathematical model for case of the application of the LED with smooth electrodes

For the model of the LED with smooth electrodes, the function in the variable subsystem of the model is (23):

$$\boldsymbol{\eta_{Ls} = 0.0088\, U_L{}^2[V] - 0.0232\, U_L[V] + \eta_0} \tag{23}$$

where the $\boldsymbol{\eta_{Ls}}$ is resulting energy efficiency, $\boldsymbol{U_L}$ the voltage applied on the LED and $\boldsymbol{\eta_0}$ the efficiency of the electrolyzer without application of the external field, calculated by the non-variable part of the model.

3.2.2.3 Mathematical model for case of the application of the LED with foam electrodes

For the model of the LED with foam electrodes, the function in the variable subsystem of the model is (24):

$$\boldsymbol{\eta_{Lf} = 0.0257\, U_L{}^2[V] - 0.0649\, U_L[V] + \eta_0} \tag{24}$$

where the $\boldsymbol{\eta_{Lf}}$ is resulting energy efficiency, $\boldsymbol{U_L}$ the voltage applied on the LED and $\boldsymbol{\eta_0}$ the efficiency of the electrolyzer without application of the external field, calculated by the non-variable part of the model.

3.3 Adaptation of the experimental results

Experimental research was limited by the number of available individual experiments that could have been conducted. Problems with the degradation of electrode surface or the achieving consistent ambient conditions in the Laboratory limited the scope of the research. On the other hand, the application of the magnetic field implied the usage of the electromagnet, and the main problem with experimental research with higher values of magnetic flux density was the heating of the electromagnet's coils. Therefore, the full potential of the range of achievable values of magnetic flux densities above 2 T was not fulfilled. It was *sacrificed* for the avoidance of

temperature fluctuations among individual experiments. To better understand the influence of the magnetic or optical fields, the mathematical model was adjusted to fill the gaps between points analyses in the experimental research.

3.3.1 Results of the adaptation for the application of the magnetic field

Adaptation success of the experimental results in the case of the application of the magnetic field and smooth electrodes was presented in Figure 20.

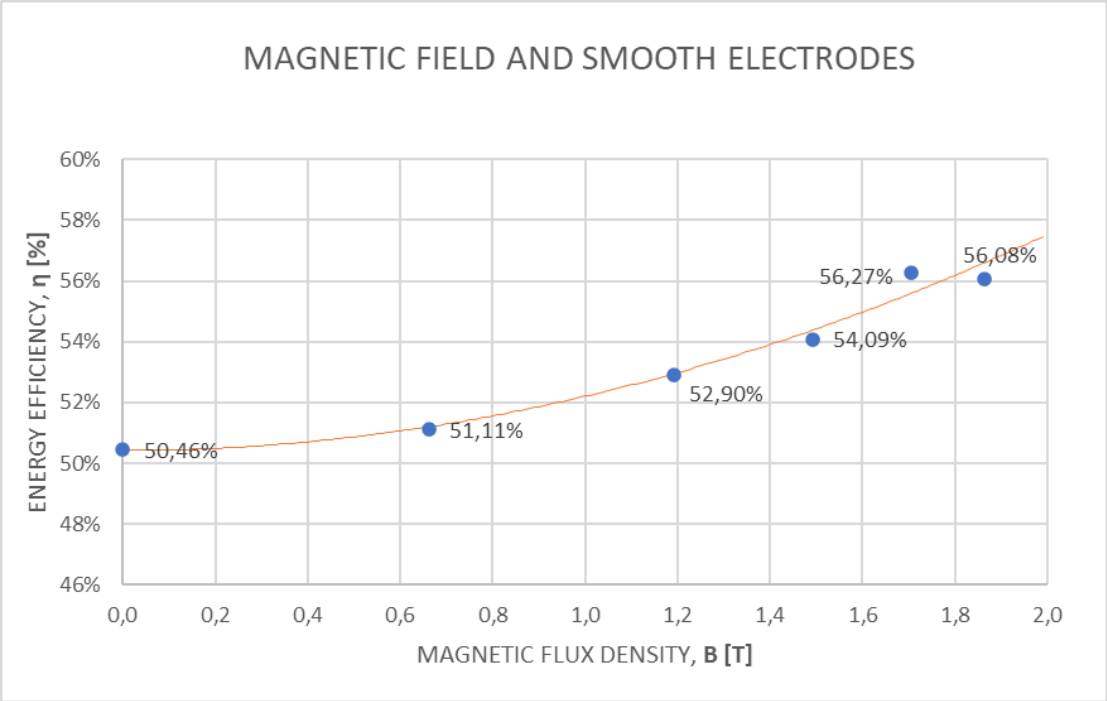

Figure 20. Adaptation success of the experimental results on the smooth electrodes with the application of the magnetic field

The analysis was conducted for the range from 0 to 2 T.

Adaptation success of the experimental results in the case of the application of the magnetic field and foam electrodes was presented in Figure 21.

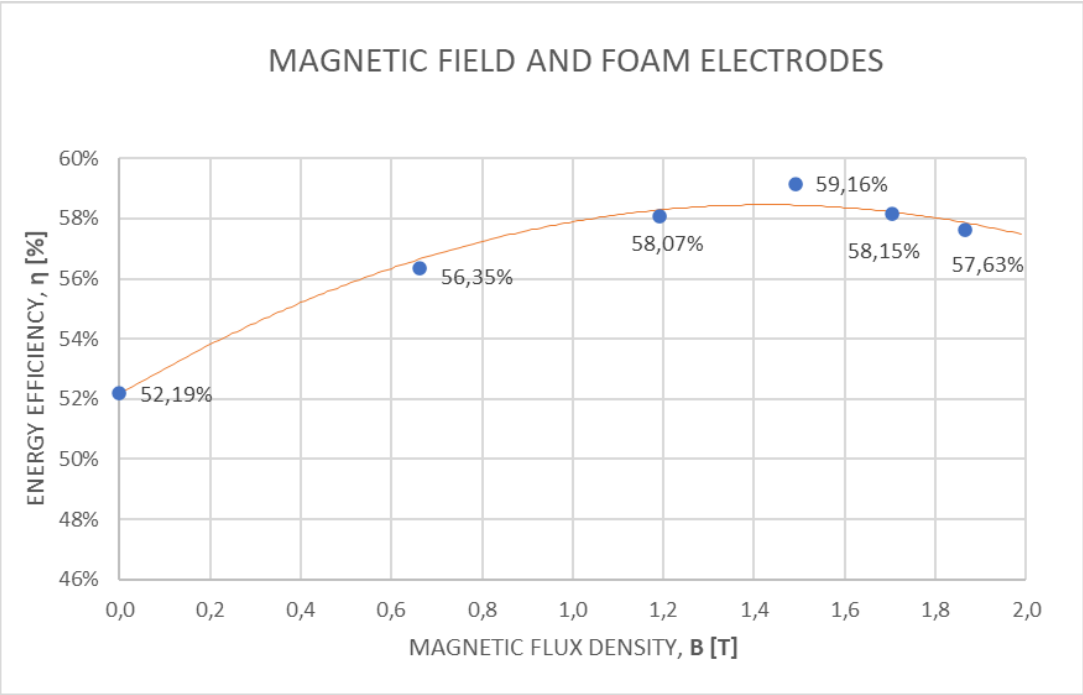

Figure 21. Adaptation success of the experimental results on the foam electrodes with the application of the magnetic field

The difference in the shapes of the graph indicates that the effects of the magnetic field on the process of the water electrolyzer vary significantly, depending on the usage of foam or smooth Ni electrodes. When the possible effect of the measurement uncertainty is considered graph's curve can change significantly. Therefore, those results, should not be taken *as law* and should be used with conditions and limitations which was analysed in mind. The comparison indicates an undeniable positive effect of the magnetic field on the process of water electrolysis.

In both cases, it was visible that the conclusion from the results of the experimental research conducted on the Electrolyzer 3, was true up to some value of the magnetic field, and then efficiency stat to decrease with further increase. Therefore, it can be concluded that there is optimal strength of the magnetic field, which varies among different electrolyzers, in which the maximum efficiency can be reached.

3.3.2 Results of the adaptation for the application of the LED

In the case of the mathematical model adjustment for the application of the LED, the main restriction was the range of the voltage used. Therefore, the results of the fitting were restricted to the voltage range of 2.8 and 3.4 V applied on the LED. For the values under the 2.8 V, the results of the fitting would not provide beneficial information since under those values of the

voltage LED does not generate any light. For those cases, the energy efficiency would be the same as if no external fields were applied. For the values above 3.4 V, it could be analysed, but in the scope of this research, it cannot be claimed that the fitting results of would follow the experimental results obtained by measurement. Adaptation success of the experimental results in the case of the application of the LED and smooth electrodes was presented in Figure 22.

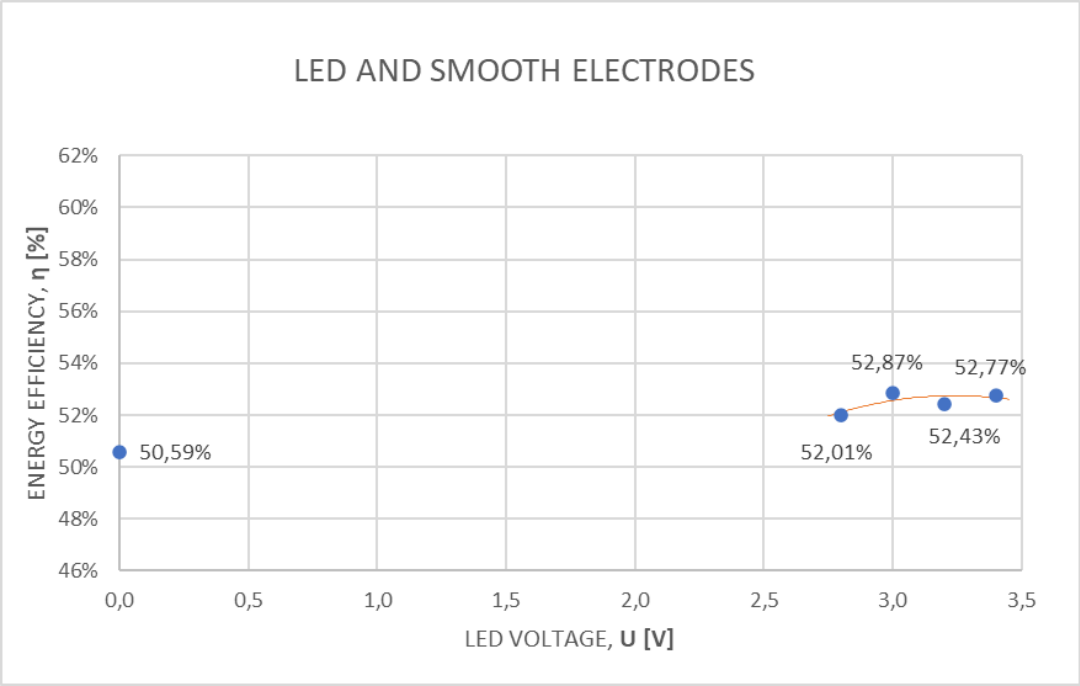

Figure 22. Adaptation success of the experimental results on the smooth electrodes with the application of the LED

Adaptation success of the experimental results in the case of the application of the LED and foam electrodes was presented in Figure 23.

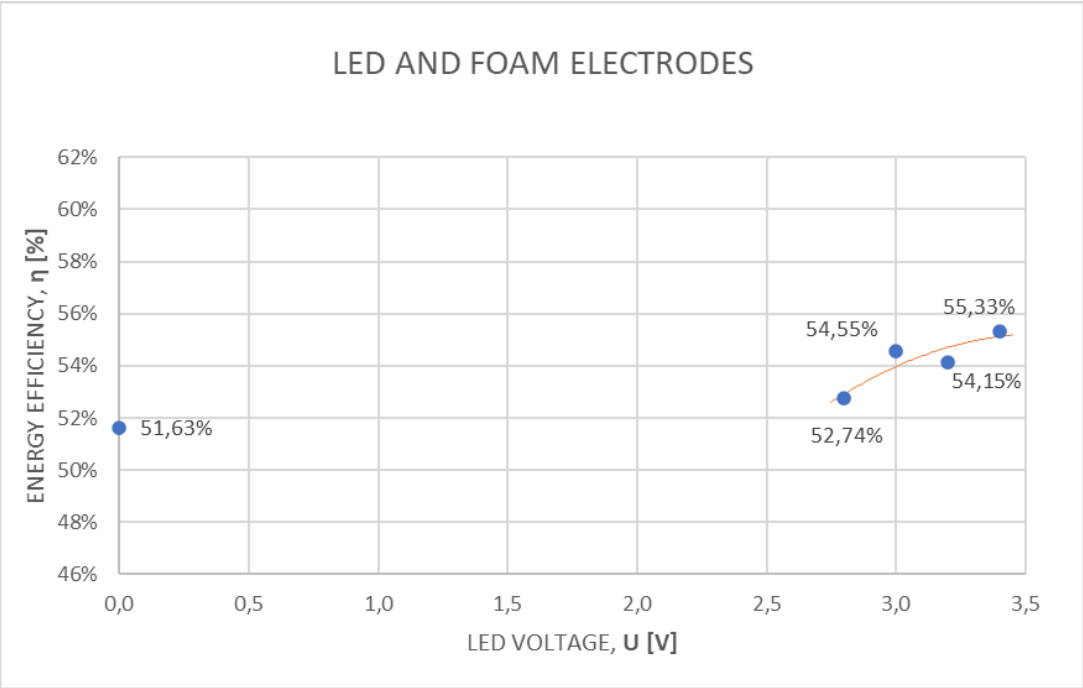

Figure 23. Adaptation success of the experimental results on the foam electrodes with the application of the LED

A notable difference between the application of the magnetic and the optical field is the trend of continuous increase of the energy efficiency with the further increase of the strength of the optical field applied in the water electrolysis process.

4. RESULTS

In this chapter, the results of the experimental research and the comparison of those results with the mathematical model were analysed. First, results of initial experimental research with Electrolyzer 3 were described and presented, then the main experimental results with Electrolyzer 4 and finally, the comparison of the mathematical model with those results were given.

4.1 Analysis of the results of experimental research of Electrolyzer 3

The first phase of the research focuses on the development of the design of the electrolyzer and the experimental setup. Therefore, initial research did not focus as much on the research of energy efficiency as on understanding the nature of the magnetic field, mapping of the magnetic field, and developing the best method of application on the main device.

4.1.1 Application of the inhomogeneous magnetic field

The investigation of the effect of the magnetic field was conducted in the early phase of the research.

4.1.1.1 Magnetic field with one pair of the permanent neodymium magnets

The first application of the magnetic field was via one pair of the permanent neodymium magnets detailed described in an earlier chapter. After the construction of the Electrolyzer 3, the first set of experiments was directed at visual confirmation of the effect of the application of the magnetic field. The direction of the magnetic field affects the direction of the created Lorentz force. Since both the directed magnetic field and the electrical current were in a horizontal plane perpendicular one to another, the resulting Lorentz force was vertical and perpendicular to the mentioned horizontal plane, but its direction could be adjusted to be directed up or down (Figure 24).

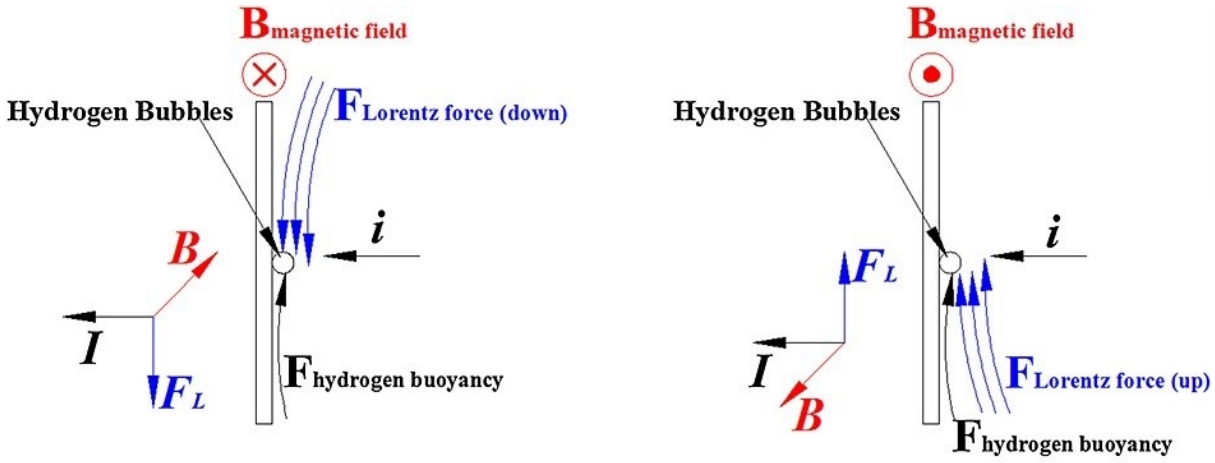

Figure 24. Differences in direction of the Lorentz force depend on the direction of the magnetic field in the relation to the direction of the electrical current [90]

The effect of the resulting Lorentz force did have a clear visual effect on the production of hydrogen and oxygen in the electrolyzer. In the comparison between the time frames of the start of the water electrolysis presented in Figure 25 and Figure 26. there was a clear difference in the way bubbles move in the volume of the upper tank. In the first case, when an electrical circuit was closed, bubble generation starts intensely and immediately since the voltage on the power supply was adjusted to 2 V. The bubbles soon started to separate from the electrodes and flow upward under the effect of buoyancy. After some time, vortices in the closed fluid, started to appear at the top of the volume of the upper tank and soon the whole volume decreases transparency due to several small bubbles of hydrogen and oxygen trapped in the electrolyte. On the other hand, when the magnetic field was applied, the fluid dynamics of the bubbles in the volume of the upper tank completely changed. Because of the Lorentz force, the bubbles immediately started creating vortices in the upper tank, circling around the electrodes, creating chaotic flow inside the upper tank. There was no clear upright flow up to the top of the upper tank. Only after enough time did the volume of the electrolyte fill up with bubbles and the transparency decreased as was the case without the application of the magnetic field. There was also a noticeable difference between the way Lorentz's force was directed. In both cases chaotic vortices were immediately created, preventing the bubbles from upright movement, but the direction of the vortices was opposite.

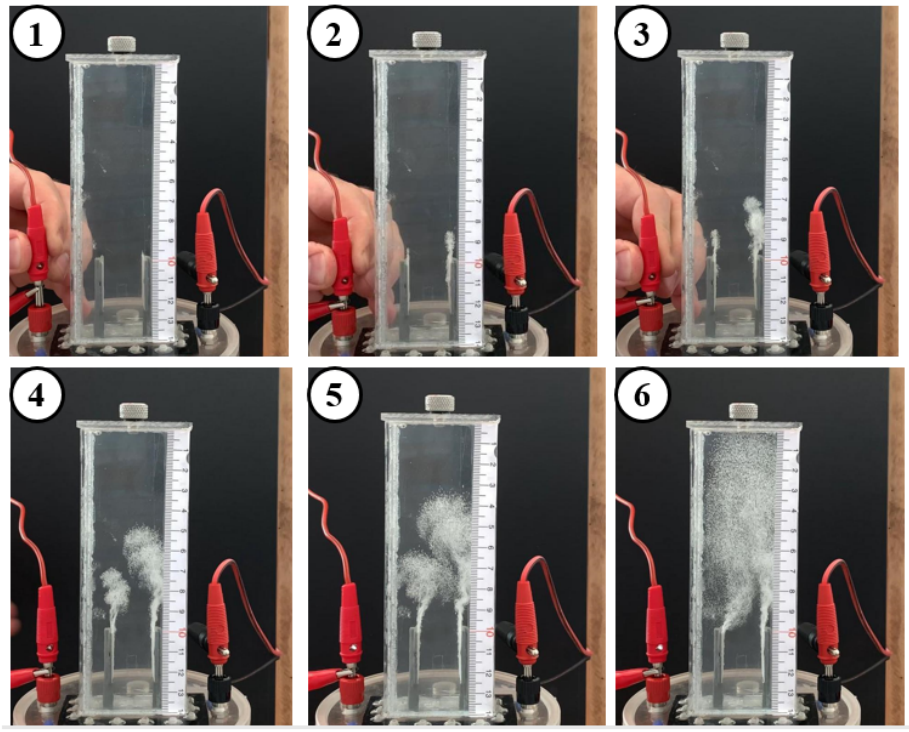

Figure 25. Frames of the first 2 seconds of the start of the water electrolysis at the voltage of 2 V without the application of the magnetic field

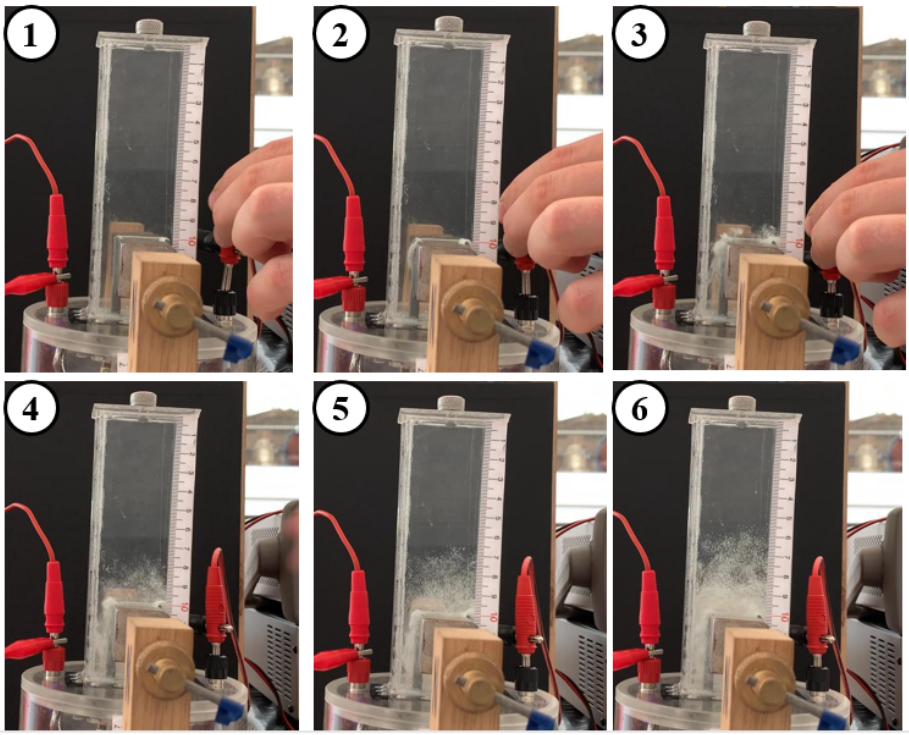

Figure 26. Frames of the first 2 seconds of the start of the water electrolysis at the voltage of 2 V with the application of the magnetic field

4.1.1.2 Magnetic field with two pairs of permanent neodymium magnets

Here the strength of the field was increased by the addition of the second pair of permanent neodymium magnets of the same size. However, the results of the addition of the second pair were not as expected. The maximum measured values of the magnetic flux density for one pair of the magnets at the distance of 25 mm were measured at the centre of the surface of the north pole of the magnet. The value of the magnetic flux density was a bit above 600 mT. After the addition of the second pair, the maximum measured value was in the centre of the surface of the north pole magnet, for the same distance of 25 mm, which amounted to 630 mT. A similar increase was recorded in the middle of the field, at the point of 12.5 mm from both surfaces of both magnets, where for one pair of magnets values amounted to 350 mT, and for two pairs of magnets amounted to 380 mT. While the increase was not expected to be doubled, the increase between 5% and 10% was disappointing, nevertheless.

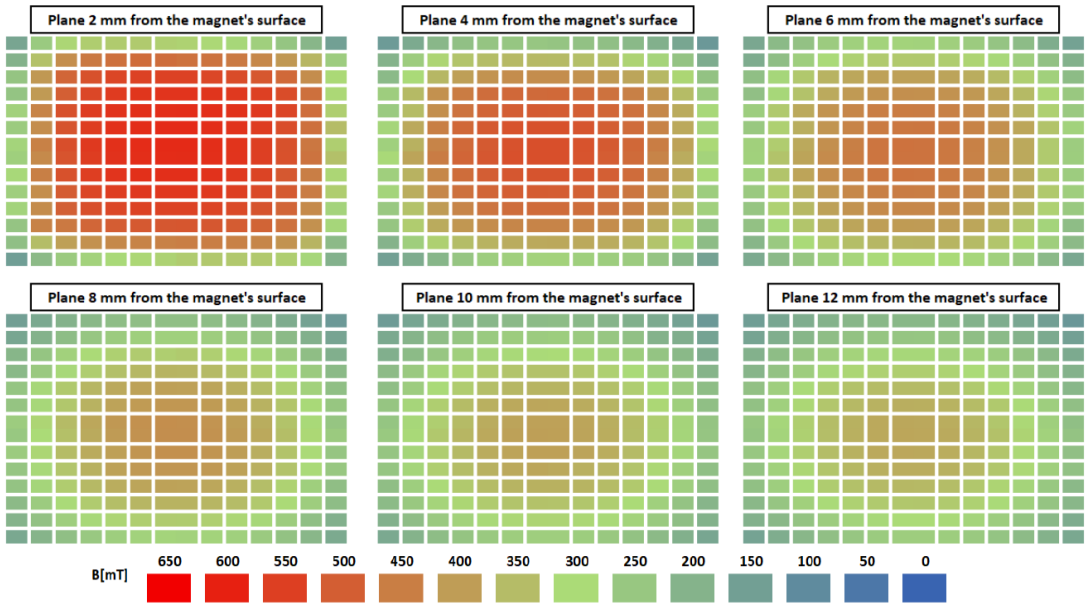

Figure 27. Progression of the magnetic flux density in inhomogeneous magnetic field as the observed plane moves away from the surface of the north magnetic pole

To better understand and visualise the shape of the magnetic field, extensive research on 3D mapping of the magnetic field was undertaken. The measurement was carried out by millimetric measurement of the planes parallel to the surface of the magnets facing each other. At the planes close to the surface of the north magnet, magnetic flux density was strongest, and equally distributed over the surface. With every other plane further away from the north side, the strength of the magnetic flux density dropped, and the shape of the field for that plane lose

coherence (Figure 27). The lowest measured values of the magnetic flux density were measured in the middle of the field and the shape of the field lost all resemblance to the square. The collected data was used for the 3D model visualisation of the field in the ParaView (Figure 28).

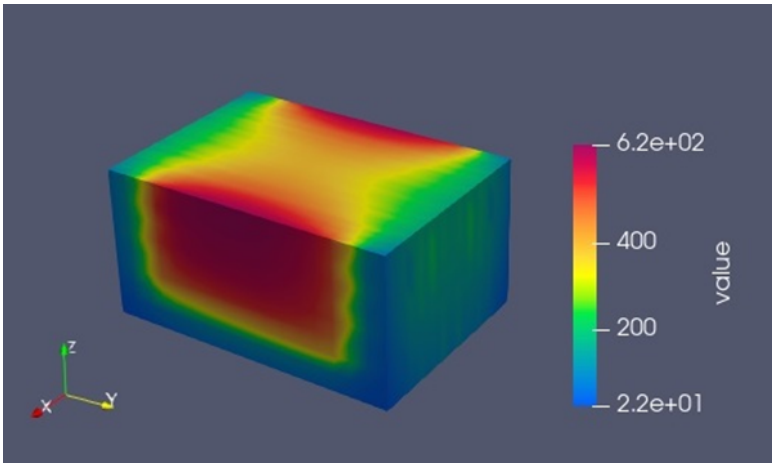

Figure 28. 3D model of the half of the magnetic field created by two pairs of permanent magnets used in the research at the distance of 25 mm

4.1.2 Energy efficiency of the research with the Electrolyzer 3

The results of all induvial experiments were analysed. In **Table 5**, results for the experiments without the application of a magnetic field are listed. Alongside data for the efficiency of every experiment, data about the average voltage and electrical current was given as well. The efficiencies for all individual experiments were averaged and the overall efficiency for the experiments without the application of magnetic field was 53.81%.

Table 5. Results of the individual experiments without the application of the magnetic field for the Electrolyzer 3

No. of exp.	**Average voltage [V]**	**Average current [A]**	**Magnets**	**Efficiency of the process [%]**
1	2.46610	0.16854	no magnets	53.32
2	2.46696	0.16642	no magnets	55.80
3	2.50783	0.20196	no magnets	54.75
4	2.51444	0.18242	no magnets	53.54
5	2.54315	0.20179	no magnets	53.22
6	2.53207	0.22289	no magnets	52.21
Avg.	**2.50509**	**0.19067**	**no magnets**	**53.81**

In **Table 6**, the results of the research with the application of one pair of magnets for the creation of a magnetic field are presented. Analog to the data for experiments with no magnets, data for average values of voltage and electrical current were also presented. The number of the experiment was higher than in the case with no magnets and with two pairs. The efficiencies for all individual experiments were averaged and the overall efficiency for the experiments with the application of magnetic field created by one pair of magnets was 54.90 %.

Table 6. Results of the individual experiments with the application of the magnetic field created with one pair of magnets for the Electrolyzer 3

No. of exp.	**Average voltage [V]**	**Average current [A]**	**Magnets**	**Efficiency of the process [%]**
7	2.54239	0.18553	1 pair	54.05
8	2.54638	0.19095	1 pair	53.45
9	2.56485	0.16352	1 pair	53.01
10	2.50256	0.15436	1 pair	55.31
11	2.50300	0.15265	1 pair	55.95
12	2.50462	0.15204	1 pair	54.80
13	2.49966	0.13600	1 pair	55.31
14	2.50230	0.13476	1 pair	55.87
15	2.50309	0.13360	1 pair	56.62
16	2.50899	0.25077	1 pair	56.58
Avg.	**2.51778**	**0.16542**	**1 pair**	**54.90**

Table 7. Results of the individual experiments with the application of the magnetic field created with two pairs of magnets for the Electrolyzer 3

No. of exp.	**Average voltage [V]**	**Average current [A]**	**Magnets**	**Efficiency of the process [%]**
17	2.48456	0.14953	2 pairs	53.20
18	2.46608	0.16835	2 pairs	56.67
19	2.51578	0.19258	2 pairs	56.50
20	2.51456	0.22210	2 pairs	55.21
21	2.50944	0.21028	2 pairs	56.01
22	2.50990	0.37388	2 pairs	55.78
Avg.	**2.50005**	**0.21945**	**2 pairs**	**55.56**

In **Table 7**, the results of the research with the application of two pairs of magnets for the creation of the magnetic field were presented. The efficiencies for all individual experiments were also averaged and the overall efficiency for the experiments with the application of a magnetic field created by one or two magnets was 55.56 %.

When analysed, data indicated that the application of the external magnetic field had a positive impact on the process of the alkaline water electrolysis. The application of the magnetic field created by one pair of the magnets increased the average efficiency in comparison to the case without the application of the magnetic field of the process from 53.81% to 54.90%. That represents an increase of 2.02%. The application of the magnetic field created by two pairs of magnets had an average value of efficiency of 55.56% which represents an increase of 3.26% in energy efficiency. Therefore, initial experimental research not only indicated that the application of the magnetic field increased the efficiency of the process, but also indicated the existence of a correlation that the stronger the magnetic field is, the higher increase in efficiency will be achieved.

4.2 Results of the experimental research

With the application of the electromagnet and Electrolyzer 4, a new phase of the research started. The principle of the experimentation and the procedures were analogue to the research with Electrolyzer 3, and therefore, qualitative conclusions of those results can be compared. Experimental research was mainly focused on the research of energy efficiency of water electrolysis as well as research on the U-I characteristic of the electrolyzer during its operation in different modes.

4.2.1 Analysis of the experimental results of the energy efficiency

Results of all individual experiments conducted with the Electrolyzer 4 were presented and analysed. All experiments were conducted following the same procedure that was established after initial trials of the experimental setup.

4.2.1.1 Example of the individual experiment

Before every experiment, the basic preparation described in previous chapters was done. When the electrolyzer was properly prepared and placed in the experimental setup, all the supporting equipment was turned on and the switch in the electrical circuit was lifted, effectively

preventing anything from happening. Before the actual experiment started, the test run was conducted, starting the electrolysis with the completely full upper tank. After a few minutes, the electrolytic gas would fill the top of the upper tank, and the level of the electrolyte in both tanks would be measured. The amount of the electrolytic gas before the experiment did not affect the measurement since mass would be subtracted from the measured produced amount in the experiment. The overall time of the experiment was 10 minutes, but the time the water electrolysis was occurring was 5 minutes. That was done for the purpose of easier and clearer data processing after the experiment was over.

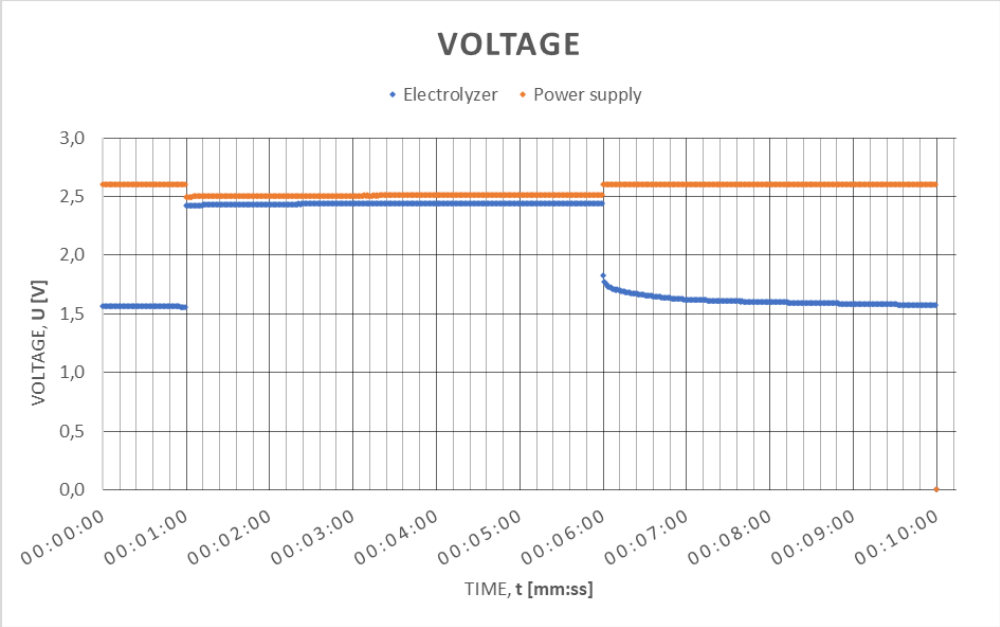

Figure 29. Measurement of the voltages in the selected experiment

Every experiment started with the start of the recording on the DAQ. The DAQ started recording data about voltage in the circuit (Figure 29) and on the resistance shunt that was later used for the calculation of the electrical current in the experiment, the temperature of the electrolytic gas and ambient temperature in lower tank and around the experimental setup (Figure 30). In the meantime, the magnetic field was activated if it was required in the scope of that experiment. At 1:00 minute of the experiment, the switch was closed, and the electrical circuit connected, i.e., the process of water electrolysis started. In the first moments of the reaction, the volume of the electrolyte was transparent and started to be filled with bubbles of hydrogen and oxygen, as the bubbles started franticly moving through the electrolyte. That effect was also visible in the measurement of the electrical current (Figure 31) and electrical resistance (Figure 32). As time progresses, the electrical resistance increases, since the interelectrode space was filled with the bubbles of hydrogen and oxygen. Since the voltage was

more or less constant in the duration of the experiment, the increase in the resistance decreased the electrical current in the process.

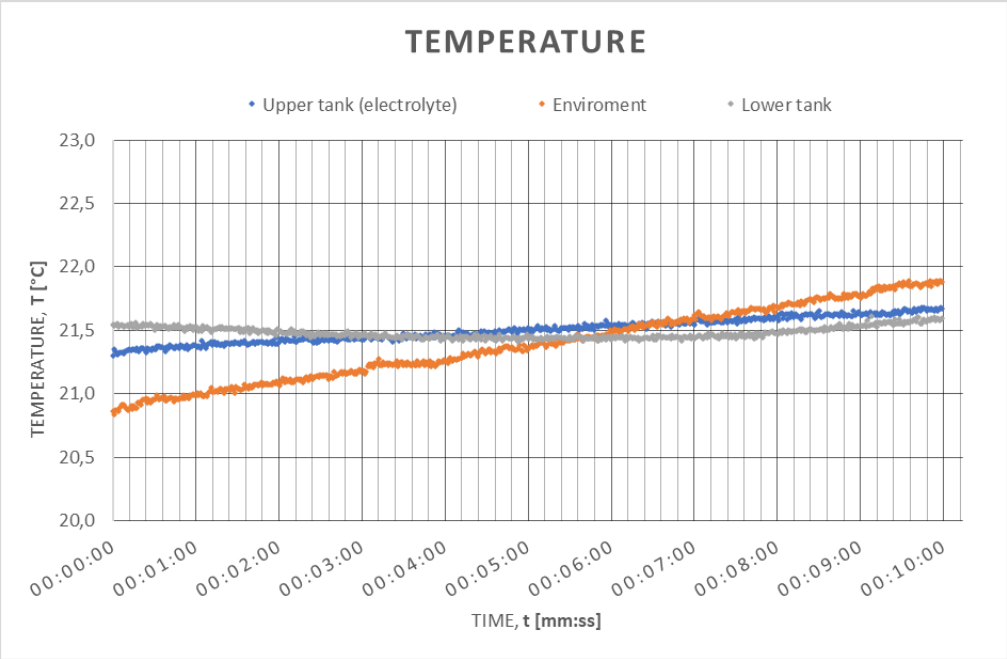

Figure 30. Measurement of the temperatures in the selected experiment

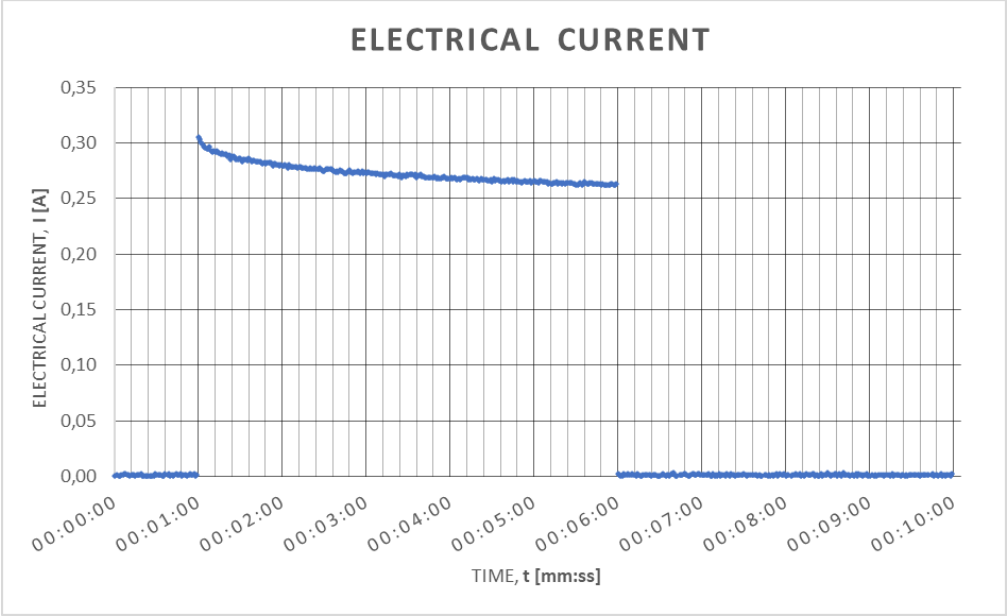

Figure 31. Measurement of the electrical current in the selected experiment

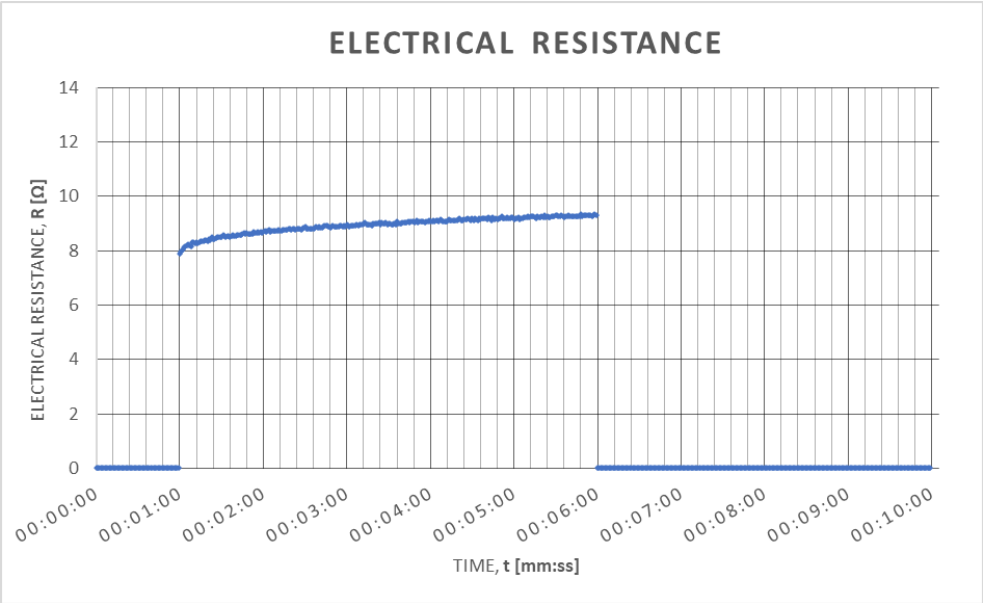

Figure 32. Measurement of the electrical resistance in the selected experiment

As the experiment progresses, the increase in the resistance was slower, and in some cases stabilises at some point. As more and more produced electrolytic gas was accumulated at the top of the upper tank, the problem of that gas reaching the tips of electrodes arised. To prevent that from happening, the experiment was limited by time and the 6:00 minute of the experiment switch was lifted again, and the process of water electrolysis was stopped. In case the electromagnet was part of the experiment, it was turned off first, while the other equipment kept recording. A couple of minutes was needed for all the bubbles of hydrogen and oxygen to reach and release in the upper part of the upper tank. In the 10:00 minute of the experiment recording in the DAQ was stopped, and consequently, the experiment. Although there was still some time spent on turning off additional equipment, from the point of data analysing, the only thing important was the measurement of the levels of the electrolyte in the lower and the upper tank and the measurement of the barometric pressure. The data for the calculation of the input energy was processed soon after. The output power in every second was integrated into the overall energy input (Figure 33), while the calculation of the produced hydrogen was calculated into overall energy output and energy efficiency was calculated.

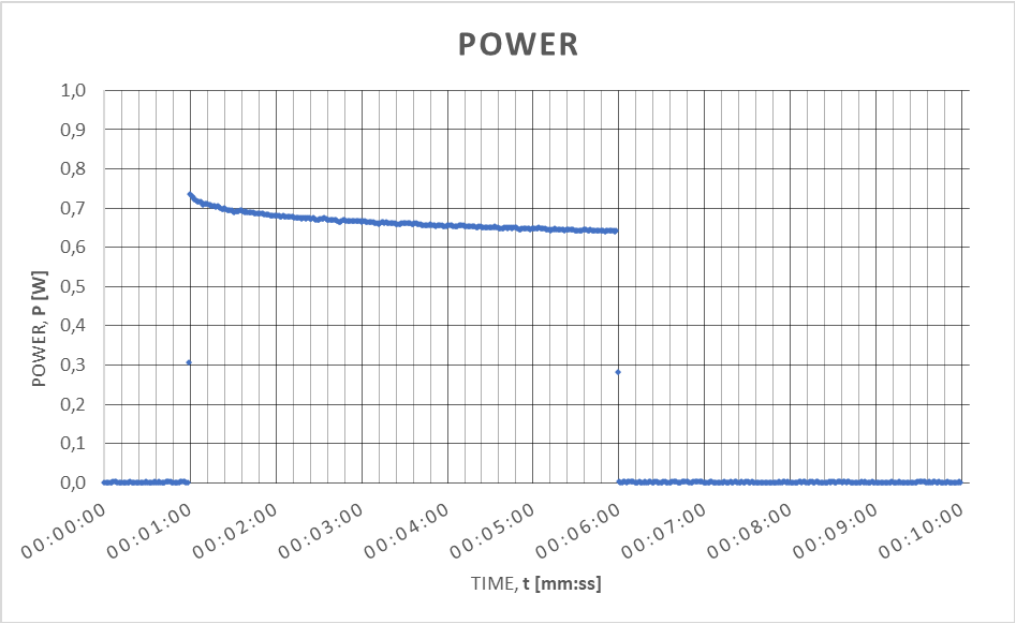

Figure 33. Output power versus experiment time duration

4.2.1.2 Analysis of the experimental results by individual effects

In the scope of the research of energy efficiency, six sets of experiments were conducted, to determine the influence of every researched influence. First, there was a difference between the usage of smooth Ni electrodes and the usage of Ni foam electrodes. The second researched influence was of the magnetic field and the third of application of the LED. The list of the set was as follows:

- With application of the magnetic field with different values of magnetic flux density on smooth Ni electrodes.
- With application of the magnetic field with different values of magnetic flux density on Ni foam electrodes.
- With application of the LED with different voltage on smooth Ni electrodes.
- With application of the LED with different voltage on Ni foam electrodes.
- Comparative analysis of the influence of both the magnetic field and LED on smooth Ni electrodes.
- Comparative analysis of the influence of both the magnetic field and LED on Ni foam electrodes.

The experiments with application of the magnetic field with different values of magnetic flux density was conducted on the same pair of electrodes with magnetic field densities of 0 T, 0.663 T, 1.191 T, 1.491 T, 1.705 T, and 1.864 T. It means that in every set of experiments, five individual experiments were conducted with the application of the magnetic field, and one without the application of the magnetic field.

For the experiments with the application of LED with different values of voltage, the same analogy was applied. Experiments were conducted at the voltages of 0 V, 2.8 V, 3.0 V, 3.2 V and 3.4 V, meaning that four experiments were conducted with the application of LED, and one without LED application. The stronger voltages were not tested due to safety reasons, while lower voltages would barely yield any green light.

For the experiment of the comparative analysis of the influence of both the magnetic field and LED, the procedure was to make four experiments on the same pair of electrodes, and then change electrodes from smooth Ni electrodes to Ni foam electrodes. The one set included the following individual experiments:

- Without application of the magnetic field or the LED.
- With application of the magnetic field with the magnetic flux density of 1.864 T
- With application of the LED at the voltage of 3.4 V
- With application of both the magnetic field with the magnetic flux density of 1.864 T and the LED at the voltage of 3.4 V

All experiments of the single set were done in a short time span with similar environment conditions, to minimise the effect of other various factors such as ambient temperature, or barometric pressure changes. In that way, the effects of only researched applications aspired to be obtained, and the effects of undesirable outer effects were mitigated.

4.2.1.2.1 Analysis of the effect of the application of the magnetic field

Out of six experiments conducted, two sets of experiments were conducted with the application of the magnetic field under the conditions described in the previous subchapter. The results of those experiments are presented in **Table 8**.

Table 8. Energy efficiency of the individual experiments conducted with the application of the magnetic field

Magnetic flux density	**Energy efficiency [%]**	
[T]	**Ni foam electrodes**	**smooth Ni electrodes**
0	52.19	50.46
0.663	56.35	51.11
1.191	58.07	52.90
1.491	59.16	54.09
1.705	58.15	56.27
1.864	57.63	56.08

The results of the experiments clearly and undoubtedly confirmed the positive influence of the magnetic field on the increase of the energy efficacy of alkaline water electrolysis. With the application of the electromagnet, stronger magnetic fields were possible to achieve.

For the experiments conducted with Ni foam electrodes, there was a clear difference in the results of energy efficiency calculation, depending on the application of the magnetic field. The results of individual experiments are presented in (Figure 34).

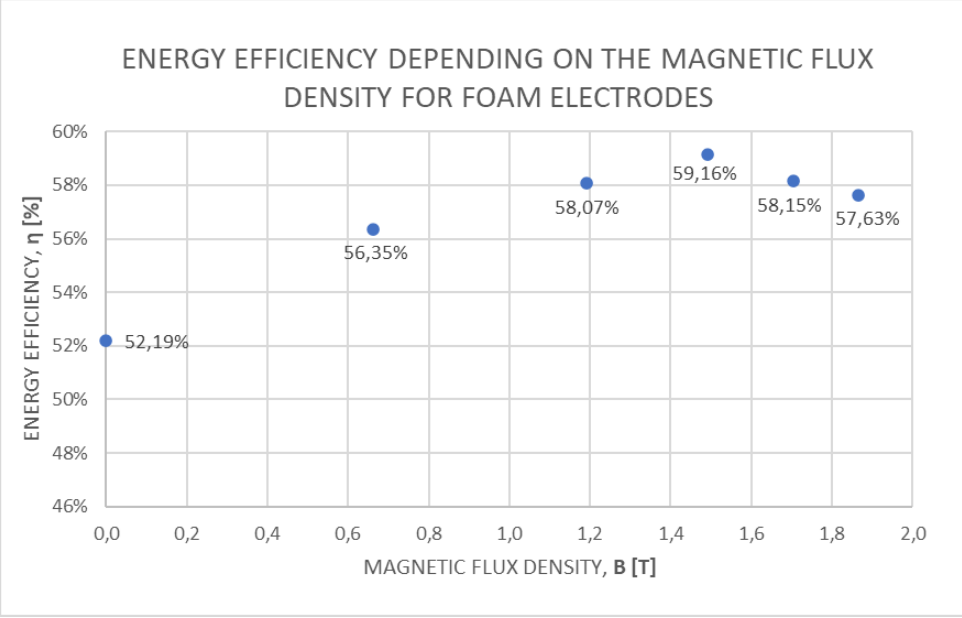

Figure 34. Electrolyzer energy efficiency of the as the function of the magnetic flux density for Ni foam electrodes

For the experiments conducted with smooth Ni electrodes, there was also a clear difference in the results of energy efficiency calculation, depending on the application of the magnetic field. The results of individual experiments are presented in Figure 35. Similarly with the Ni foam electrodes, here can be noted that the increase in the magnetic field does not result in the increase in the energy efficiency indefinitely. Although overall energy efficiency is lower for smooth electrodes, the influence of the magnetic field had an expected effect.

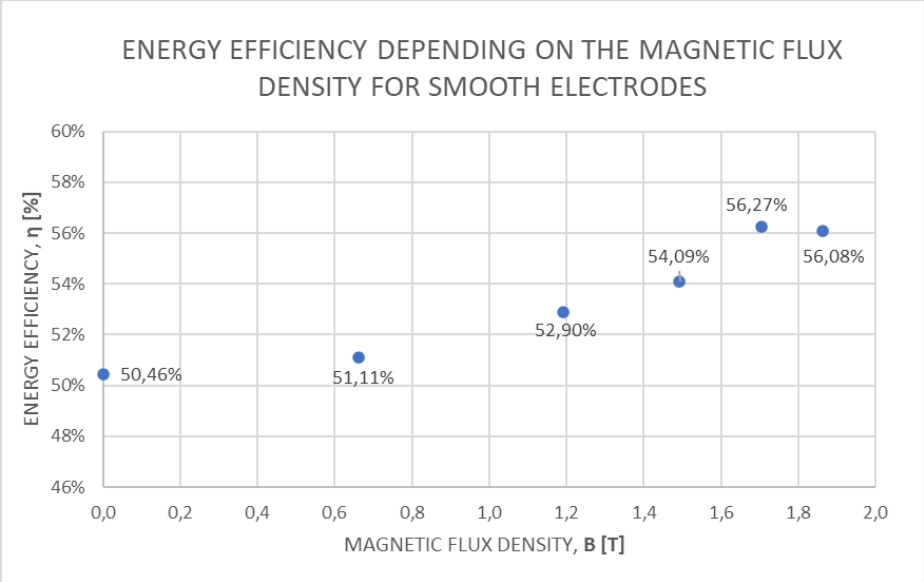

Figure 35.. Electrolyzer energy efficiency as the function of the magnetic flux density for smooth Ni electrodes

4.2.1.2.2 Analysis of the effect of the application of the LED

Out of six experiments conducted, two sets of experiments were conducted with the application of the LED under the conditions described in the previous subchapter. The results of those experiments are presented in **Table 9**.

Table 9. Electrolyzer energy efficiency with the application of the LED

Voltage	**Energy efficiency [%]**	
[V]	**Ni foam electrodes**	**smooth Ni electrodes**
0	51.63	50.59
2.8	52.74	52.01
3.0	54.55	52.87
3.2	54.15	52.43
3.4	55.33	52.77

The experimental results indicate positive impact of the LED application. The positive effect of the LED is not as notable as it was the case with the application of a magnetic field, but it is still apparent. The experimental results for the Ni foam electrodes are presented in Figure 36.

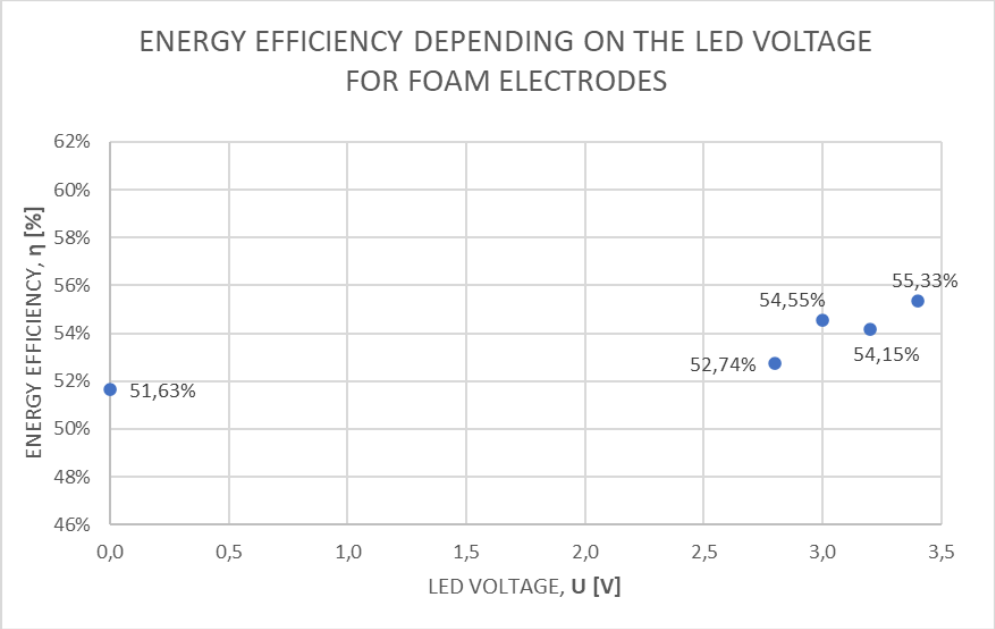

Figure 36. Electrolyzer energy efficiency versus LED voltage for Ni foam electrodes

For the experiments conducted with smooth Ni electrodes, the results point out to the same conclusion. The results of individual experiments are presented in Figure 37. In the case of smooth electrodes, the difference is not as significant.

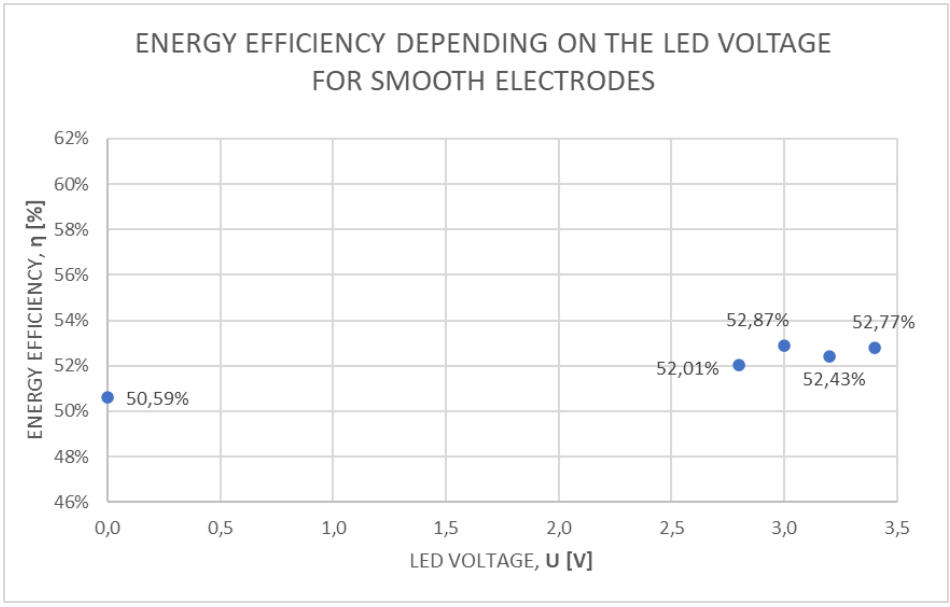

Figure 37. Electrolyzer energy efficiency versus LED voltage for smooth Ni electrodes

4.2.1.2.3 Analysis of the effect of the application of the magnetic field and LED

Out of all six sets of experiments conducted, two sets were conducted with the goal to determine the difference among the eight modes of electrolyzer defined in the previous chapter. Although some results from experimental sets analysed in two previous subchapters could serve as potential references for this analysis as well, the results of those experiments could have been affected by some other effects like temperature or barometric pressure. Also, for every set, electrodes were prepared separately to minimise the effects of degradation of the surface of the electrodes due to extended exposure to the alkaline electrolyte. Therefore, separate experimental sets were conducted. In the experimental research of one set, four types of conditions were applied, for both foam and smooth electrodes:

- Without application of the magnetic field or the LED.
- With application of the magnetic field with the magnetic flux density of 1.864 T.
- With application of both the magnetic field with the magnetic flux density of 1.864 T and the LED at the voltage of 3.4 V
- With application of the LED at the voltage of 3.4 V

The results of those two experiment sets are presented in **Table 10**.

Table 10. Energy efficiency of the individual experiments conducted with the application of the LED

Electrode	Electromagnets	LED	Efficiency
Foam	**Yes (1.864 T)**	**Yes (3.4 V)**	59.13 %
Foam	**Yes (1.864 T)**	No	59.60 %
Foam	No	**Yes (3.4 V)**	52.59 %
Foam	No	No	50.34 %
Smooth	**Yes (1.864 T)**	**Yes (3.4 V)**	57.25 %
Smooth	**Yes (1.864 T)**	No	55.88 %
Smooth	No	**Yes (3.4 V)**	52.48 %
Smooth	No	No	50.19 %

From the experimental results, it can be concluded that influence of the application of the magnetic field has a high positive influence on the electrolyzer energy efficiency. In comparison to the results when no fields applied, the effect of the magnetic field showed an increase of

energy efficiency 18.36% for foam electrodes and of 11.34% for smooth electrodes. The influence of LED was also notable but not as significant as with magnetic field. The effect of the optical field showed an increase of energy efficiency of 4.47% for foam electrodes and 4.56% for smooth electrodes, in comparison with no fields applied. When both applications were combined, the results showed no significant additive effects, and energy efficiency was in the range of those when only a magnetic field was applied. The combined effect of both applied fields shows an increase of energy efficiency of 17.46% for foam electrodes and an increase of energy efficiency of 14.07% for smooth electrodes, in comparison with no fields applied.

The experimental results followed the trend of the results from previous experiments with different magnetic flux densities and different voltages applied. There were some deviations in how much significant the increase was with the application of both fields. The best example can be found in this experimental set where the energy efficiency of combined effects was higher than only the magnetic field for foam electrodes, while it was lower for smooth electrodes.

4.2.1.2.4 Analysis of the effect of the application of the Ni foam electrodes

In this research, three experimental sets were conducted with Ni foam electrodes and three sets with smooth Ni electrodes. Those experiments were conducted to determine the effects of the magnetic and optical field on the process of alkaline water electrolysis. However, those experiments were conducted with a secondary objective as well, to compare the effect of the usage of Ni foam electrodes instead of smooth Ni electrodes. That is why all experiments were essentially the repetition of the experimental set but with different pair of electrodes. To analyse the effect of different types of electrodes, the results of complementary sets of experiments were analysed. In Figure 38, data from **Table 8** are presented for experiments with the usage of magnetic fields. It is visible that for every case of the applied magnetic field, calculated energy efficiency was higher for the foam electrodes than for the smooth ones. In this analysis, it can be determined that the replacement of smooth electrodes by foam will increase energy efficacy by 6.99%.

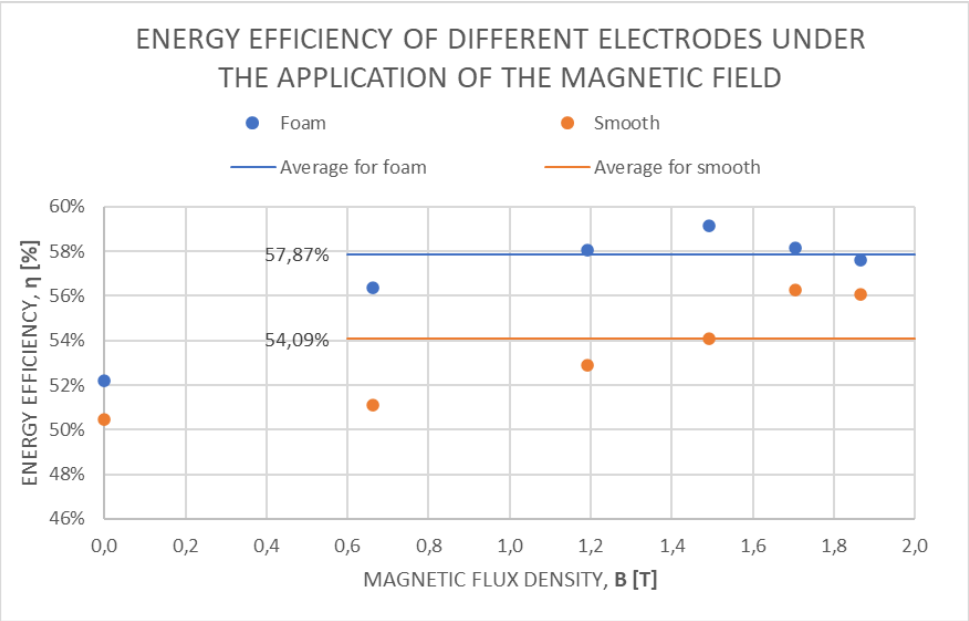

Figure 38. Electrolyzer energy efficiency with both types of electrodes under the application of the magnetic field

Data analysed for the application of LED from **Table 9** is presented in Figure 39. The effect of the foam electrodes is not as visible. In some cases, calculated energy efficiency for the smooth electrodes under the LED of the same voltage was higher than for the foam electrodes. In this analysis, it can be determined that the replacement of smooth electrodes by foam will increase energy efficiency by 3.18%.

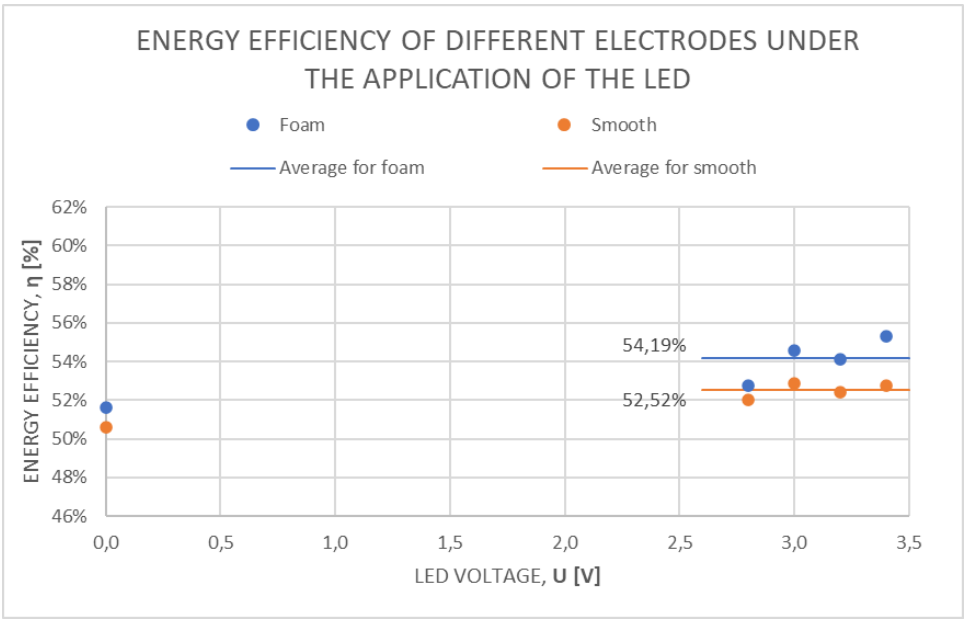

Figure 39. Electrolyzer energy efficiency with both types of electrodes under the application of the LED

Data analysed from the experiments that include both the magnetic field and the LED also had varying results. As it was presented in **Table 10** for the cases with application of both fields and only magnetic field, the energy efficiency was higher for the foam electrodes. For the case when only the LED was applied the energy efficiency was higher with application of smooth electrodes. In this case, without the application of any field, the results were showing similar effect, with the energy efficiency higher when foam electrodes were applied. The average electrolyzer energy efficiency with foam electrodes was 51.34%, while for the smooth electrodes it was 50.46%. That determines the increase of 1.73% if smooth electrodes were replaced by foam electrodes.

Finally, if all data points measured in all experiments for the Electrolyzer 4 were averaged, the average electrolyzer energy efficiency with foam electrodes was 55.54% while with smooth electrodes it was 53.16%. In other words, the replacement of smooth electrodes by foam electrodes will result in an increase of the energy efficiency for a 4.29%.

4.2.1.3 Analysis of the effect of other factors

Values of average voltage, electrical current, electrical resistance, average temperature of the electrolyte and average ambient temperature were analysed as well. The average value for each factor was calculated from experimentally collected data. Data was collected in one sample per second rate. As it was presented, it cannot be determined that the influence of other measured factors was influencing the results of the energy efficiency.

The values of the average voltage in the experiments are presented in Figure 40. As it is shown earlier, during the experiment, the voltage did not change much. It cannot be concluded that the voltage average value in the process affected the results because there is no clear indication that higher values of voltage increase or decrease the energy efficiency.

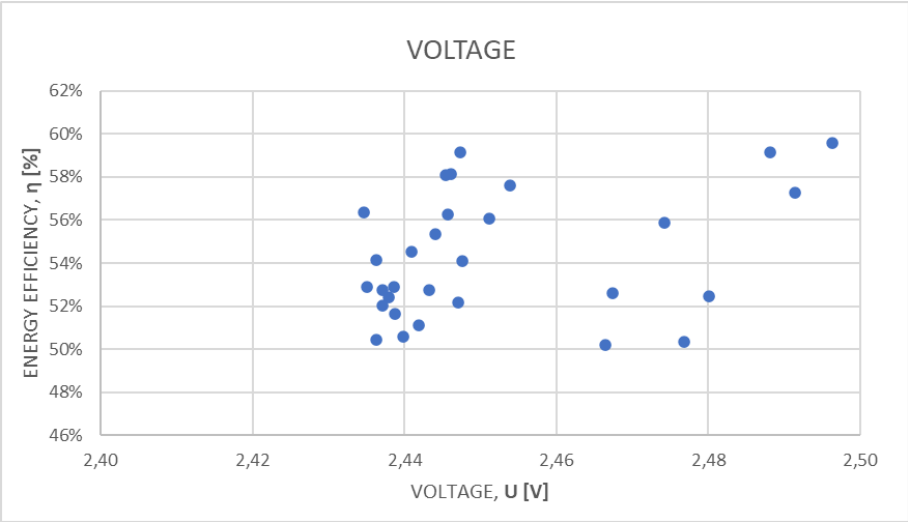

Figure 40. Average voltage in each experiment in corelation with the energy efficiency

The values of the average electrical current in the experiments are presented in Figure 41. Different to the values of the voltage in the duration of the experiment, the electrical current did change its values drastically. From maximum values at the start of the experiment, values would drop, first rapidly, then slightly until the balanced state was reached. From the analysed data there cannot be concluded that the average value of the electrical current in the process affected the results of the research since there is no clear indication that higher values of electrical current increase or decrease the energy efficiency.

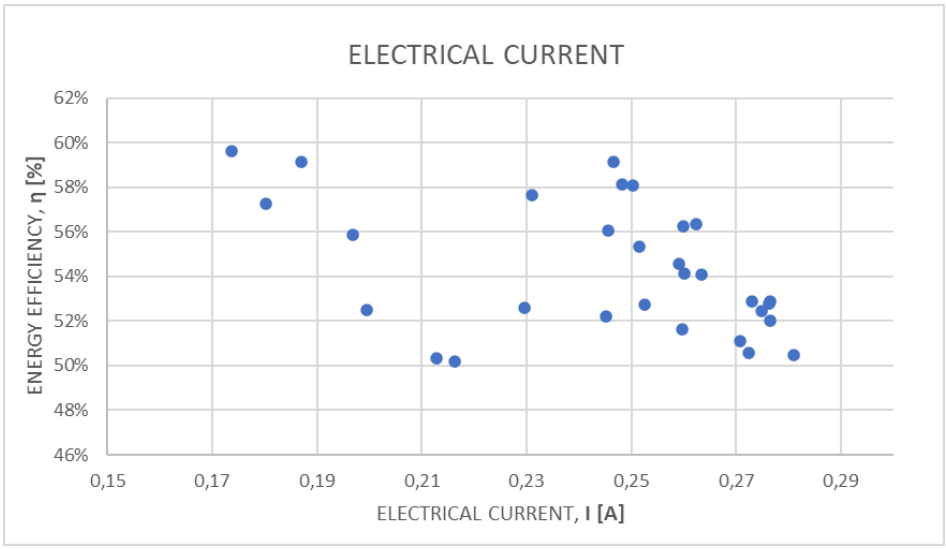

Figure 41. Average electrical current in each experiment in corelation with the energy efficiency

The values of the average electrical resistance in the experiments are presented in . Since the voltage was constant for the duration of the experiment, it was logical that the values of the

resistance changed in the opposite direction than the electrical current. Its values would at the beginning rise rapidly from their minimum values until the balanced state was reached. From the analysed data there cannot be concluded that the average value of the electrical resistance in the process affected the results of the research since there is no clear indication that higher values of electrical resistance increase or decrease the energy efficiency.

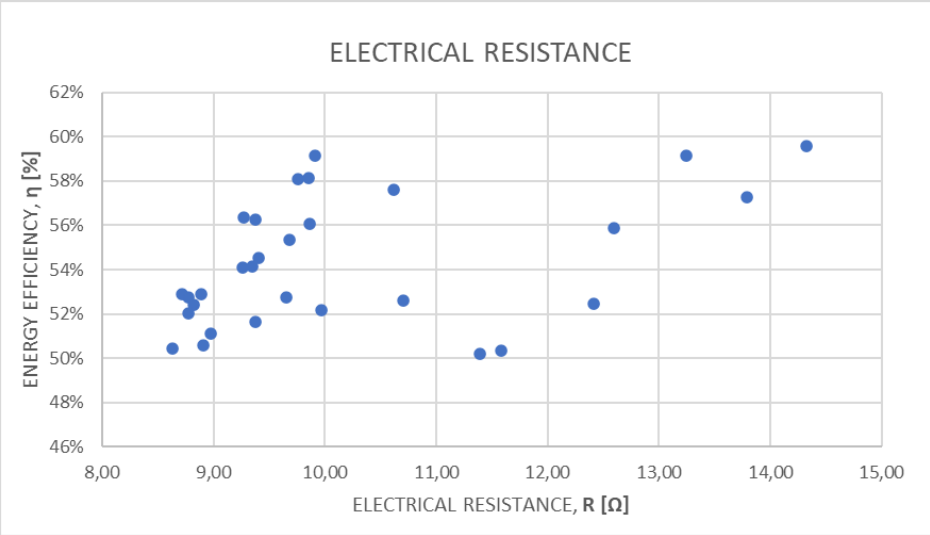

Figure 42. Average electrical resistance in each experiment in corelation with the energy efficiency

The values of the average temperature of the produced electrolytic gas in the upper tank in the experiments were presented in Figure 43. The values of temperature were measured using K-type thermocouple and were mostly constant with experiments without the application of the magnetic field. The temperature rose in the duration of the experiments with the application of the magnetic field due to heating of the coils. From the analysed data there cannot be concluded that the average value of the temperature of the produced electrolytic gas in the process affected the results of the research since there is no clear indication that higher temperatures increase or decrease the energy efficiency.

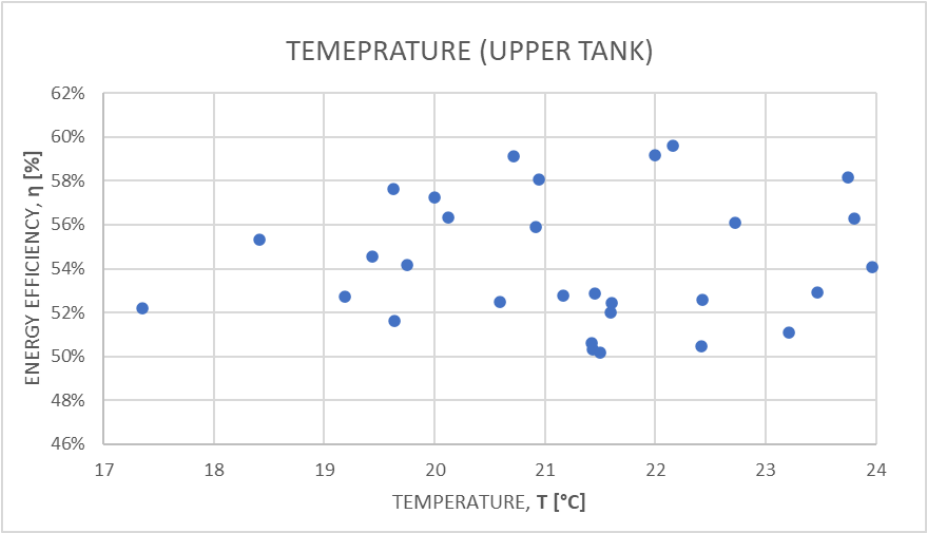

Figure 43. Average temperature of electrolytic gas in each experiment in corelation with the energy efficiency

The values of the average ambient temperature in the experiments are presented in Figure 44. The values of temperature were measured using K-type thermocouple and were mostly constant during all experiments. From the analysed data there cannot be concluded that the average value of the ambient temperature affected the results of the research since there is no clear indication that higher temperatures increase or decrease the energy efficiency.

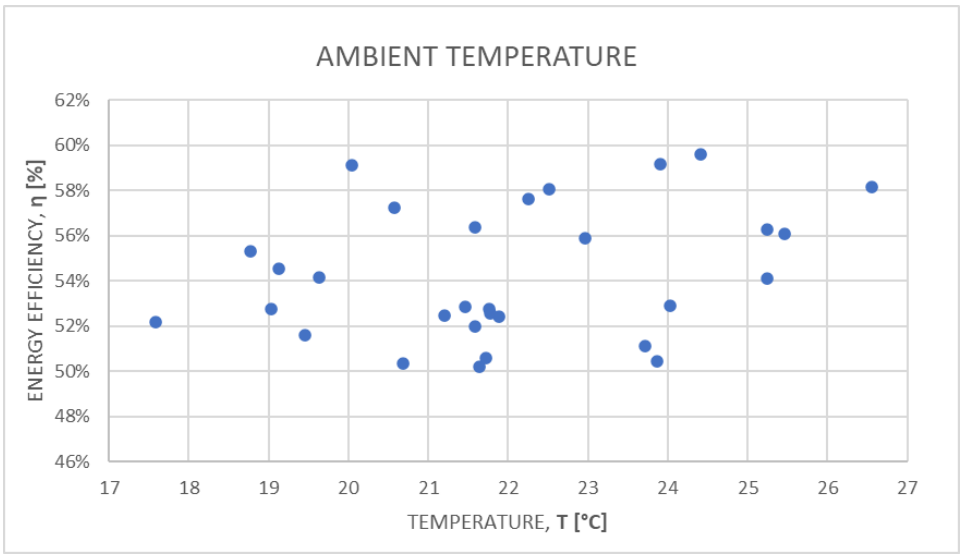

Figure 44. Average ambient temperature in each experiment in correlation with the energy efficiency

4.2.2 Analysis of the U-I characteristic of the Electrolyzer 4

Analysis of the U-I characteristics was done for the mode of the experiments with the smooth electrodes and the application of the LED. The voltage of the LED was set at 3.4 V and constant during the recording of the U-I characteristics. The magnetic field was not applied in this set pf experiments.

4.2.2.1 Example of one U-I characteristic

The recording of the U-I characteristic was conducted in a way that voltage was slowly increased in constant intervals for the same step, until the maximum voltage was reached, then in the same intervals it was decreased, by the same step (Figure 45). The time of the interval and the size of the step differs. In the longer version, which lasted 20:00 minutes, the intervals lasted 10 seconds, and the step was 0.05 V, while in the shorter version, the intervals lasted 5 seconds and the step was 0.1 V. As the voltage was increased, the electrical current increased as well (Figure 46). During the research, the stationary state of the electrolysis was not achieved during the recording of U-I characteristics. After combining the recorded data, the U-I characteristic of a single experiment was generated (Figure 47).

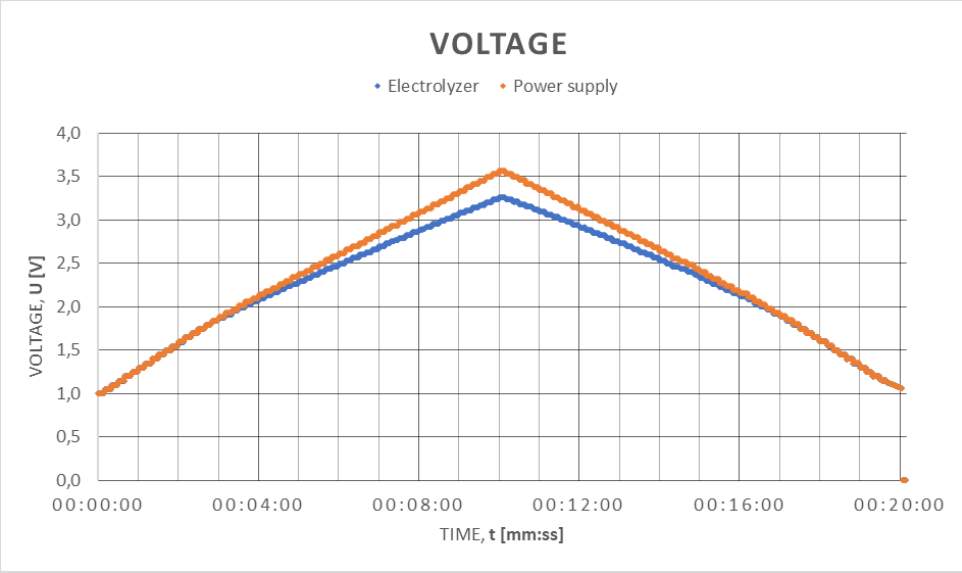

Figure 45. Change of the voltage during recording of the U-I characteristic

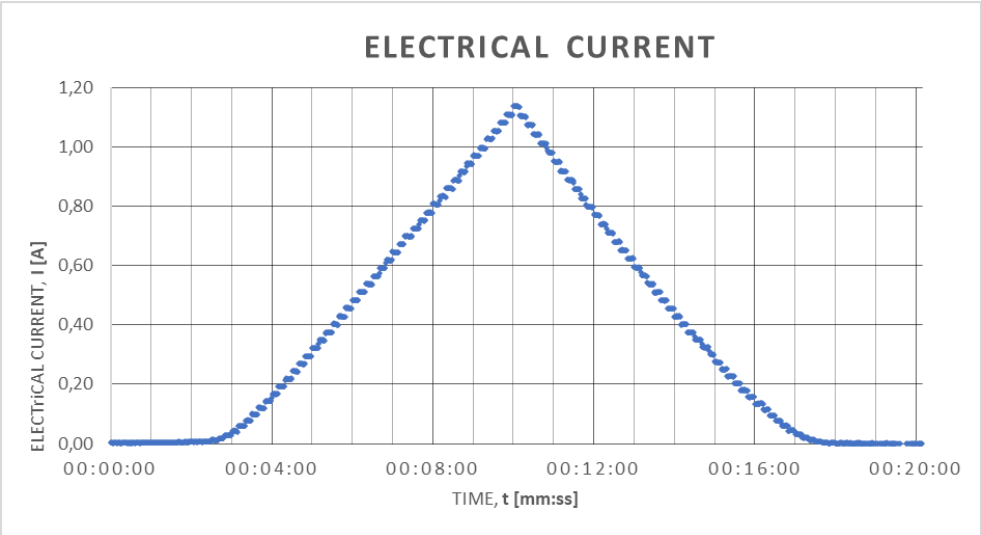

Figure 46. Change of the electrical current during recording of the U-I characteristic

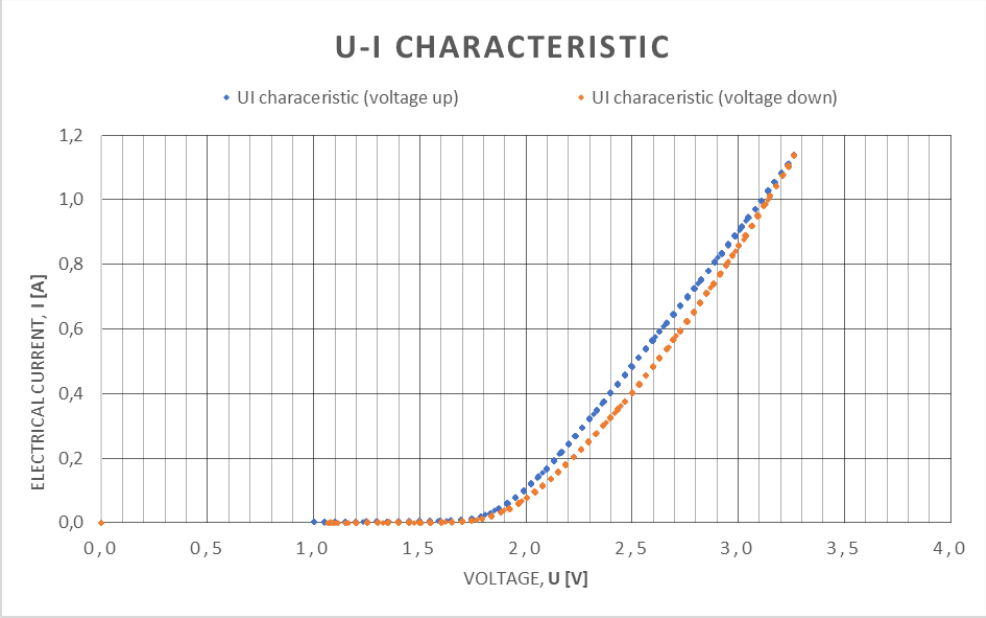

Figure 47. U-I characteristic of the experiment example

4.2.2.2 Comparative analysis of the U-I characteristics for the same mode of operation

As initial research conducted on the Electrolyzer 3 showed, the recording of the U-I characteristics of the electrolyzer proved problematic since the results that are supposed to repeat themselves, did not. Therefore, experimental research was conducted, analysing the influence of outside factors that shape the U-I characteristic of the electrolyzer. In each recording, LED was applied at the voltage of 3.4 V, while the magnetic field was excluded. As results show, for the recording that was conducted on the same day, the U-I characteristics does follow the same path (Figure 48). However, when recordings of the U-I characteristics were

conducted over a period of a few days, the data does not overlap as expected and the deviations are significant (Figure 49). Therefore, it can be concluded that the influence of the ambient conditions had significant effect on the shape of the U-I characteristic.

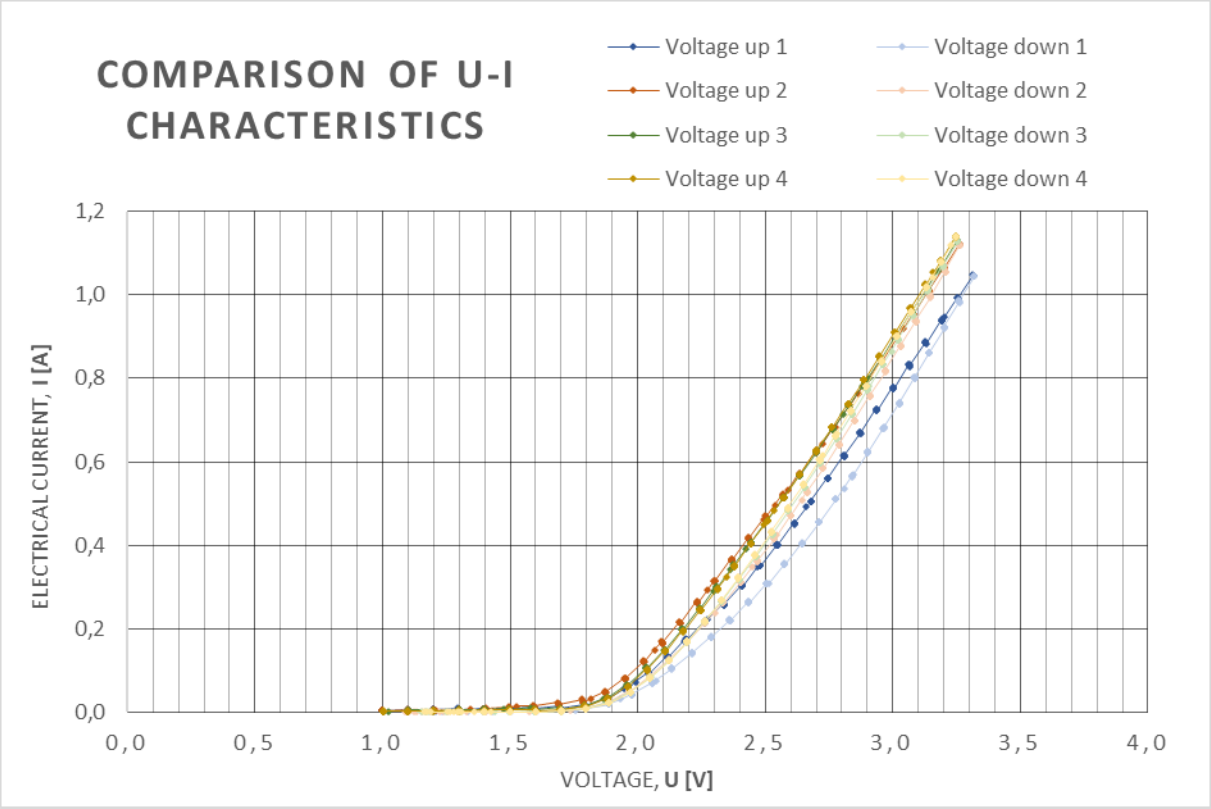

Figure 48.. Four U-I characteristics recorded in the same day

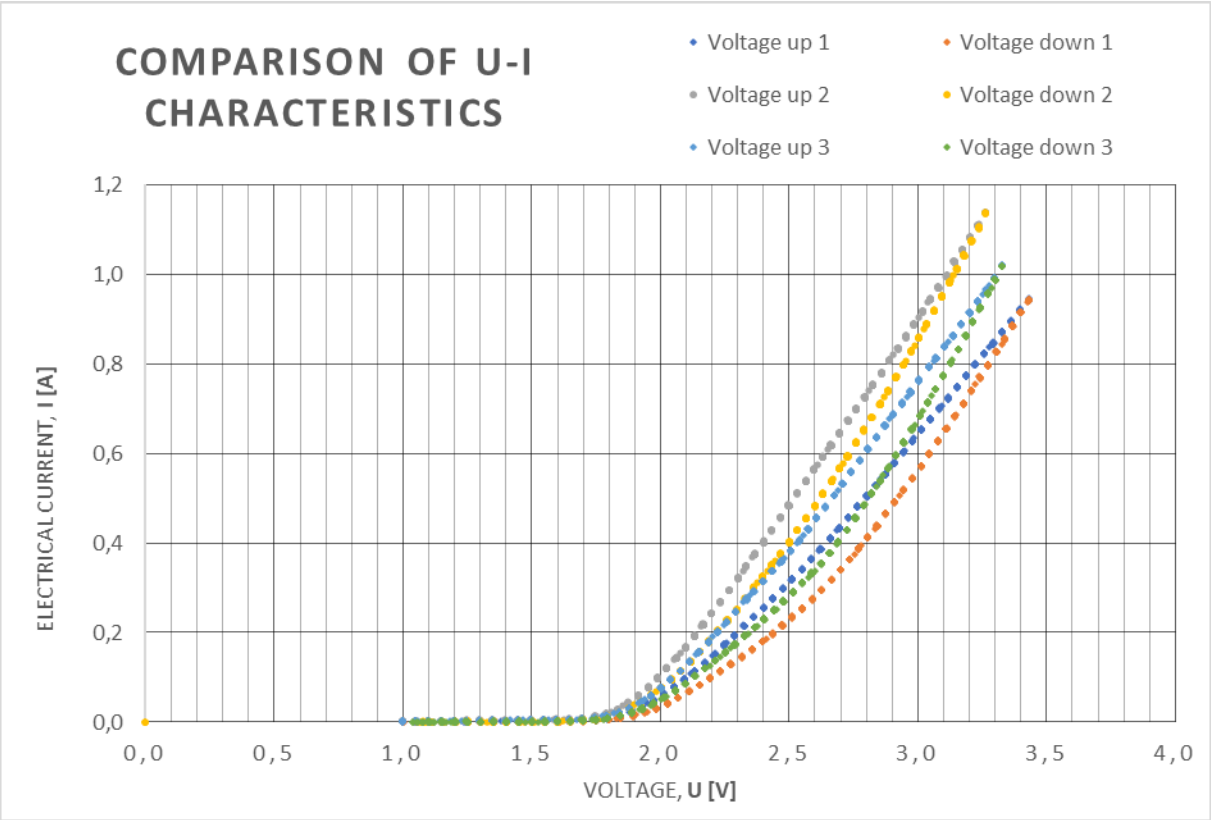

Figure 49. Three U-I characteristics recorded in different days

5. CONCLUSION

The research objectives set in the planning phase of this doctoral dissertation were achieved, and the research plan was respected. The experimental research was well planned and organised, the experimental setup was designed accordingly, and experiments were conducted. In the duration of the research, many subsystems of the experiment were constantly upgraded, better techniques were adopted, improving the quality of the research.

The main goal was to investigate the effects of the application of the magnetic and optical field, and the implementation of the Ni foam electrodes in the process of alkaline water electrolysis. The result of the experimental research undoubtedly confirms the positive impacts of all three implementations in the alkaline electrolyzer.

The most significant impact has the implementation of the magnetic field. The application of the electromagnet enabled the creation of a wide range of strength of the magnetic field, with the magnetic flux density up to 2 T. And while results vary significantly, with the highest increase of energy efficiency calculated to be 13.36% for the 1.49 T with the foam electrodes and the lowest increase in the to be 1.29% for the 0.66 T for the smooth electrodes, compared to the case without the usage of the magnetic field, it undoubtedly confirms significant positive impact on the process. Furthermore, when comparing different strengths of the magnetic fields, differences in the results are not so drastic. But in general, it can be concluded that the increase of the magnetic flux density of the applied magnetic field increases the efficiency of the water electrolysis process. The circulation of the bubbles in the electrolyte becomes ever more chaotic with the strengthening of the magnetic field. Thus, it can be assumed that at some point further increase of the magnetic flux density starts to have a slight negative impact on the energy efficiency.

Regarding optical field in the form of the LED, the results seem to point to a lesser but still positive impact on the energy efficiency of the water electrolysis process. As in a case with the magnetic field, the results vary significantly, with the highest increase of energy efficiency calculated to be 7.17% and the lowest increase to be 2.15% compared to the case without the usage of LED. Furthermore, when comparing different strengths of the optical fields, differences in the results show that the increase of the strength of the applied light increases the energy efficiency of the process, although the differences are not so distinctive and are in the

limit of measurement uncertainty. It can be concluded that the maximum efficiency was not reached due to the limitation of the equipment used and that with further increase of the strength of the optical field, further increase in the efficiency is to be expected.

The application of the foam electrodes proved to have a positive impact as well. Analysis of the results shows that the average energy efficiency for the foam electrodes in all experiments was 55.54%, while for the smooth electrodes, it was 53.16%. That determines the increase of 4.29% when smooth electrodes are replaced with foam electrodes. The increase in energy efficiency might be the least significant of all three analysed applications, but on another hand, are most trustworthy, due to the large number of comparable results analysed.

The results of the combined effects of more than one application were analysed. From a design point of view, the easiest combinations could be achieved by combining the foam with either of two external fields. However, the combination of magnetic field and LED with and without the foam electrodes was analysed as well. Based on the results, it was concluded that the dominant effect in the increase of energy efficiency has the application of the magnetic field. When applied with the LED, the effects of the LED are mitigated, due to the chaotic flow of bubbles in the electrolyte caused by the magnetic field. Bubbles lower the visibility of the electrolyte, effectively blocking the reach of the optical field to the inter-electrode space. When compared with the similar research main difference in this research is the way data is obtained. The data is obtained by physical measurement of produced hydrogen, while similar research conducted did not measure the amount of hydrogen produces in the process, but the units such as voltage to determine the voltage efficiency or Faraday efficiency. Other research focused on the rate of hydrogen production concluding that the implementation of the magnetic and the optical field resulted in the nine times higher hydrogen yields in comparison to conventional water electrolysis [79].

Results of the mathematical model adjustment are based on the results of the experimental research and provide further possibilities to better organise the future experimental research. Undoubtedly, the mathematical model will have a decisive economic impact, improving the financial viability of future research, by directing spending in the efficient direction.

Finally, it can be concluded, that the main hypothesis of the scientific research:

"The application of an external magnetic and optical field to the process of alkaline water electrolysis increases the efficiency of the alkaline electrolyzer with Ni foam electrodes."

was proven since the results indicate that application of an external magnetic and optical field in an alkaline electrolyzer with Ni foam electrodes increases the efficiency of the water electrolysis process.

5.1 Scientific contributions

Scientific contributions produced in this doctoral thesis are as follows:

- Research conducted in the scope of this research confirmed the hypothesises that the application of an external magnetic and optical field to the process of water electrolysis in an alkaline electrolyzer with Ni foam electrodes increases the efficiency of the water electrolysis process
- Extensive experimental research was conducted with the laboratory-made alkaline electrolyzer with restricted resources and limited available equipment, proving that complex and ambitious research can be conducted under those conditions
- Valuable knowledge and experience in the organisation, design and conduct of the experimental research, as in the following scientific procedures was gained in the duration of the research, which enabled the doctoral candidate for future work on the highest quality level

5.2 Future research

Future research will focus on further development of the usage of the effects of magnetic and optical fields. First, the main effort will be directed into exploiting its benefits in the design and manufacturing of prototype or the stronger electrolyzer with higher hydrogen production capacity. In purpose of that, the development and construction of a completely different geometry and size of the device will be needed, combining this research with the previous research conducted in the PEL. Since the positive impact on the energy efficiency has been established, restriction of the influence of the other effects, like temperature and pressure cease to exist, enabling the creative freedom in the upgrade of the design. The second part of the development will be based on the current design with the continuation of the research. The main goals will be to optimise the utilisation of the magnetic field and the LED, to achieve a positive impact with consideration of the economical perspective and overall energy efficiency. For the

application of LED, results showed that there is a potential in the usage of a stronger optical field, while the potential for the magnetic field was reached.

In the scope of this study, overall energy efficiency, that for example calculates the power supply for the electromagnet and LED was not analysed. Since the electromagnet alone is an energy device with the consumption power of a few kilowatts, the sheer amount of the energy consumption of the electromagnet would neglect any positive impacts of the study by a margin of a few magnitudes. If the power for the electromagnets would be utilised by the RES, for example PV power station, then the ecological aspect would be satisfied, However, produced electricity could have more beneficial usage, and should not be wasted lightly. Therefore, optimisation of the process must be conducted to achieve the best cost-efficient and energy-efficiency solutions available.

Finally, the work on the current equipment and experiments will continue. The results may vary a lot and measurement uncertainty may affect some measurements, by a significant margin. To mitigate those effects, the most cost-effective solution is the repetition of the experiments, expander of points that were analysed which will serve to the further development of the mathematical model, and the application of more precise measurement techniques, like the measurement of the level of the electrolyte in the upper tank. With a more reliable system of measurement, the effects of the measurement uncertainty on the results can be drastically reduced. That and the increased number of the experiment would improve the effects of the statistical errors making the results more reliable.

LITERATURE

[1] A. Kovač, M. Paranos, D. Marciuš, Hydrogen in energy transition: A review, International Journal of Hydrogen Energy 46 (2021) 10016-10035

[2] J. Proost, Critical assessment of the production scale required for fossil parity of green electrolytic hydrogen, International Journal of Hydrogen Energy 45 (2020) 17067-17075

[3] S.A. Sherif, F. Barbir, T.N. Veziroglu, Towards a Hydrogen Economy, The Electricity Journal 18 (2005) 62-76

[4] M. Groll, Can climate change be avoided? Vision of a hydrogen-electricity energy economy, Energy 264 (2023) 126029

[5] Craig A. Grimes, Oomman K. Varghee, Sudhir Ranjan, Light, Water, Hydrogen - The Solar Generation of Hydrogen by Water Photoelectrysis, Springer (2008)

[6] Volker Quaschning, Understanding Renewable Energy Systems, Earthscan (2005)

[7] Ankica Đukić, Proizvodnja vodika elektrolizom vode pomoću sunčeve energije i fotonaponskog modula, doktorski rad, Fakultet strojarstva i brodogradnje (2013)

[8] Frano Barbir, PEM Fuel Cells: Theory and Practice, Elsevier (2005)

[9] A. Đukić, V. Alar, M. Firak, S. Jakovljević, A significant improvement in material of foam, Journal of Alloys and Compounds 573 (2013) 128-132

[10] A. Đukić, V. Alar, M. Firak, Corrosion behaviour of the nickel based materials in an alkaline solution for hydrogen evolution, Indian Journal of Chemical Technology 24 (2017) 88-92

[11] M. Motalleb, A. Đukić, M. Firak, Solar hydrogen power system for isolated passive house, International Journal of Hydrogen Energy 40 (2015) 16001-16009

[12] A. Kovač, D. Marciuš, L. Budin, Solar hydrogen production via alkaline water electrolysis, International Journal of Hydrogen Energy 44 (2019) 9841-9848

[13] A. Đukić, Autonomous hydrogen production system, International Journal of Hydrogen Energy 40 (2015) 7465-7474

[14] A. Kovač, M. Paranos, Design of a solar hydrogen refuelling station following the development of the first Croatian fuel cell powered bicycle to boost hydrogen urban mobility, International Journal of Hydrogen Energy 44 (2019) 10014-10022

[15] A. Kovač, D. Marciuš, M. Paranos, Thermal management of hydrogen refuelling station housing on an annual level, International Journal of Hydrogen Energy 46 (2021) 29400-29410

[16] M. Firak, A. Đukić, Hydrogen transportation fuel in Croatia: Road map strategy, International Journal of Hydrogen Energy 41 (2016) 13820-13830

[17] Hrvatska strategija za vodik do 2050. godine, Hrvatski Sabor (2022)

[18] A. Kovač, Uloga vodikovih gorivnih članaka u procjeni razvoja prometnog sektora u Republici Hrvatskoj, Radovi Zavoda za znanstveni rad Varaždin 29 (2018) 349-359

[19] J. Šimunović, I. Pivac, F. Barbir, Techno-economic assessment of hydrogen refueling station: A case study in Croatia, International Journal of Hydrogen Energy 47 (2022) 24155-24168

[20] D. Marciuš, A. Kovač, M. Firak, Electrochemical hydrogen compressor: Recent progress and challenges, International Journal of Hydrogen Energy 47 (2022) 24179-24193

[21] M. Amin, H. H. Shah, A. G. Fareed, W. U. Khan, E. Chung, A. Zia, Z. U. R. Farooqi, C. Lee, Hydrogen production through renewable and non-renewable energy processes and their impact on climate change, International Journal of Hydrogen Energy 47 (2022) 33112-33134

[22] S. Nižetić, F. Barbir, N.b Djilali, The role of hydrogen in energy transition, International Journal of Hydrogen Energy 44 (2019) 9673-9674

[23] J. M. Low, R. S. Haszeldine, J. Mouli-Castillo, Refuelling infrastructure requirements for renewable hydrogen road fuel through the energy transition, Energy Policy 172 (2023) 113300

[24] Ikäheimo, T. J. Lindroos, J. Kiviluoma, Impact of climate and geological storage potential on feasibility of hydrogen fuels, Applied Energy 342 (2023) 121093

[25] S. Takeda, H. Nam, A. Chapman, Low-carbon energy transition with the sun and forest: Solar-driven hydrogen production from biomass, International Journal of Hydrogen Energy 47 (2022) 24651-24668

[26] F. Barbir, PEM electrolysis for production of hydrogen from renewable energy sources, Solar Energy 78 (2005) 661-669

[27] T. Capurso, M. Stefanizzi, M. Torresi, S.M. Camporeale, Perspective of the role of hydrogen in the 21st century energy transition, Energy Conversion and Management 251 (2022) 114898

[28] H. Zhang, G. Lin, J. Chen, Evaluation and calculation on the efficiency of a water electrolysis system for hydrogen production, International Journal of Hydrogen Energy 35 (2010) 10851-10858

[29] K. Ayers, High efficiency PEM water electrolysis: enabled by advanced catalysts, membranes, and processes, Current Opinion in Chemical Engineering 33 (2021) 100719

[30] M. Carmo, D. L. Fritz, J. Mergel, D. Stolten, A comprehensive review on PEM water electrolysis, International Journal of Hydrogen Energy 38 (2013) 4901-4934

[31] Z. Zou, K. Dastafkan, Y.Shao, C. Zhao, Q. Wang, Electrocatalysts for alkaline water electrolysis at ampere-level current densities: a review, International Journal of Hydrogen Energy (2023) In Press

[32] E. Açıkkalp, O. Altuntas, H. Caliskan, G. Grisolia, U. Lucia, D. Borge-Diez, E. Rosales-Asensio, Sustainability analyses of photovoltaic electrolysis and magnetic heat engine coupled novel system used for hydrogen production and electricity generation, Sustainable Energy Technologies and Assessments 52 (2022) 102094

[33] S. Wang, Z. Geng, S. Bi, Y. Wang, Z. Gao, L. Jin, C. Zhang, Recent advances and future prospects on Ni3S2-Based electrocatalysts for efficient alkaline water electrolysis, Green Energy & Environment (2023) In Press

[34] X. Wei, T. Kakimoto, Y. Umehara, H. Nakajima, K. Ito, H. Inagaki, S. Mori, Improvement of the critical current density of alkaline water electrolysis based on the hydrodynamic similarity between boiling and water electrolysis, International Journal of Heat and Mass Transfer 214 (2023) 124420

[35] C. Lamy, P. Millet, A critical review on the definitions used to calculate the energy efficiency coefficients of water electrolysis cells working under near ambient temperature conditions, Journal of Power Sources 447 (2020) 227350

[36] R. Qi, M. Becker, J. Brauns, T. Turek, J. Lin, Y. Song, Channel design optimization of alkaline electrolysis stacks considering the trade-off between current efficiency and pressure drop, Journal of Power Sources 579 (2023) 233222

[37] T. Wu, Y. Hu, M. Li, B. Han, Z. Liang, D. Geng, Enabling efficient decoupled alkaline water electrolysis using a low-cost sodium manganate solid-state redox mediator, International Journal of Hydrogen Energy (2023) In Press

[38] N. A. Burton, R. V. Padilla, A. Rose, H. Habibullah, Increasing the efficiency of hydrogen production from solar powered water electrolysis, Renewable and Sustainable Energy Reviews 135 (2021) 110255

[39] J.Zhang, J. Dang, X.Zhu, J. Ma, M. Ouyang, F. Yang, Ultra-low Pt-loaded catalyst based on nickel mesh for boosting alkaline water electrolysis, Applied Catalysis B: Environmental 325 (2023) 122296

[40] S. K. Mazloomi, N. Sulaiman, Influencing factors of water electrolysis electrical efficiency, Renewable & Sustainable Energy Reviews 16 (2012) 4257-4263

[41] F. Scheepers, M. Stähler, A. Stähler, E. Rauls, M. Müller, M. Carmo, W. Lehnert, Temperature optimization for improving polymer electrolyte membrane-water electrolysis system efficiency, Applied Energy 283 (2021) 116270

[42] R. Phillips, C. W. Dunnill, Zero gap alkaline electrolysis cell design for renewable energy storage as hydrogen gas, Rsc Advances 6 (2016) 100643-100651

[43] J. Kuang, Y. Huang, Research on improvement of electrode efficiency of water electrolysis on Ni-P electroless plating by appended RE, Journal of Rare Earths 28 (2010) 469-473

[44] S. Li, C. Wang, C. Chen, Water electrolysis in the presence of an ultrasonic field, Electrochimica Acta 54 (2009) 3877-3883

[45] Z. Dobó, A. B. Palotas, Impact of the voltage fluctuation of the power supply on the efficiency of alkaline water electrolysis, International Journal of Hydrogen Energy 41 (2016) 11849-11856

[46] Z. Dobó, A. B. Palotas, Impact of the current fluctuation on the efficiency of Alkaline Water Electrolysis, International Journal of Hydrogen Energy 42 (2017) 5649-5656

[47] S. F. Amireh, N. N. Heineman, P. Vermeulen, R. L. G. Barros, D. Yang, J. van der Schaaf, M. T. de Groot, Impact of power supply fluctuation and part load operation on the efficiency of alkaline water electrolysis, Journal of Power Sources 560 (2023) 232629

[48] N. Demir, M. F. Kaya, M. S. Albawabiji, Effect of pulse potential on alkaline water electrolysis performance, International Journal of Hydrogen Energy 43 (2018) 17013-17020

[49] Q. de Radigues, G. Thunis, J. Proost, On the use of 3-D electrodes and pulsed voltage for the process intensification of alkaline water electrolysis, International Journal of Hydrogen Energy 44 (2019) 29432-29440

[50] I. A. Poimenidis, N. Papakosta, A. Klini, M. Farsari, M. Konsolakis, P. A. Loukakos, S. D. Moustaizis, Electrodeposited Ni foam electrodes for increased hydrogen production in alkaline electrolysis, Fuel 342 (2023) 127798

[51] F. Rocha, R. Delmelle, C. Georgiadis, J. Proost, Effect of pore size and electrolyte flow rate on the bubble removal efficiency of 3D pure Ni foam electrodes during alkaline water electrolysis, Journal of Environmental Chemical Engineering 10 (2022) 107648

[52] X. Lyu, J. Li, C. J. Jafta, Y. Bai, C. P. Canales, F. Magnus, Á.S. Ingason, A. Serov, Investigation of oxygen evolution reaction with Ni foam and stainless-steel mesh electrodes in alkaline seawater electrolysis, Journal of Environmental Chemical Engineering 10 (2022) 108486

[53] N. Bidin, S. R. Azni, M. A. Abu Bakar, A. Johari, D. Munap, M. F. Salebi, S. N. A. Razak, N. S. Sahidan, S. N. A. Sulaiman, The effect of sunlight in hydrogen production from water electrolysis, International Journal of Hydrogen Energy 42 (2017) 133-142

[54] F. Si, M. Wei, M. Li, X. Xie, Q. Gao, X. Cai, S. Zhang, F. Peng, Y. Fang, S. Yang, Natural light driven photovoltaic-electrolysis water splitting with 12.7% solar-to-hydrogen conversion efficiency using a two-electrode system grown with metal foam, Journal of Power Sources 538 (2022) 231536

[55] S. Hu, B. Guo, S. Ding, F. Yang, J. Dang, B. Liu, J. Gu, J. Ma, M. Ouyang, A comprehensive review of alkaline water electrolysis mathematical modelling, Applied Energy 327 (2022) 120099

[56] K. Górecki, P. Górecki, J. Zarębski, Electrical model of the alkaline electrolyser dedicated for SPICE, International Journal of Circuit Theory and Applications 46 (2018) 1044-1054

[57] J. C. Garcia-Navarro, M. Schulze, K. A. Friedrich, Detecting and modeling oxygen bubble evolution and detachment in proton exchange membrane water electrolyzers, International Journal of Hydrogen Energy 44 (2019) 27190-27203

[58] H. Liu, L.Pan, Q.Qin, P.Li, Experimental and numerical investigation of gas-liquid flow in water electrolysis under magnetic field, Journal of Electroanalytical Chemistry 832 (2019) 293-302

[59] O. Aaboubi, Hydrogen evolution activity of Ni–Mo coating electrodeposited under magnetic field control, International Journal of Hydrogen Energy 36 (2011) 4702-4709

[60] J. A. Koza, S. Muhlenhoff, P. Zabinski, P. A. Nikrityuk, K. Eckert, M. Uhlemann, A. Gebert, T. Weier, L. Schultz, S. Odenbach, Hydrogen evolution under the influence of a magnetic field, Electrochimica Acta 56 (2011) 2665-2675

[61] M. Y. Lin, L. W. Hourng, C. W. Kuo, The effect of magnetic force on hydrogen production efficiency in water electrolysis, International Journal of Hydrogen Energy 37 (2012) 1311-1320

[62] M. Y. Lin, W. N. Hsu, L. W. Hourng, T. S. Shih, C. M. Hung, Effect of Lorentz force on hydrogen production in water electrolysis employing multielectrodes, Journal of Marine Science and Technology-Taiwan 24 (2016) 511-518

[63] M. Y. Lin, L. W. Hourng, J. S. Hsu, The effects of magnetic field on the hydrogen production by multielectrode water electrolysis, Energy Sources Part a-Recovery Utilization and Environmental Effects 39 (2017) 352-357

[64] M. Y. Lin, L. W. Hourng, C. H. Wu, The effectiveness of a magnetic field in increasing hydrogen production by water electrolysis, Energy Sources Part a-Recovery Utilization and Environmental Effects 39 (2017) 140-147

[65] S. Zhan, Y. Huang, W. Zhang, B. Li, M. Jiang, Z. Wang, J. Wang, Experimental investigation on bubble growth and detachment characteristics on vertical microelectrode surface under electrode-normal magnetic field in water electrolysis, International Journal of Hydrogen Energy 46 (2021) 36640-36651

[66] G. Bilgiç, B. Öztürk, S. Atasever, M. Şahin, H. Kaplan, Prediction of hydrogen production by magnetic field effect water electrolysis using artificial neural network predictive models, International Journal of Hydrogen Energy 48 (2023) 20164-20175

[67] A. Zeeshan, N. Ijaz, A. Majeed, Analysis of magnetohydrodynamics peristaltic transport of hydrogen bubble in water, International Journal of Hydrogen Energy 43 (2018) 979-985.

[68] Y. Liu, S. Li, H. Wu, Y. Shi, Impact of electrode-normal magnetic field on oxygen bubbles generated by alkaline water electrolysis at low current densities, Journal of Electroanalytical Chemistry 945 (2023) 117679

[69] H. B. Liu, D. H. Zhong, J. X. Han, L. M. Pan, Y. Liu, Hydrogen bubble evolution from magnetized nickel wire electrode, International Journal of Hydrogen Energy 44 (2019) 31724-31730

[70] H. Matsushima, T. Iida, Y. Fukunaka Gas bubble evolution on transparent electrode during water electrolysis in a magnetic field, Electrochimica Acta 100 (2013) 261-264

[71] X. Yang, K. Eckert, S. Mühlenhoff, S. Odenbach, On the decay of the Lorentz-force-driven convection in vertical concentration stratification during magnetoelectrolysis, Electrochimica Acta 54 (2009) 7056-7065

[72] H. Matsushima, D. Kiuchi, Y. Fukunaka, Measurement of dissolved hydrogen supersaturation during water electrolysis in a magnetic field, Electrochimica Acta 54 (2009) 5858-5862

[73] P. Purnami, N. Hamidi, M. N. Sasongko, D. Widhiyanuriyawan, I. N. G. Wardana, Strengthening external magnetic fields with activated carbon graphene for increasing hydrogen production in water electrolysis, International Journal of Hydrogen Energy 45 (2020) 19370-19380

[74] Y. Liu, L. Pan, H. Liu, Water electrolysis using plate electrodes in an electrode-paralleled non-uniform magnetic field, International Journal of Hydrogen Energy 46 (2021) 3329-3336

[75] P. Zhao, J. Wang, W. He, H. Xia, X. Cao, Y. Li, L. Sun, Magnetic field Pre-polarization enhances the efficiency of alkaline water electrolysis for hydrogen production, Energy Conversion and Management 283 (2023) 116906

[76] M. F. Kaya, N. Demir, M. S. Albawabiji, M. Taş, Investigation of alkaline water electrolysis performance for different cost effective electrodes under magnetic field, International Journal of Hydrogen Energy 42 (2017) 17583-17592

[77] Y. Liu, L. M. Pan, H. B. Liu, T. M. Chen, S. Y. Yin, M. M. Liu, Effects of magnetic field on water electrolysis using foam electrodes, International Journal of Hydrogen Energy 44 (2019) 1352-1358

[78] H. B. Liu, H. T. Xu, L. M. Pan, D. H. Zhong, Y. Liu, Porous electrode improving energy efficiency under electrode-normal magnetic field in water electrolysis, International Journal of Hydrogen Energy 44 (2019) 22780-22786

[79] N. Bidin, S. R. Azni, S. Islam, M. Abdullah, M. F. S. Ahmad, G. Krishnan, A. R. Johari, M. A. A. Bakar, N. S. Sahidan, N. Musa, M. F. Salebi, N. Razali, M. M. Sanagi, The effect of magnetic and optic field in water electrolysis, International Journal of Hydrogen Energy 42 (2017) 16325-16332

[80] Electromagnet with variable Air Gap AGEM 5520 - Maunual, Schwarzbeck mess-elektronik (2020)

[81] Jürgen Garche, Chris K. Dyer, Patrick T. Moseley, Zempachi Ogumi, David A. J. Rand, Bruno Scrosati, Encyclopedia of Electrochemical Power Sources, Elsevier (2009)

[82] Tomislav Filetin, Ivan Kramer, Gojko Marić, Metalne pjene, Hrvatsko društvo za materijale i tribologiju (2003)

[83] Thomas G. Beckwith, Roy D. Marangoni, John H. Lienhard V, Mechanical Measurements Fifth Edition, Addison-Wesley Publishing Company (1995)

[84] IFA for Databases on hazardous substances (GESTIS), Potassium hydroxide 25% water solution - Safety data sheet, RCI Labscan Limited (2021)

[85] Antun Galović, Termodinamika I, Fakultet strojarstva i brodogradnje (2011)

[86] Boris Halasz, Antun Galović, Ivanka Boras, Toplinske Tablice, Fakultet strojarstva i brodogradnje (2010)

[87] The Engineering ToolBox

[88] Antun Galović, Termodinamika II, Fakultet strojarstva i brodogradnje (2010)

[89] Colleen Spiegel, PEM Fuel Cell Modeling and Simulation Using MATLAB®, Academic Press (2008)

[90] M. Martin, L. W. Hourng, Effects of magnetic field and pulse potential on hydrogen production via water electrolysis, International Journal of Energy Research 38 (2014) 106-116

BIOGRAPHY

Matej Paranos was born on June 18, 1993, in Zagreb. He grew up in Ivanić Grad, where he finished Primary and Secondary school. In 2011 he enrolled in undergraduate studies of mechanical engineering at the Faculty of Mechanical Engineering and Naval Architecture in Zagreb. During his undergraduate and graduate studies, he worked on numerous student jobs, outside and within the engineering profession.

He finished his undergraduate studies in 2017 and in the same year enrolled in his graduate studies, which ends in 2019. During his graduate studies, he became very interested in the issue of climate change, clean energy transition, and energy efficiency, with a special emphasis on hydrogen technologies.

After completing his studies in the same year, within the Croatian Science Foundation project, he was employed as a Research Project Assistant at the Faculty of Mechanical Engineering and Naval Architecture and worked in the Power Engineering Laboratory, Department of Energy, Power, and Environmental Engineering, under the guidance of Ankica Kovač and enrolled in doctoral study at the same faculty.

In addition to the scientific work on the project, as a part of the work in the Power Engineering Laboratory, he was involved in working with students, creating projects and studies, cooperating with industry and other state institutions, and numerous other tasks. He participated in numerous international conferences in Croatia and abroad. In 2022, he became a head of the Power Engineering Laboratory, and in the same year, he was appointed the alternative legal representative of the University of Zagreb, Faculty of Mechanical Engineering and Architecture in Hydrogen Europe Research.

Matej serves as a Technical Chair of the Renewable Hydrogen Energy Convention, and a member of a Local Organizing Committee of the Global Conference on Global Warming.

He spends his free time in the company of friends, through walks, cinema, and pub quizzes. As the handball player and former tennis player, Matej has been connected to sports his whole life. His favourite hobbies are windsurfing, chess and football, he likes history, traveling and going out to concerts, festivals, and football matches.

PUBLISHED WORK

Journals

[1] Ankica Kovač, Matej Paranos, Doria Marciuš, Hydrogen in energy transition: A review // International journal of hydrogen energy, 46 (2021), 16; 10016-10035 https://doi.org/10.1016/j.ijhydene.2020.11.256

[2] Ankica Kovač, Matej Paranos, Design of a solar hydrogen refuelling station following the development of the first Croatian fuel cell powered bicycle to boost hydrogen urban mobility // International journal of hydrogen energy, 44 (2019), 20; 10014-10022 https://doi.org/10.1016/j.ijhydene.2018.11.204

[3] Ankica Kovač, Doria Marciuš, Matej Paranos, Thermal management of hydrogen refuelling station housing on an annual level // International journal of hydrogen energy (2021) https://doi.org/10.1016/j.ijhydene.2020.11.013

Conferences

[1] Matej Paranos, Ankica Kovač, Analysis of experimental application of permanent neodymium magnets in alkaline electrolyzer for green hydrogen production // Abstract Book - WHEC2022 - 23rd World Hydrogen Energy Conference Istanbul, Turkey, 2022. pp. 56-56 (lecture, international peer review, full paper, scholarly))

[2] Matej Paranos, Mihajlo Firak, Ankica Kovač, Application of magnetic field in green hydrogen production // Book of Abstracts: The 1st Renewable Hydrogen Energy Conference (RH2EC-2021) Zagreb, Hrvatska, 2021. pp. 6-6 (lecture, international peer review, abstract, scholarly)

[3] Matej Paranos, Ankica Kovač, Application of Permanent Neodymium Magnets in Green Hydrogen Production // 16th SDEWES conference Dubrovnik 2021: Book of Abstracts, Dubrovnik, Hrvatska, 2021. pp. 672-672 (lecture, international peer review, abstract, scholarly)

[4] Doria Marciuš, Ankica Kovač, Matej Paranos, Hydrogen Refuelling stations: State of the Art and perspectives // TUBA World Conference on Energy Science and Technology: Book of Abstracts, held virtually, 2021. pp. 305-306 (lecture, international peer review, short communication, scholarly)

[5] Marciuš Doria, Matej Paranos, Ankica Kovač, The role of hydrogen in the new era of transport // Nova era prometa 2022 Zagreb, 2022. pp. 30-30 (lecture, local peer review, abstract, scholarly)

[6] Ankica Kovač, Matej Paranos, Željko Penga, Dinko Brezak, Tessa Uroić, Doria Marciuš, Advanced methods of green hydrogen production and its transportation // Book of Abstracts Zagreb, 2021. pp. 320-320 (lecture, international peer review, abstract, scholarly)